

Assessing Pain from Neurophysiological Signals: Machine Learning Approaches Using Functional Connectivity

Yiyuan Han

A thesis submitted for the degree of

Doctor of Philosophy

School of Computer Science and Electronic Engineering

University of Essex

June 2024

Abstract

The assessment of pain remains a significant challenge in healthcare, which always relies on subjective measures based on behaviour. However, the unresponsive patients, e.g., the ones with the disorder of consciousness, cannot self-report pain. Addressing this challenge, this thesis develops machine learning approaches for pain assessment using electroencephalography (EEG).

This research initially quests the suitable neural biomarkers of pain, which firstly analysed the neural biomarkers of integration. By examining functional connectivity and cross-frequency coupling, phase-based functional connectivity from the alpha band emerged as a robust feature, excelling in both prediction accuracy and computational efficiency. Consequently, it was employed in subsequent model development. Considering the individual variability in pain processing, this study adopted cross-domain transfer learning strategies, targeting unresponsive patients as they cannot provide training labels. Inspired by the contributions of deep learning models to transfer learning, a convolutional neural network (CNN) was implemented. The CNN model demonstrated good performances in both pain prediction and subject recognition with the subject involved

in model training, which suggested its potential role in cross-subject transfer learning. Furthermore, the study figured out the activation patterns of functional connectivity produced by the CNN using Gradient-weighted Class Activation Mapping (Grad-CAM). The patterns revealed the critical involvement of frontal, parietal, and occipital brain regions in functional connectivity specific to pain assessment, in line with established physiological findings. Nevertheless, the work also identified the challenge of isolating pain-specific features due to the extensive distribution of functional connectivity contributing to subject recognition.

Overall, this thesis emphasises the potential of phase-based functional connectivity from the alpha band as an ideal neural biomarker for pain and individual differences. It also introduces CNN-based transfer learning as a promising avenue for cross-subject pain assessment.

Acknowledgements

First and foremost, I would like to express my deepest gratitude to my supervisors, Dr. Sebastian Halder and Dr. Elia Valentini, for their outstanding and patient support, guidance and supervision. Their expertise and insight in interdisciplinary research are a true treasure for my research and future career development. More importantly, their abundant encouragement has sustained me through the challenges of this journey, especially through uncertainty during the pandemic. It is my great pleasure to have had the opportunity to work with these distinguished researchers.

I also extend my heartfelt thanks to my colleagues at the Essex Brain-Computer Interface and Neural Engineering Laboratory (BCI-NE Lab), the School of Computer Science and Electronic Engineering and the Department of Psychology. To all the members of the BCI-NE Lab, thank you for creating an environment of curiosity and academic rigour. I am grateful to have been part of such an inspiring and supportive community. I would like to express my gratitude and best wishes to my peers, including Eirini, Milan, Lena, Istvan, Ahmet, Federica, Wenxin, Mushfika, Zilu, Idorenyin, Khetam, and Alberto. I am sincerely grateful to Dr. Serafeim Perdikis and Dr. Zilong Liu as the members of my su-

pervisory panel, who gave me insightful feedback on my research. I would like to thank Dr. Ana Matran-Fernandez for giving me the wonderful opportunity for external training.

To my friends living around the world, I would say thanks to their friendship making so much joy and comfort, including Fangqing, Fernanda, Jiaxing, Jingyi, Jinyan, Lei, Lu, Shiyu, Siyi, Wenxian, Xiaokang, Xiaonan, Xin, Yajie, Yang, Yao, Yilin, and Zihao. I am also thankful to my undergraduate supervisor Prof. Fei Chen from my Alma Mater, Southern University of Science and Technology, for leading me into the world of research. Otherwise, I appreciate Mr. Adrian Wallwork for the training in academic writing.

I would like to acknowledge the scholarship provided by the Faculty of Science and Health, University of Essex, without which this PhD research would not have been possible. I would also like to acknowledge the use of the High-Performance Computing Facility (Ceres) and its associated support services in the completion of this work.

I am indebted to my beloved parents, Mr. Wenwu Han and Mrs. Xiaolan Liu, whose unconditional love and unwavering belief supported my growth and built my confidence to face all the challenges. I would say many thanks for their constant encouragement by always being there when I needed listening ears when we were thousands of miles away.

I dedicate this work to my late grandmother, Mrs. Gaihua Qin, who passed away in December 2022. Her love and kindness live in my heart, I know she is watching over me as I complete this journey.

Some people said *Pain is temporary, but a Ph.D. is forever*. As a Ph.D. student studying pain, I hope my work can help make pain less and weaker, while health, happiness, and peace move ever closer to being forever in this turbulent world.

Contents

List of Abbreviations	xi
List of Figures	xvii
List of Tables	xxix
1 Introduction	1
1.1 Motivation and Background	1
1.1.1 Assessing Pain with Efficient and Portable Electrophysiological Equip- ment	1
1.1.2 Electrophysiological Representation of Complex Pain Processing . .	4
1.1.3 Development of Machine Learning	6
1.2 Research Questions	8
1.2.1 Neural Marker: Feature in Machine Learning	8
1.2.2 Machine Learning Model	9
1.3 Contributions of the Thesis	10
1.4 Thesis Outline	12
1.5 List of Publication	14

1.5.1	Journal Publication and Manuscript	14
1.5.2	Conference Publication	15
1.5.3	Conference Abstract	15
2	Literature Review	17
2.1	What is Pain?	17
2.1.1	Pain as a Global Health Crisis	17
2.1.2	Types of Pain	19
2.1.3	Neuroanatomy and Neurophysiology of Pain	22
2.2	Pain Management and Assessment	27
2.2.1	Pain Management	27
2.2.2	Toward Treatment and Management: Why We Need to Assess Pain	29
2.2.3	Behavioural and Verbal Assessment	31
2.2.4	Physiological Assessment	36
2.2.5	Other Novel Approaches in Pain Assessment	41
2.3	Electroencephalography (EEG) in Pain Assessment	43
2.3.1	Principles and Advantages of EEG	43
2.3.2	Brain Rhythms and Electrophysiology of Pain	44
2.3.3	Discovering Neural Biomarker: Neurophysiological Measure from EEG in Pain Assessment	48
2.4	Machine Learning	57
2.4.1	Machine Learning Algorithm	59

2.4.2	Transfer Learning	63
3	Experiment and Signal Pre-processing	65
3.1	Participants	65
3.2	Experimental Condition and Procedure	66
3.3	Signal Pre-processing	68
3.3.1	Filtering and Artifact Removal	68
3.3.2	Re-referencing	69
4	Accurate and Efficient Prediction of Pain: A Comparative Electroencephal-	
	ography Study of Functional Connectivity and Cross-Frequency Coupling	71
4.1	Introduction	72
4.2	Methodology	78
4.2.1	EEG pre-processing	78
4.2.2	Functional connectivity and cross-frequency coupling	78
4.2.3	Machine learning	82
4.3	Results	85
4.3.1	Prediction accuracy	85
4.3.2	Computational efficiency	91
4.3.3	Significant neural markers of integration	91
4.4	Discussion	99
4.4.1	From the <i>ideal</i> feature to the <i>ideal</i> setting	99
4.4.2	Topographical regions of interest in tonic pain prediction	104

4.5	Conclusions	108
5	EEG-based Cross-Subject Pain Prediction I: EEG-Based Pain Assessment	
	Model Using Convolutional Neural Networks	111
5.1	Introduction	112
5.2	Methodology	116
5.2.1	Experimental Conditions	116
5.2.2	Data Re-organisation	117
5.2.3	Machine Learning	119
5.2.4	Grad-CAM	127
5.3	Results	131
5.3.1	Basic Cross-Subject Pain Prediction	131
5.3.2	Subject Recognition	134
5.3.3	Selective Transfer Learning	138
5.3.4	Activated Functional Connectivity	138
5.4	Discussion	140
5.4.1	Improvement of Generalisation in Pain Assessment Model	140
5.4.2	Functional Connectivity of Interests in Pain Assessment Revealed by Deep Learning	144
5.5	Conclusions	145
6	EEG-based Cross-Subject Pain Prediction II: EEG-Based Transfer Learning	
	Approaches for Pain Assessment	147

6.1	Introduction	148
6.2	Methodology	152
6.2.1	Experiment and Signal Pre-processing	152
6.2.2	Feature Extraction	152
6.2.3	Dataset Generation	153
6.2.4	Model Training and Validation	153
6.3	Framework	156
6.3.1	Neural Network Model	159
6.3.2	Pattern Analysis	162
6.4	Results	165
6.4.1	Performances of Transfer Learning Frameworks	165
6.4.2	Correlation between Similarity Measure and Accuracy	171
6.4.3	Grad-CAM Pattern	171
6.5	Discussion and Conclusion	175
7	Conclusion	182
7.1	Main Contributions	182
7.1.1	Phase-based Functional Connectivity from the Alpha Band: Ideal Neural Marker of Integration for Pain Prediction	183
7.1.2	Discovery of Deep Learning: Convolutional Neural Network for Cross-subject Pain Assessment	185
7.1.3	Physiological Interpretability of the Features Extracted by CNN Model	186

7.2	Limitations and Future Work	187
7.2.1	Robust Strategy of Cross-subject Pain Assessment	187
7.2.2	Generalisation and Standardisation of Datasets for EEG-based Pain Assessment	188
7.2.3	BCI-based Online Pain Assessment System	189
	Bibliography	191

List of Abbreviations

ACC Anterior Cingulate Cortex.

AI Artificial Intelligence.

AUC Area Under ROC Curve.

BCI Brain-Computer Interface.

BPS Behavioural Pain Scale.

CFC Cross-Frequency Coupling.

CNN Convolutional Neural Network.

CNS Central Neural System.

COVID-19 Coronavirus Disease 2019.

CPOT Critical Care Pain Observation Tool.

CSD Current Source Density.

CSP Common Spatial Pattern.

CV Computer Vision.

DBS Deep Brain Stimulation.

DOC Disorder of Consciousness.

DRG Dorsal Root Ganglion.

ECG Electrocardiography/Electrocardiogram.

EEG Electroencephalography/Electroencephalogram.

FFT Fast Fourier Transform.

fMRI Functional Magnetic Resonance Imaging.

fNIRS Functional Near-Infrared Spectroscopy.

FPS Functional Pain Syndrome.

GAN Generative Adversarial Network.

Grad-CAM Gradient-weighted Class Activation Mapping.

GUI Graphical User Interface.

HIV Human Immunodeficiency Virus.

IASP International Association for the Study of Pain.

ICU Intensive Care Unit.

ISPC Inter-Site Phase Clustering.

LFP Local Field Potential.

LOO Leave-One-Out.

LSTM Long Short-Term Memory.

MCS Minimally Conscious State.

MEG Megnetoencephalography/Magnetoencephalogram.

mPFC Medial Prefrontal Cortex.

NAcc Nucleus Accumbens.

NCA Neighbourhood Component Analysis.

NLP Natural Language Processing.

NPS Neurologic Pain Signature.

NRS Numeric Rating Scale.

NSAID Non-Steroidal Anti-Inflammatory Drug.

OFC Orbitofrontal Cortex.

ODU Opioid Use Disorder.

PAF Peak Alpha Frequency.

PAG Periaqueductal Gray Matter.

PAINAD PainAssessment in Advanced Dementia.

PCC Posterior Cingulate Cortex.

PDC Partial Directed Coherence.

PDN Painful Diabetic Neuropathy.

PDR Pupillary Dilation Reflex.

PET Positron Emission Tomography.

PHN Post-Herpetic Neuralgia.

PPG PhotoplethysmographyPhotoplethysmogram.

PRI Pain Rating Index.

PSD Power Spectral Density.

ROC Receiver Operating Characteristic.

RVM Rostroventromedial Medulla.

SCA Skin Conductance Algesimeter.

SMA Supplementary Motor Area.

SNR Signal-to-Noise Ratio.

STFT Short-Term Fourier Transform.

SVM Support Vector Machine.

TCA Transfer Component Analysis.

tDCS transcranial Direct Current Stimulation.

TENS Transcutaneous Electrical Nerve Stimulation.

TG Trigeminal Ganglia.

TL Transfer Learning.

VAS Visual Analogue Scale.

VRS Verbal Rating Scale.

WHO World Health Organization.

WT Wavelet Transform.

List of Figures

2.1	The diagram outlines neural structures in pain processing [1]. It shows that pain perception starts from the transmission system with transduction (lower left), where a stimulus creates nerve impulses conducted to the spinal cord and then relayed via diverse pathways toward the cerebral cortex. The pain-modulation inputs from different regions (i.e., the frontal association cortex and the hypothalamus) weaken the intensity of perceived pain. (DRG: dorsal root ganglion.)	23
2.2	Common pain rating scales [2]. From top to bottom: Visual analogue scale (VAS), numerical rating scale (NRS), and verbal rating scale (VRS). .	33
2.3	The McGill Pain Questionnaire [3]. The questionnaire includes four groups of word descriptors: sensory (1-10), affective (11-15), evaluative (16) and miscellaneous (17-20). The rank value of each descriptor increases from top to bottom. The sum of the rank values is defined as the pain rating index (PRI).	34
2.4	Five typical frequency bands which are studied as the brain rhythms from EEG.	43

2.5	An example of spectrogram computed with the EEG signals recorded in different brain regions [4]. The strength of each point represents the amplitude computed with STFT, the x- and y-axis represent the scales of time and frequency. Each spectrogram was averaged across the electrodes in a brain region within the same subject.	51
2.6	The pipeline of machine learning model's development. According to the neuroanatomy and neurophysiology of pain, neurophysiological measures were developed. Hence, neurophysiological measures can serve as neural biomarkers inputting the machine learning model as features. In the meantime, the behavioural and verbal measures can play the role of labels in the machine learning model's training. Using an appropriate machine learning model, pain-related states can be predicted.	58
2.7	Procedure of a two-dimensional CNN [5]. After adding the padding for processing the effects of edges, the convolutional kernels were slid on the input, and then the output patterns were processed by max pooling.	62

3.1	The experimental procedure for recording the pain-related EEG signals. During the matching phase, the participants were requested to match the pain rating with the unpleasantness induced by the Dound condition (S). The EEG signals started to be recorded after the matching phase, in which each condition lasted five minutes, and there were two phases of baselines (Eyes-Open [O] and Eyes-Closed [C]) before and after stimulus conditions (Hot [H], Warm [W] and Sound [S]).	69
4.1	(a) Pre-processing pipeline: First, delta (0.5-4 Hz), theta (4-7 Hz), alpha (8-12Hz), and low beta (12.5-16 Hz) bands were extracted from the raw EEG data. I then computed power and phase using Hilbert transform. Then, I extracted the neural markers representing functional connectivity or cross-frequency coupling. (b) Model training and testing pipeline: I split data into two groups. While one dataset was used for feature selection, the other was used to train and test the classifiers with the selected features using 10-fold cross-validation. Subsequently, feature-selection and model-training datasets would be swapped.	79

4.2 **Boxplots of binary classification accuracy versus feature type.** Each plot represents the median of prediction accuracy (y axis) for the 100 features dataset across experimental conditions. The box edges are the 25th and 75th percentiles, the outlines indicate the 95th percentile, the plus sign indicate values out of the confidence interval. The labels 'O' and 'C' represent 'eyes-open' and 'eyes-closed', while 'H' and 'W' mean 'hot' and 'warm'. Alpha-phase connectivity ('PhaCon'), alpha-power connectivity ('PowCon'), phase-based CFC ('PhaCou'), and power-based CFC('PowCou') are displayed on the x axis according to different trial lengths (arranged by different degrees of gray). Each subplot represents one pair of binary classification. 92

4.3 **Brain topography of z-scored signal amplitude versus conditions and frequency bands.** Each plot represents the z-scored brain topography of the median signal amplitudes calculated as the square roots of power spectral density (PSD) across pain-related conditions and frequency bands. Each row of plots represents the topography from the same frequency band, and each column of plots represents the same experimental condition. All of the topography does not involve any significant differences from the other one in the same frequency band, the green background represents the topography has significantly high similarity with at least one of the topography within the same band (**p<.001). 93

4.4	Brain topography of z-scored exponential phase versus conditions and frequency bands. Each plot represents the z-scored brain topography of the median signal amplitudes calculated as the square roots of power spectral density (PSD) across pain-related conditions and frequency bands. Each row of plots represents the topography from the same frequency band, and each column of plots represents the same experimental condition. The topography with blue backgrounds involves significant similarity to at least one in the same frequency band (* $p < .05$), while the others are significantly different.	94
4.5	Prediction accuracy of each pairwise classification versus the feature number. Each line represents the effects of feature numbers to the prediction accuracy within one pairwise binary classification, in which the tested feature numbers were discrete with a step of 10 between 10 and 100.	95
4.6	The effects of feature type, trial length and the number of features to the time cost in feature extraction and classification. The unit of time is the logarithm second [$\ln(T)$], the box plots show the total running time for extracting features with specific number (i.e. 20, 40, 60, 80, and 100) and type and then predicting the class of each sample with the extracted features. In the boxplot, the central line represents the median value of the time cost's logarithms, and the outlines show the boundary of the 95th percentile, while the markers represent the time costs beyond the confidence interval.	97

4.7	Time cost versus the number of features, the feature types were categorized with phase and power: The bar-plots show the distribution of time cost in seconds with studied feature numbers. The findings of time cost revealed the absence of significant differences between phase-based and power-based features, thus the time is categorized according to the features' origin, i.e., phase or power. The dots represent the outliers outside 1.5 times the inter-quartile range above the third quartile.	98
4.8	Features showing the characteristics selected from each type of neural marker of integration: After selecting 40 features with NCA from each type of feature, the ones shared by at least two binary classifiers containing every individual condition were selected to represent the characteristics, the rows represent the conditions, while the column is for the feature type. In the last two columns showing the selected features from coupling features, the color of each square represents the frequency band involved in the CFC at the corresponding channel (red- delta, green- theta, blue- alpha, yellow- low beta).	105

4.9	Selected features from alpha-phase connectivity features of each condition versus the other conditions. Except for the diagonal from top-left to right-bottom, the row represents each targeting conditions, the column represents the other condition in the corresponding binary classifiers, in which the features are shared by at least two classifiers containing the targeting condition, such features were marked with blue lines in the figure. And the ones on the diagonal show the significant features of every condition, which were shared by all classifiers containing the corresponding condition, which are marked in red.	106
5.1	Two types of decision trees in pain prediction: (a) classifying if the thermal stimulus was induced before distinguishing the intensity of the thermal stimulus, (b) targeting at recognising the pain, then classifying the non-pain conditions, respectively.	117
5.2	The map of EEG channels used for feature extraction this this chapter. The highlighted channels with labels were used for generating features in this chapter and Chapter 6.	118
5.3	An example of the re-organised ISPC feature matrix. Each sample of an ISPC matrix was a 32×32 square matrix, in which the columns and rows represented the EEG channels, and the orders of channels were consistent.	119

5.4	An example of the cumulative evidence involving 5 trials. (The values are only examples instead of real predictions) The red trial represents the target to be predicted. Two classes are represented by labels 0 and 1, x is the prediction score of class 0 and y is the prediction score of class 1. The prediction labels are shown at top right from two strategies. The original prediction is only produced with the target trial itself.	127
5.5	The pipeline of selective transfer learning. The testing set of both models on the figure is all the data of the excluded subject. The subject recognition model predicted the subject most similar to the excluded subject. The pain prediction model then predicted the pain-related labels, where the subject-wise pain prediction model was trained with the data from the excluded subject (i.e., Pain Classifier k).	128
5.6	The curves of mean accuracy versus the time duration of classification between conditions O and H with cumulative evidence. The curves represent the mean accuracy across excluded subjects from the two paradigms based on cumulative evidence, and the original curves represent the accuracy produced by only the target trial in the corresponding test.	135

5.7 **The clustering result of all subjects based on the alpha-phase functional connectivity.** The column represents the true subject s , and the row represents the clustered group's number c . The value on each cell represents the ratio of samples clustered into group c belonging to the subject s 137

5.8 **The proportion of subject ID predicted with the data from the subject whose pain labels were predicted.** The rows represent the subjects to be tested, whose pain-related labels were predicted. The columns represent the predicted subject IDs produced by the subject recognition model, the ones with the highest ratio were selected as the most similar subjects to the ones in the rows. The models were then trained with each *most similar subject* to predict pain in the respective subject in the rows. 139

5.9 The absolute values of arithmetic differences among the activated patterns out of layer 7 in Table 5.1 between each pair of conditions. These differences can show the cogent regions reflecting the connectivity capable of significantly classifying the corresponding conditions: Hot [H], Warm [W], Eyes-open [O], and Eyes-closed [C]. 141

6.1	Architecture of transfer learning frameworks. Two transfer learning frameworks processed the input of ISPC matrices. Both frameworks aimed to minimise the loss in training the pain prediction model. (a) The upper is the adversarial learning framework. An encoder was shared by two classifiers, and two networks were trained at the same time. (b) The lower one is the partial fine-tuning framework. This framework trained encoder 1 to recognise subjects ahead. Then encoder 2 was added to frozen encoder 1 and trained toward pain prediction.	163
6.2	The accuracy of subject-wise pain prediction models trained and tested with each pairwise subjects. (Classification between O and H) Each row represents a subject x involved in training a subject-wise model, and each column represents the subject y whose pain-related labels were predicted with the model trained with x , the accuracy of pain prediction is shown as the value in (x, y) . In particular, the values on the diagonal should be ignored.	168
6.3	Mean loss curves of training different frameworks across 36 LOO tests respectively. The curves were made with the classification between O and H.	169
6.4	The effects of time length involved in cumulative evidence. The bold curves represent the mean curves of cumulative evidence's effects on accuracy across the all the LOO tests, and the grey curve represents the accuracy curve of cumulative evidence from each LOO test.	170

6.5 The mean KL divergence between the distributions of ISPC values between the same channel of pairwise subjects. Since KL divergence is not symmetrical, P and Q represent subjects' IDs, where the KL divergence was computed with $D_{KL} = \sum P(x)\log(P(x)/Q(x))$. Each KL divergence was computed as the mean values of the KL-divergences acquired from the same channel from subjects P and Q respectively. The values of KL divergence represent the directed similarity from P to Q. 173

6.6 The scatter plot of KL divergence versus the subject-wise accuracy, with a fitted linear regression line $y_{acc} = -0.0478x_{KL} + 0.6341$; $R^2 = 0.0992$, $ *p < .001$.** 174

6.7 Grad-CAM feature maps produced in the model recognising subjects. The map was generated based on the subject recognition model in Chapter 5, which was the basis of the subject recognition models in adversarial learning and partial fine-tuning frameworks. 176

6.8 The Grad-CAM feature maps of the models predicting pain. The activation patterns were produced from the last hidden convolutional layer in each architecture, the strength of each region represents the contributions in pain prediction. 177

List of Tables

2.1	Properties of primary afferent fibres [6, 7].	24
2.2	Typical Power-based Measures of Neural Integration. The power-based measures utilise the time-frequency information from signals, which both involve the power- and phase-based properties. In the meanwhile, phase-based measures quantify the synchronisation between signal series by using the phases extracted with the Hilbert transform [8, 9]	56
2.3	Typical Phase-based Measures of Neural Integration. The phase-based measures quantify the synchronisation between signal series by using the phases extracted with the Hilbert transform [8, 9]	57
4.1	Comparisons of sensitivity and accuracy affected by different settings using 100 features in each test. The prediction sensitivity and accuracy of each setting of trial lengths and feature types were shown in the form of mean sensitivity/accuracy(\pm standard deviation (%)).	86

4.2 Summary of post-hoc comparisons to the accuracy for the trial lengths and feature types. Asterisks represent statistical two-tailed significance out of Holm-Bonferroni method were produced (* < 0.05, ** < 0.01, *** < 0.001). In the columns, A and B represent the values of the same property to be compared in the post-hoc analysis, where the accuracy produced with the properties of A or B were compared statistically. For example, the first column shows the differences of the accuracy produced by the trials with lengths of 10 and 5 seconds. 87

4.3 Summary of comparisons between power and phase z-score topography as represented with Pearson correlations (r-value, p-value). Asterisks represent statistical two-tailed significance (Significance level $\alpha = 0.05$, **p<0.01, *p<0.05). 89

4.4 Summary of pairwise comparisons across power magnitude's z-score topography as represented with Pearson correlations (r-value, p-value). Asterisks represent statistical two-tailed significance (Significance level $\alpha = 0.05$, ***p<0.001). 90

4.5 Summary of pairwise comparisons across exponential phase's z-score topography as represented with Pearson correlations (r-value, p-value). Asterisks represent statistical two-tailed significance (Significance level $\alpha = 0.05$, *p<0.05). 90

5.1	Architecture of the CNN model: Three basic structures (layers 1-9) were applied, in which the activation function of each convolutional hidden layer was a rectified linear unit (ReLU) function. The 2D sizes in brackets involved in 'Size/Parameter' represent the kernel size of the corresponding layer, and the parameter multiplied with the kernel size in each hidden layer is the number of filters.	120
5.2	The encoder's architecture for feature extraction	122
5.3	The architecture for the classifying pain and non-pain conditions	123
5.4	The architecture for recognising individuals (Number of subjects: N)	124
5.5	Performance of binary classification with CNN and SVM models: (1) 'All': the models were trained with the data from all subjects. (2) 'LOO': Each training excluded a subject, here shows the accuracy of predicting the pain-related labels of the excluded subject's data.	130

5.6 **Accuracy produced in different testing modes in the classification between conditions O and H.** Three columns represent three different testing modes in the study without pooling layers. (1) Within-subject (WS): the models were trained and tested with the data from the same subject. (2) Leave-one-out (LOO): in each test, the model training excluded the subject in the corresponding row. (3) Mean accuracy of cumulative evidence (Mean CE): The accuracy was from the results applied with cumulative evidence, where the mean values across all the studied time length represented the average level produced by cumulative evidence. The bold value in each row represented the larger value between the accuracy from LOO and Mean CE. 132

5.7 **Accuracy produced by the individual recognition and pain assessment models under different validation modes.** For the tests about generalisation, including the leave-one-out (LOO) and selective transfer learning (STL) tests, it showed the original accuracy without cumulative evidence, and the maximum accuracy produced by mean and voting mechanisms of cumulative evidence. 136

6.1 **The subject-based mean accuracy out of cumulative evidence.** This table shows the mean accuracy produced with the cumulative evidence in each subject. Conditions of warm (H), warm (W), and eyes open (O) were involved in the analysis. Under each classification, the first three columns represent the accuracy of the basic CNN model (Basic), adversarial learning (Adversarial), and partial fine-tuning (Fine-tuning) frameworks. The bold values highlight the maximum accuracy produced among the three frameworks. The last column in each classification represents the maximum accuracy of the subject-wise pain prediction. 166

6.2 **Performances produced by different models without and with TCA.**
The bold values show the maximum mean accuracy in each row. 172

Chapter 1

Introduction

This chapter introduces the motivations and objectives of this research. The scientific questions and the engineering objectives are declared in this chapter. The structure of this thesis and related publications are listed at the end of this article.

1.1 Motivation and Background

1.1.1 Assessing Pain with Efficient and Portable

Electrophysiological Equipment

Nowadays, the pain has become a worldwide health burden. In both developed and developing countries, 20% – 40% adults are affected by chronic pain every year [10, 11]. Although the duration of acute pain is shorter than chronic pain, it is more common as a symptom that appears along with many diseases [12]. More seriously, neuroplasticity can cause the transition from acute pain to chronic pain [13]. Especially during

and after the pandemic of Coronavirus Disease 2019 (COVID-19), such a transition has caused a serious global health crisis [14]. Such a scenario raises the requirement for pain assessment. Therefore, it is possible to remind users or their caregivers of concurrent or potential health problems by monitoring pain-related status. Pain assessment in responsive individuals depends on self-report, for which they can report pain directly or express it through behaviour such as facial expressions [15]. However, such a subjective report must be put on a quantitative scale for clinical use. For this purpose, some numeric scale-based tools were designed to *measure* pain in the clinical environment, such as the McGill Pain Questionnaire [16, 17] and the Visual Analogue Scale (VAS) [18]. These numeric scales help clinicians assess the quality and intensity of subjective pain, especially showing the relative change in pain in a specific individual, but they cannot quantify or assess the physiologically objective state of pain related to it. Fortunately, with the rapid development of electrophysiology, I can acquire physiological signals as the source of biomarkers correlated with pain, making objective pain assessment feasible.

The lack of objective approaches from physiological properties is not the only concern in pain assessment, a more crucial challenge is thrown by unresponsive patients. Unlike responsive individuals, non-responsive patients (e.g., those with a disorder of consciousness or locked-in syndrome) cannot report pain by behaviour voluntarily. This specificity blocks their caretakers from perceiving pain in unresponsive patients, so biosensors that record electrophysiological signals can benefit the pain assessment in unresponsive patients as a key.

In the development of approaches for assessing pain from electrophysiological sig-

nals, the diversity of biosensors and the corresponding equipment created considerable solutions. Based on the physiological indicators that can be recorded with mature technology, including heart rate, pulse, and blood pressure, some methods have been implemented to assess pain [19, 20, 21]. However, these ways can be only applied to responsive individuals since they rely on self-report as the basis for model training, and their precision is also limited [22]. Benefitting from neurophysiological signal recording technology, researchers investigated biomarkers extracted from neural signals that correlate with pain. Some machine learning models have been successfully validated with signals recorded by functional magnetic resonance imaging (fMRI) or positron emission tomography (PET), which are potentially tools for pain prediction [23]. However, the clinicians or caregivers of unresponsive patients are supposed to perceive the pain of the patients at the bedside, where the fMRI and PET equipment cannot be applied. Thus, electroencephalography (EEG) is an ideal choice to record neural signals at the bedside as a portable and noninvasive tool.

Hence, we can use EEG with its convenience for both the daily health monitoring requirements of responsive individuals and the more serious needs of unresponsive patients. Although such research is still based on laboratory data, it can produce system stereotypes to assist clinical practice as translational research [24].

1.1.2 Electrophysiological Representation of Complex Pain

Processing

Aiming to assess pain with electrophysiological recording equipment, especially EEG, the fundamental is the neural biomarkers correlated to the neurophysiological mechanism of the brain's responses to pain, which can be measured from the electrophysiological recording. Many researchers have made efforts to disclose neural markers that contribute to pain processing.

As an *unpleasant sensory and emotional experience* by definition [25], both psychological and social pain should be involved in the analysis of the brain regions and rhythms associated with pain processing [26, 27, 28, 29]. From the research in [27] and [28], various regions of the brain were suggested to contribute to pain processing, including the somatosensory, insular, anterior cingulate, prefrontal cortices, and thalamus, etc. From the perspective of neuronal oscillations, that is, frequency bands, the delta, theta, and beta bands are associated with brain's responses to pain, while the alpha and gamma bands reflect pain sensitivity, the level at which an individual perceives and reacts to painful stimuli [29, 30]. These studies suggested one main focal point this thesis must consider: the complexity of the neural mechanism processing pain. Consequently, the electrophysiological measurement of pain should indicate such complexity in at least some aspects in the regions and frequency bands of brain signals.

In the line of studies focusing on the electrophysiological representation of pain, some studies focused on the contributions of specific components, while others discussed integ-

ration involving diverse regions or bands. These ideas shaped two paradigms to develop a biomarker for pain. The first paradigm only uses the signals within an independent source, such as a neuronal oscillation or a brain region. Whereas the second involves the integration of neuronal oscillations or brain regions.

One paradigm is based on the theoretical basis for developing measures for pain assessment. Typically, the alpha and gamma bands were concentrated among neuronal oscillations to find the correlation between pain perception and electrophysiological signals. Regarding the brain regions, the parietal, prefrontal, and occipital lobes are usually crucial in electrophysiological research. For example, the peak alpha frequency is correlated with pain sensitivity [31, 32], and the prefrontal gamma band can be an indicator of pain intensity [33].

The other paradigm prioritises the integration of different components from different signal sources of the neural recordings, where the signals' frequencies of the oscillations and locations of electrodes to be analysed can be neuronal oscillations or brain regions. This paradigm does not limit itself with independent brain regions or neuronal oscillations but synthesises the signals from different regions or frequency bands, with the aim of quantifying the complexity of neural activities in pain processing. A typical measure is cross-frequency coupling. In deep brain structures, Liu et al. found that pain-related gamma responses are coupled with theta and alpha bands [34]. Another integration is functional connectivity, Ploner et al. disclosed that prestimulus functional connectivity is a determinant element in perception of pain [35]. However, how to use such integrations to assess pain as neural biomarkers is still under discovery.

These two approaches inspired me to do research on the integration across different brain regions or neuronal oscillations. Taking into account the diversity of integrations, e.g. phase-power cross-frequency coupling, I used the control variable method toward the frequency bands or the brain regions. In this research, I attempted to quantify functional connectivity across brain regions within the same frequency band from EEG, or cross-frequency coupling at the same scalp site. Therefore, complexity can be quantified in an inherent form, which can expose the intrinsic characteristics correlated to pain processing from EEG signals. Considering the usability at the bedside as expressed in Section 1.1.1, this work also addressed the basic properties of the neural markers of integration that may affect the prediction performances, such as the length of trials for computing the measures.

1.1.3 Development of Machine Learning

Just like many other challenges in translational research, pain assessment from neurophysiological signals has benefited from the rapid development of machine learning [36, 37]. In such a context, the research on neural markers of pain has gone beyond the box of physiological analysis. Especially, as a subjective experience, it can be studied in a *more objective* way with machine learning, which could at least distinguish the occurrence of nociception from the nonpainful states [38]. Since 2012, the pain decoding study from EEG has attracted many efforts [37, 39]. By applying machine learning methods, multiple purposes have been demonstrated in practical assessment of pain, including the classification of pain phenotypes [40], distinguishing pain from resting states, and

even predicting the intensity of pain in a relatively objective way according to the intensity of the stimulus [41, 42]. Although sometimes the machine learning methodology is doubted as a *grey box* or even a *black box*, many researchers studying pain with machine learning highlighted the interpretability of models. In the aspect of neuronal oscillations, many works analysed the contributions of different frequency bands by controlling their participation in feature generation [41, 43, 44]. Moreover, machine learning can also reveal the cortical characterisation [45, 40]. Consequently, by extracting the neural markers of integration declared in Section 2.3.3, they were input into machine learning models to test their performances. Furthermore, one of the main objectives of this research is to develop machine learning models to assess pain. Like the trial length studied as a basic property for the potential application at the bedside to the patients, this thesis involved the settings related to machine learning as well, especially the number of features used in model training.

However, a significant obstacle still blocks the development of most EEG-based machine learning models, the individual differences of neural responses [46]. In particular, in pain research, pain sensitivity has a strong individual variation among different human individuals [31]. In the machine learning models developed for pain assessment, most were only evaluated in within-subject tests; generalisability was seldom discussed. In a recent systematic review of machine learning models for pain assessment with EEG, fewer than ten studies reported cross-subject performance out of 44 studies reviewed [37]. This is not surprising at all due to individual variation, but it is very concerning for the need for unresponsive patients who cannot provide labelled data to train the mod-

els. Therefore, our aim is to develop models to be transferred to individuals with only unlabelled data.

One of the key solutions is to adopt transfer learning in order to mitigate the interference associated with individual differences. Transfer learning is the technique to transfer a trained model to a new task, where the *task* can be a new problem or a new domain [47]. Almost during the same decade when machine learning approaches for pain assessment were studied in its early era, transfer learning went through explosive growth, benefiting from the development of deep learning [48]. The question of improving the generalisability of pain assessment models can be simplified into a typical domain transfer learning objective. Correspondingly, the data from each subject can be treated as one domain, where the prediction model learnt from the labelled domains can be generalised to the unlabelled domain. Therefore, this research set its main objective to develop the transfer learning model with deep learning to predict pain from unlabelled individuals. For interpretability, the features extracted by such transfer learning models should be analysed, whose correlations with individual specificity and pain would be discovered and compared with physiological findings.

1.2 Research Questions

1.2.1 Neural Marker: Feature in Machine Learning

Q1-1 Can neural integration be measured in a concise way that can reflect the intrinsic mechanism of pain processing?

Q1-2 How can neural markers of different neural integration (e.g., functional connectivity and cross-frequency coupling) be mathematically comparable?

Q1-3 Which components of neural integration are important in pain assessment?

Q1-4 With neural markers producing good accuracy and efficiency, how can we use them in a suitable setting for pain prediction? In particular, how many features can be sufficiently specific to the characteristics related to pain? How long should the cropped data trials be?

1.2.2 Machine Learning Model

Q2-1 What deep learning models can distinguish pain from non-pain conditions accurately using the ideal neural marker?

Q2-2 Can training the model with data from multiple participants improve the model's sensitivity to pain across subjects? How about applying it to the novel participants not involved in the training phase?

Q2-3 Do the ideal features of pain assessment carry patterns indicating individual specificity?

Q2-4 Is it practical to use only the neural marker of pain processing to develop a transfer learning model applied to participants without labelled data?

Q2-5 Are the feature patterns extracted by the deep learning models consistent with the physiological principles?

1.3 Contributions of the Thesis

- **The strong specificity of the phase from the alpha band was disclosed.** This study involved the novel analysis of topographical patterns of phase and power from different low-frequency bands, which presented significant differences across the phase patterns in different conditions, which did not appear in the power patterns. While using power-based and phase-based features to train support vector machine (SVM) models to predict pain, phase-based features also drove higher accuracy.
- **This research revealed an efficient way to use phase-based functional connectivity of the alpha band in pain prediction with machine learning.** Two typical integration neural biomarkers attended the comparison in comparable forms, including functional connectivity from the alpha band and cross-frequency coupling (CFC) in four bands. Based on the finding of the advantage of phase-based measures, within both phase-based measures, functional connectivity requires less time in feature extraction than CFC. Hence, phase-based functional connectivity from the alpha band is an ideal neural marker to predict pain. Otherwise, the important functional connectivity that strongly represents pain specificity is revealed by neighbourhood component analysis (NCA), which can help reduce the dependency on abundant electrodes.
- **Within the data from the same subjects for both training and testing, a convolutional neural network (CNN) model predicts pain or not very accurately.**

Naturally, the functional connectivity measure can be organised as square matrices, whose rows and columns represent the electrodes in EEG research. With functional connectivity as input features, a CNN model with three hidden layers produced a good performance in the classification among painful, innocuous thermal conditions and resting states. For interpreting the performance, the activation patterns generated by the CNN architectures match the functional connectivity specific to pain revealed in qualified research.

- **By using a CNN model with the functional connectivity of the alpha phase as input features, individual identification can be accurately recognised.** Inspired by the physiological study that proposes the specificity of the functional connectivity from the alpha band to pain, another CNN model is trained to recognise pain with features of the functional connectivity. This model shows very high sensitivity to individual identification of subjects, which suggests the CNN model's potential to detect individual specificity while predicting pain. Furthermore, it also reveals the possibility of utilising the functional connectivity from the alpha band in identification recognition for other purposes.
- **Two transfer learning (TL) frameworks utilise the performances of CNN with alpha-phase functional connectivity.** Toward the limitation of data size and the need for generalisation, a fine-tuning and adversarial learning framework uses the sensitivity of functional connectivity in the alpha band to both pain-related states and individual differences. Although they did not significantly improve gen-

eralisability, their convolutional hidden-layer activation patterns provide good interpretability. More importantly, the good performances of some subject-wise TL models trained with only one subject for predicting pain from another novel subject suggest another solution for generalisation, which raises the need for further work to quantify the similarity among subjects from EEG.

1.4 Thesis Outline

This thesis is organised as follows. Chapter 1 provides an overview of the motivation and research objectives in this research. This chapter covers the fundamental background of related fields, and the main inspirations published before and during this research were mentioned in both physiological findings and technical development. This work summarises the objectives of each part of this research and the corresponding contributions.

Chapter 2 is a systematic review of the literature on the scientific and technical background related to this research. As interdisciplinary research on pain, starts with the basic conceptions, classifications of pain, and the global health crisis related to pain is introduced. Naturally, the anatomy and physiology of pain are reviewed, which focusses on how the nociceptive system works. Following scientific principles, I present different strategies and measures for pain assessment. In requests for pain assessment, the strategies that rely on straightforward feedback and mature technology that uses electrophysiological signals occupy most of the review. The third and fourth sections concentrate on the technical background. Given that this research aims to assess pain with EEG,

I express the principles of EEG recording and the methodology of EEG signal processing. Beyond EEG, the other important technical tools in this research involve machine learning and TL. Therefore, this thesis reviews the methodologies of machine learning and TL which have been proven to be applicable for pain assessment.

Chapter 3 introduces the experimental design for collecting the EEG data used in this research. The mechanism and methods to induce tonic pain in the experimental environment are described. In detail, the basic information about the participants, the technical settings, and the experimental procedure are listed. After the description of the experiment, how the data was pre-processed is illustrated.

I present the novel research from Chapters 4 to 6. The structure can be split into three stages: Chapter 4 for feature discovery, Chapters 5 and 6 about model development and the corresponding interpretability.

Chapter 4 discovers neural biomarkers of integration for pain assessment. Two typical neural integrations, functional connectivity and CFC, participated in the analysis, which were measured in comparable forms. This chapter describes how the neural biomarkers attended the SVM classifier, and presents the accuracy produced by these neural markers quantified as phase- or power-based features. Based on the ideal neural marker for pain prediction, phase-based functional connectivity from the alpha band, I tested the effects of trial lengths and the number of features. Furthermore, feature selection algorithms provide interpretability to the neural marker.

Chapters 5 and 6 indicate attempts to develop deep learning models using the ideal neural marker declared in Chapter 4, phase-based functional connectivity from the alpha

band.

Chapter 5 proposes a novel CNN architecture for pain assessment. Based on this CNN model, this chapter presents the results of within-subject pain assessment. For interpretability, Gradient-weighted Class Activation Mapping (Grad-CAM) provides primary evidence of the functional connectivity's patterns specific to pain brain responses to pain.

Toward the challenge of improving generalisability for participants who do not have labelled data, Chapter 6 describes the frameworks designed for transfer learning. This chapter first explores the specificity of functional connectivity to individual variation. Synthesising the CNN models and feature's specificity, it compares the proposed CNN model's cross-subject performances, and tests two transfer learning frameworks. Beyond these, this chapter poses potential strategies to measure the similarity between subjects for subject-wise model training. Grad-CAM also plays a role in the interpretation of the results of these evaluations and suggests future improvement.

Chapter 7 is the end of this thesis, which demonstrates the main conclusions and achievements in this thesis. It discusses the potential approach to utilise this work in future research as well.

1.5 List of Publication

1.5.1 Journal Publication and Manuscript

[1] Han, Y., Ziebell, P., Riccio, A., & Halder, S. (2022). Two sides of the same coin: adaptation of BCIs to internal states with user-centered design and electrophysiological

features. *Brain-Computer Interfaces*, 9:2, 102-114. (Chapters 2 and 4)

[2] **Han, Y.**, Valentini, E., & Halder, S. (2024). Accurate and Efficient Prediction of Pain: A Comparative Study of Functional Connectivity and Cross-Frequency Coupling from Electroencephalogram. *Human Brain Mapping*, Under review. (Chapter 4)

1.5.2 Conference Publication

[1] **Han, Y.**, Valentini, E., & Halder, S. (2022). Classification of Tonic Pain Experience based on Phase Connectivity in the Alpha Frequency Band of the Electroencephalogram using Convolutional Neural Networks, *44th Annual International Conference of the IEEE Engineering in Medicine and Biology Society*, Glasgow, Scotland, UK. (Chapter 5)

[2] **Han, Y.**, Valentini, E., & Halder, S. (2023). Validation of Cross-Individual Pain Assessment with Individual Recognition Model from Electroencephalogram, *45th Annual International Conference of the IEEE Engineering in Medicine and Biology Society*, Sydney, Australia. (Chapter 5)

1.5.3 Conference Abstract

[1] **Han, Y.**, Valentini, E., & Halder, S. (2021). Prediction of Tonic Pain Using Support Vector Machines with Phase-based Connectivity Features, *The 8th International BCI Meeting*, Online. (Chapter 4)

[2] **Han, Y.**, Valentini, E., & Halder, S. (2023). Offline Prediction of Prolonged Acute Pain by Means of Convolutional Neural Network Model Applied to Electroencephalographic

Oscillatory Connectivity, *The 10th International BCI Meeting*, Brussel, Belgium. (Chapter 6)

Chapter 2

Literature Review

This chapter is a systematic review of the background related to pain assessment. The rationale follows the components that we should consider when developing the approach to pain assessment, which involves the social impact caused by pain, the anatomy and physiology of pain, the general methods of pain assessment, and the techniques used in this research.

2.1 What is Pain?

2.1.1 Pain as a Global Health Crisis

Pain has become a global social health burden, which became even more serious during and after COVID-19 [14]. It is not surprising, given the diversity of its origins. According to some surveys, at least 10%, more generally 20% of the adult population around the world experience chronic pain, which can reach 25% in some regions, for example, it

can even reach 34.5% among Americans [49, 50, 51]. As tonic pain is the result of injury, it can have more casual and more profound effects on people [50].

Unfortunately, such a wide distribution and strong effects did not generate sufficient interest in medical education. For example, only 3% of the medical schools in the United States have a specific curriculum on pain. The time devoted to it is also quite limited; the typical time on this topic is less than 10 hours in the United States, around 12 hours in the United Kingdom [52, 53]. Such a scenario makes the concern about inadequate acute pain treatment last for years and is still under resolution.

Moreover, the abuse of opioids has attracted a great deal of societal interest in pain treatment [54]. A survey exposed most 77% of opioid-related overuse, and, more seriously, it has become the leading reason for death from drug overdose, for example, in the United States, 66.4% of drug-related death in 2016 involved opioids [55, 56]. Beyond death, such abuse has induced a serious increase in health and economic costs relevant to opioid use disorder (OUD) [57]. Although the assessment of pain cannot directly lead to the optimisation of pain treatment, it can help improve the efficacy of the diagnostic and treatment evaluation processes [58]. Moreover, it can play the role in guiding the neuromodulation of pain [59]. Simply, the neuromodulation strategies, such as deep brain stimulation and spinal cord stimulation, can respond to pain more efficiently if pain is assessed. Thus, optimising the development of alternative treatment for pain can help reduce the reliance on opioids.

2.1.2 Types of Pain

Classification by Pathophysiological Mechanism

By definition, pain is *an unpleasant sensory and emotional experience associated with, or resembling that associated with actual or potential damage*, as defined by the International Association for the Study of Pain (IASP) [25]. Therefore, naturally, the sources of pain are diverse and can involve biological, psychological, and social factors. Due to the diversity, the types of pain also varied.

According to pathophysiological mechanisms, pain can be classified into four types: nociceptive, inflammatory, neuropathic, and functional pain, which can also be simply classified as receptor pain and non-receptor pain [60, 61]. As typical receptor pain, nociceptive pain is elicited by the responses of nociceptors, which are the specialised sensory receptors to actual or potential damage [25, 62]. In particular, the types of noxious stimuli are various, including extremes of temperature and mechanical and chemical insults [63]. Therefore, the nociceptors respond to each particular stimulus. In a sense, inflammatory pain is a special type of nociceptive pain caused by the activation of nociceptors toward inflammatory mediators [64, 65]. Unlike receptor pain, inflammatory and neuropathic pain is not induced by specific receptors [60, 61]. Neuropathic is defined as *pain that arises as a direct consequence of a lesion or disease that affects the somatosensory system* [66]. Specifically, it is mainly induced by diseases or injuries that could damage the central or peripheral nervous system, such as post-herpetic neuralgia (PHN), painful diabetic neuropathy (PDN), and human immunodeficiency virus (HIV)

[12]. Functional pain syndrome (FPS), or dysfunctional pain, is special compared to the aforementioned, stating pain and related symptoms and disability without clear etiology [67]. In addition to these physical pains, social pain is also worth studying. Although the term pain mostly tends to be physiological, as described in its definition, social pain or emotional pain, i.e., painful feelings from negative social conditions, induces warning signals to potential damage as well [68]. However, the controversy between psychological and physiological pain mechanisms has received much research over the past decades [69, 70].

Acute Versus Chronic Pain

According to its temporal characteristics, pain is also classified as acute and chronic pain [71]. In general, surgery, trauma, or acute illness induce acute pain, which is the physiological response to an adverse stimulus [72]. On the other hand, chronic pain is defined as *persistent or recurrent pain that lasts more than three months, leading to the decline of functional ability and emotional distress* [73]. The main causes of chronic pain involve damage to the peripheral or central nervous systems and failure of the pain suppression system [1, 74]. Although literally the dichotomy between acute and chronic pain originated from its duration after the onset, this classification was challenged by clinical trials. For example, some acute pain related to new tissue damage can last more than 6 months in some cases [75].

Ignoring the controversy associated with the duration, the classification between acute and chronic pain is tenable considering the transition between them. At the onset,

acute pain arises from the extensive, persistent, nociceptive, and behavioural cascade induced by tissue damage [76]. Despite the short duration of most acute pain, some of them can progress to chronic pain [72]. In general, neuroplasticity occurs with the onset of persistent acute pain, in which glial cells, as pain-transmitting neurones, become more sensitive and react more sensitively to nociceptive stimuli [77]. This neuroplasticity causes peripheral and central sensitisation related to the changes of activity-dependent phenotype in the dorsal horn neurones and other structures of the central neural system (CNS). With peripheral, central, or even nociceptive sensitisation, acute pain tends to turn into chronic pain. From the perspective of the pathway (see Section 2.1.3), chronicification of pain can also be explained as activity-induced plasticity of the limbic-cortical circuitry, which causes neocortex reorganisation [78]. Furthermore, although researchers have not fully understood the neural mechanisms of acute and chronic pain, the first-in-human study of chronic pain prediction suggested significant differences in their biomarkers using machine learning [79]. Therefore, acute and chronic pain can be distinguished from both chemical and electrophysiological activities in neural processing. In this study, the main objective is experimental tonic pain, which is a kind of acute pain induced in laboratories.

Unlike acute pain, it is still challenging to study chronic pain in the laboratory; even clinical neurophysiological studies that focus on it were just recently launched and benefit from the frontier intracranial devices [79]. In most of the work to discover neural biomarkers of pain, researchers used the data recorded in experiments with inducing acute pain. As a study of experimental tonic pain, this Ph.D. thesis covers only research

on acute pain induced in laboratories. However, it can be fundamental to detect chronic pain and the transition between acute and chronic pain in the future.

2.1.3 Neuroanatomy and Neurophysiology of Pain

As a subjective experience that warns of potential tissue damage or actual tissue damage, the anatomy and physiology of pain are concentrated on the nervous system [1, 25]. Therefore, the discussions about the physiological mechanism of pain and the relative anatomy start from three perspectives: how the *pain receptors* perceive pain, how the signals of pain are transmitted from the receptor to the central neural system (CNS), and the mechanism of the CNS to process pain. Following the neural pathway along these aspects, the neural system processing pain mainly consists of four steps, including transduction, transmission, modulation and perception, Figure 2.1 presents the basic neural structures working in pain processing [1]. The *pathway* covers the parts of the transduction and transmission from the nociceptor to the CNS, as long as the pathways and CNS are integrating in the modulation of pain and finally control pain.

Nociceptor

Nociceptors are sensory receptors perceiving the stimuli which potentially damage the organism, which is seen as superficial pain receptors sending the 'neural messages' about the acute pain [80, 81]. The soma of nociceptors is located mainly in the dorsal root ganglia (DRG) or trigeminal ganglia (TG), whose axons extend to the terminals to innervation targets, which can be found in the skin, joints, deep tissues and cornea [82].

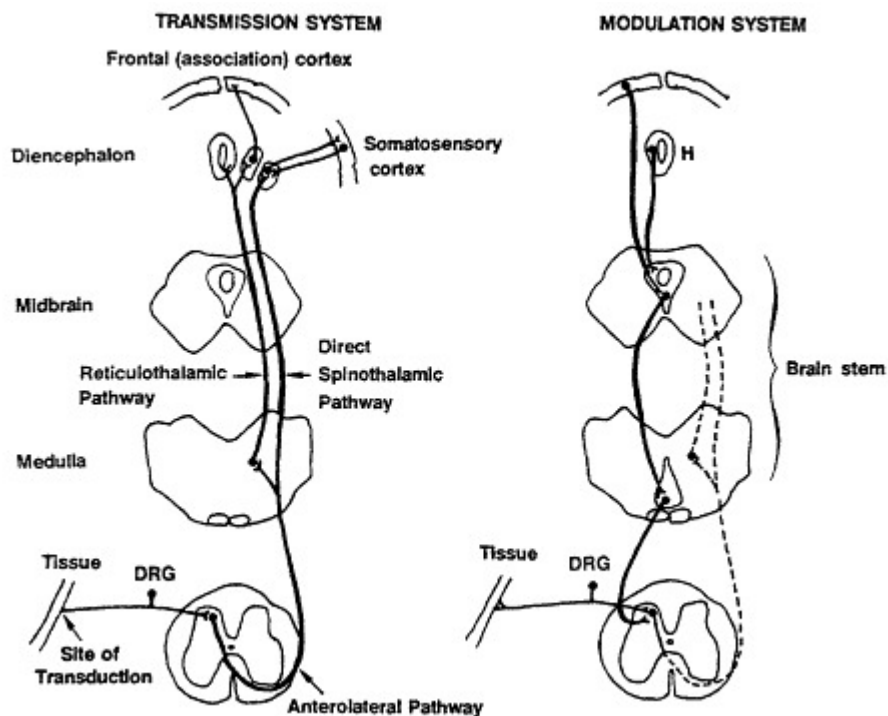


Figure 2.1: The diagram outlines neural structures in pain processing [1]. It shows that pain perception starts from the transmission system with transduction (lower left), where a stimulus creates nerve impulses conducted to the spinal cord and then relayed via diverse pathways toward the cerebral cortex. The pain-modulation inputs from different regions (i.e., the frontal association cortex and the hypothalamus) weaken the intensity of perceived pain. (DRG: dorsal root ganglion.)

They respond to mechanical (typically pressure), thermal, and chemical stimuli in the way of detecting signals from damaged tissue as described in the definition of acute pain in Section 2.1.2, or indirectly responding to chemicals released from damaged organism [1].

Conventionally, nociceptors are the nerve endings of two types of primary afferent

Table 2.1: **Properties of primary afferent fibres** [6, 7].

Fibre Type	A_{β}	A_{δ}	C
Diameter	5 – 12 μm	1 – 5 μm	< 1 μm
Myelination	Thickly	Thinly	None
Conduction Velocity	30 – 70m/s	3 – 30m/s	< 2m/s
Sensation on Stimulation	Light touch, nonnoxious	Rapid, sharp, localised pain	Slow, diffuse, dull pain

fibres, including myelinated A fibres (including A_{δ} and A_{β} fibres) and unmyelinated C fibres, which respectively process the primary and secondary acute pain responses according to the neural transmission speed (see Section 2.1.3 about transmission) [6]. While A_{β} fibres are thickly myelinated and conduct neural signals at the fastest speed among the main nociceptors, A_{δ} fibres are thinly myelinated, and their conduction velocity is significantly faster than C fibres [83]. C fibres are the majority of nociceptors and are associated with nonmyelinating Schwann cells and form Remak bundles [84]. The aforementioned morphological and electrophysiological characteristics decide the end percept originating from the nociceptors linked to these fibres, A_{δ} fibre is associated with rapid and sharp pain and A_{β} is more sensitive to light touch and non-noxious stimuli, but the activation of the fibre C mainly results in enduring and persisting pain [85]. Correspondingly, the differences between the contributions of the fibre A and C can also reflect the differences between acute and chronic pain [86]. Table 2.1 summarises the main properties of the fibres.

Nociceptive Pathways

After the nociceptors transduce potentially harmful stimuli into action potentials, this signal travels through the axon of the primary afferent fibre from the peripheral nervous system to the central nervous system [1]. The nociceptive pathway is a type of complex sensory system, which involves not only the transmission of the protective response to noxious stimuli, but also integrates with cognitive, emotional, and behavioural elements [87].

Structurally, the A and C fibres carry the nociceptor signals and transmit them to the CNS and later higher centres of the CNS (*vide infra*) (see Figures 2.1) [7, 82]. Cell bodies of primary afferent fibres are found in the dorsal root ganglion (DRS) [82]. Cell bodies synapse into different kinds of cells, including cells in the spinal dorsal horn [82, 88], nociceptor-specific inhibitory and excitatory neurons in Rexed lamina I and II (substantia gelatinosa) [88], and projection neurons in the deep areas of the dorsal horn [89].

As shown in Figure 2.1, the ascending nociceptive pathway begins with the decussation of projection neurons from the dorsal horn, and it ascends in the lateral spinothalamic tract before ending in the ventral posterolateral nuclei of the thalamus [88]. Finally, the ascending nociceptive pathway affects the somatosensory cortex and the periaqueductal grey matter (PAG). In particular, the ascending pathway transmits the information of pain and touch to the brain regions associated with memory and affective components of pain, for example, the amygdala, hypothalamus, and PAG [90].

The descending pain modulatory system can control nociception in a bidirectional

way with the interaction of the ascending pathway [91]. Bidirectional control occurs through the activation of the midbrain and medullary sites. In the facilitation of descending pain, the PAG plays a role as analgesic after receiving nociceptor signals, and the rostroventromedial medulla (RVM) facilitates and executes the final relay [92].

Central Processing of Pain

Different from specific auditory or visual cortices, the cortical representation is distributed extensively underlying pain [93]. In decades of studies using functional brain imaging studies, including functional magnetic resonance imaging (fMRI), electroencephalography (EEG), and magnetoencephalography (MEG), researchers have revealed the contributions of various brain areas in pain processing. Classical research on the responses of the brain to pain concentrated in the primary and secondary somatosensory cortices (i.e., S1 and S2/parietal operculum), the insula and the ACC in humans and primates [94]. Some studies also reported some other cortical areas that receive and process neural signals from the nociceptive, for example, the cerebellum, amygdala, nucleus accumbens (NAcc), and other nuclei from the basal ganglia [95, 96, 97, 98, 99]. By synthesising these findings, the investigators declared the *neuromatrix*, and later derived it into the *pain matrix* in central pain processing, which involves the thalamus, anterior cingulate cortex (ACC), posterior cingulate cortex (PCC), insula, amygdala, primary and secondary somatosensory cortices (S1 and S2) and PAG [100, 101].

The participation of cognition in pain processing also contributes to distributed brain regions, which occurs in the bidirectional progress of pain sensation and modulation

[102, 103]. One typical example of the bidirectional effect is attention, although a continuous nociceptive stimulus will reduce attention to the main task, attention control can help manage pain effectively [104, 105, 106]. Another cognitive element that is influenced by pain is memory. Along with chronic pain, structural and biochemical changes occur in the hippocampus and amygdala, which adversely affect working memory, recall, and recognition memory [107, 108]. Beyond attention and memory, some evidence suggests the negative effects of pain on processing, executive function, decision making, psychomotor efficiency, and reaction time [103]. In summary, the cortical regions that process the corresponding cognitive activities present changes compared to the normal state in pain processing. Therefore, in pain studies, we must consider the participation of brain regions related to these cognitive elements, which may show great contributions in neural biomarkers of pain.

2.2 Pain Management and Assessment

2.2.1 Pain Management

Pain management has a long history, and the development of modern medicine has led to the evolution of acute and chronic pain treatment [109]. Treatment of acute pain became the focus of anesthesiologists in the 1980s [110, 111]. And earlier, as a notable work in pain research, gate control theory suggested a new potential solution that contributes to the management of chronic pain [112]. However, the development within decades both enlightened the hope of analgesia and disclosed some additional risks in

pain management.

In the medical relief of pain, the selection of pharmaceutical drugs is quite strict. The World Health Organization (WHO) suggests physicians and pharmacists to use a *pain ladder* in the management of medical pain, especially when managing chronic pain [113]. According to the ladder, if treatment does not work effectively, doctors should consider the next step of treatment. Toward different types of pain, the common initial drugs include paracetamol, non-steroidal anti-inflammatory drugs (NSAIDs), antacids, antidepressants, etc. When severe pain occurs in patients, opioids are recommended for use in many conditions [114].

Physical approaches are widely used in pain management, whose side effects are more controllable than some medical treatments, especially opioids [115]. Traditionally, physical treatment includes passive and active approaches [116]. Patients can receive passive treatment, such as heat or electrotherapy, or do exercises (e.g., Tai Chi and yoga) by themselves to relieve pain [116]. In the passive perspective, the development of technology also provided some new solutions, including transcutaneous electrical nerve stimulation (TENS) and transcranial direct current stimulation (tDCS), which stimulated specific locations with electrical impulses in non-invasive ways [116, 117]. Similarly, deep brain stimulation (DBS) is also being studied as a potential device for long-term and invasive pain management [118].

2.2.2 Toward Treatment and Management: Why We Need to Assess Pain

In many cases, although medical treatment such as analgesic interventions for a specific disease is independent of the assessment of pain, by noticing the symptoms reflected in pain and communicating with the patient more efficiently, physicians and caregivers can treat the ongoing patient's pain more precisely. The most significant difficulty in pain management is probably the subjectivity of pain assessment, which can create obstacles for clinicians to make a precise decision about treatment.

The intensity of stimuli that induce pain is objectively quantifiable under many conditions, such as the prickle force and the temperature of the water, thus we could match the sensation of pain according to the stimuli in laboratories [20, 33, 119]. However, the pain experience is subjective, which presents strong individual differences [31]. This individual variation could be the result of differences in past experience and future prediction about the stimulus [120]. To face such subjective differences, some doctors suggested trusting the descriptions of the patients in most cases according to their practise [121]. However, the standard quantification system is still necessary, as the original verbal description is sometimes unclear and insufficient to be matched under different conditions [122, 123].

Unfortunately, regular pain assessment approaches based on behaviour or verbal communication cannot work in some special environments. A common barrier in pain assessment comes from patients' disabilities, since approaches depend on communica-

tion, such approaches cannot work in noncommunicative individuals, for example those with intellectual or developmental disabilities [124]. Beyond disabilities, clinicians cannot also apply these communication-based assessment strategies in clinical settings. For example, in intensive care units (ICUs), patients with temporary loss of communication ability cannot report pain voluntarily [125]. Assessment approaches that do not rely on communication are essential to assess pain in such individuals. Therefore, the behaviour of patients is a type of reference for evaluating pain without communication, and observation measures of pain were designed for such purposes.

In the perspective of how to assess pain independently of communication, one other *extreme* condition focused on in this work is worth declaring. In this study, I considered an even more serious condition, the care of unresponsive patients. These typically have disorders of consciousness (DOCs), partially or completely losing their ability to interact with the surrounding environments [126]. Consequently, they cannot report pain through any behaviour, including verbal communication and motor, although they still have conscious experience, including the sensation of pain [127, 128].

Taking into account those who are unable to report pain temporarily or permanently, researchers developed approaches based on quantitative physiological measures to assess pain. Most of such methods rely on physiological signals, such as heart rate, blood pressure, and various electrophysiological signals such as EEG, EMG, etc. [129]. Benefiting from the development of artificial intelligence (AI), some researchers also proposed novel strategies using data with an indirect relationship with pain, for example, facial expressions [130]. The following sections will introduce the details of different

approaches to pain assessment. Generally, apart from particular strategies, most pain assessment approaches aim to quantify or recognise pain with relatively *objective* quantification of some factors. Furthermore, these measures can serve as the basis for building machine learning models for pain assessment (Section 2.4), where the behavioural and verbal measures can be labels and the physiological signals are the source of features in machine learning.

2.2.3 Behavioural and Verbal Assessment

Self-report Measure

Theoretically, self-report measures are consistent with pain's definition because they completely follow the subjectivity. Therefore, it is seen as the gold standard for pain assessment [131]. In clinical applications, it is also the most convenient approach to assess pain when patients can communicate. Some studies doubted its validity in chronic pain and its intrinsic correlation with physical disabilities, and its standardisation is not seriously tenable in individuals and time [132]. However, the good performance of the self-report measure in assessing acute pain and efficiency makes it still a popular tool in clinical diagnosis, which can access direct expressions related to pain [133]. In general, self-report measures include rating scales and questionnaires.

Two common rating scales in pain assessment are the visual analogue scale (VAS) and the numeric rating scale (NRS) [18], Figure 2.2 presents these scales. The VAS is a 10-cm line with anchors at each end, which represents *no pain* and *worst imaginable pain*.

The patient is requested to draw a 100mm line horizontally or vertically, and then the pain score is measured on a millimetre scale, i.e., there are 101 levels of pain intensity in the VAS [134, 135]. It is apparent that VAS is reliable in different environments and patients due to fixed length, but it also makes it not feasible enough, for example, the length may change in the paper copy or the electronic display [2], and the direction of VAS also affects its validity considering the reading habits of users [136, 137]. Designed with a similar paradigm, the NRS does not have such limitations. NRS does not rely on visual scale bars, which could involve 11, 21 or 101 levels of intensity of pain, from no pain to the most intolerable pain [138]. Furthermore, there is a *verbal version* of NRS, the verbal rating scale (VRS), which describes the intensity of pain verbally (see Figure 2.2). Although the intensities were rated with numerical scales, they do not have objectively consistent intervals between different individuals, the misunderstanding caused by the inconsistent intervals made them not applicable in statistical analysis under most conditions [139].

The rating scales are straightforward in subjective self-report but too simple, and their designs ignored the factors influencing personal responses to pain, including physiology, personality, life experiences, and culture. For example, pain tolerance has variation between different ethnic groups and genders based on reports of pain [140]. Although direct rating is not reliable enough within such variations, therapists can use more descriptive details in pain assessment based on adjectives, which are mostly organised as questionnaires. Therefore, the pain experience can possibly be presented in a statistical analysis between individuals, and the factors correlated with pain are covered in a

comprehensive way [141]. The McGill Pain Questionnaire is the most popular and typical example of this type of tool [141]. In 1975, Melzack published the first version of McGill Questionnaire, and the questionnaire consists of four major categories of words, including sensory, affective, evaluative and miscellaneous descriptors (see Figure 2.3). With the questionnaire, patients are supposed to select words specifying their subjective pain experience. When analysing the numerical pain rating index (PRI), the number of words chosen, and the intensity of pain reported on a 5-level scale, the pain assessment can be statistically quantitative [3, 16]. In addition to the McGill Pain Questionnaire, there are also some other questionnaires that are used in clinics as well, such as the Pain Self-Efficacy Questionnaire [142] and a brief Pain Inventory [122].

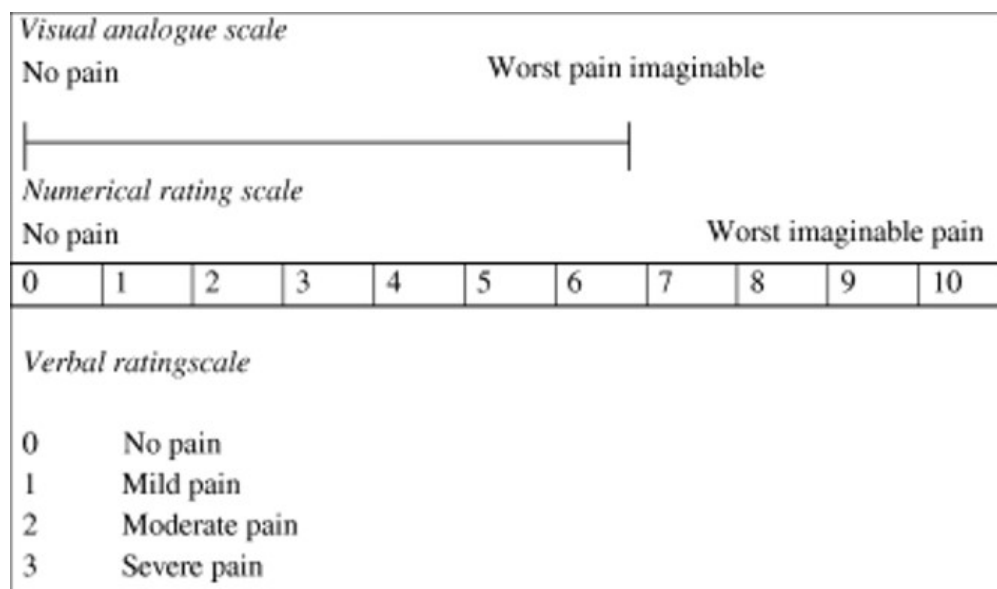


Figure 2.2: **Common pain rating scales [2]**. From top to bottom: Visual analogue scale (VAS), numerical rating scale (NRS), and verbal rating scale (VRS).

McGILL PAIN QUESTIONNAIRE
RONALD MELZACK

Patient's Name _____ Date _____ Time _____ am/pm

PRI: S _____ A _____ E _____ M _____ PRI(T) _____ PPI _____
(1-10) (11-15) (16) (17-20) (1-20)

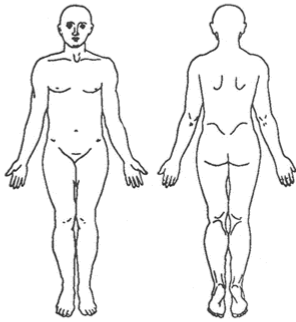
<p>1 FLICKERING QUIVERING PULSING THROBBING BEATING POUNDING</p> <p>2 JUMPING FLASHING SHOOTING</p> <p>3 PRICKING BORING DRILLING STABBING LANCINATING</p> <p>4 SHARP CUTTING LACERATING</p> <p>5 PINCHING PRESSING GNAWING CRAMPING CRUSHING</p> <p>6 TUGGING PULLING WRENCHING</p> <p>7 HOT BURNING SCALDING SEARING</p> <p>8 TINGLING ITCHY SMARTING STINGING</p> <p>9 DULL SORE HURTING ACHING HEAVY</p> <p>10 TENDER TAUT RASPING SPLITTING</p>	<p>11 TIRING EXHAUSTING</p> <p>12 SICKENING SUFFOCATING</p> <p>13 FEARFUL FRIGHTFUL TERRIFYING</p> <p>14 PUNISHING GRUELLING CRUEL VICIOUS KILLING</p> <p>15 WRETCHED BLINDING</p> <p>16 ANNOYING TROUBLESOME MISERABLE INTENSE UNBEARABLE</p> <p>17 SPREADING RADIATING PENETRATING PIERCING</p> <p>18 TIGHT NUMB DRAWING SQUEEZING TEARING</p> <p>19 COOL COLD FREEZING</p> <p>20 NAGGING NAUSEATING AGONIZING DREADFUL TORTURING</p> <p style="text-align: center;">PPI</p> <p>0 NO PAIN 1 MILD 2 DISCOMFORTING 3 DISTRESSING 4 HORRIBLE 5 EXCRUCIATING</p>	<table border="1" style="width: 100%; border-collapse: collapse;"> <tr> <td>BRIEF</td> <td>RHYTHMIC</td> <td>CONTINUOUS</td> </tr> <tr> <td>MOMENTARY</td> <td>PERIODIC</td> <td>STEADY</td> </tr> <tr> <td>TRANSIENT</td> <td>INTERMITTENT</td> <td>CONSTANT</td> </tr> </table> <div style="text-align: center; margin-top: 20px;">  </div> <div style="text-align: center; margin-top: 10px;"> <table border="1" style="width: 60%; margin: auto;"> <tr> <td>E = EXTERNAL</td> </tr> <tr> <td>I = INTERNAL</td> </tr> </table> </div> <div style="margin-top: 20px;"> <p>COMMENTS:</p> <div style="border: 1px solid black; height: 80px; width: 100%;"></div> </div> <p style="text-align: right; font-size: small;">© R. MELZACK, 1975</p>	BRIEF	RHYTHMIC	CONTINUOUS	MOMENTARY	PERIODIC	STEADY	TRANSIENT	INTERMITTENT	CONSTANT	E = EXTERNAL	I = INTERNAL
BRIEF	RHYTHMIC	CONTINUOUS											
MOMENTARY	PERIODIC	STEADY											
TRANSIENT	INTERMITTENT	CONSTANT											
E = EXTERNAL													
I = INTERNAL													

Figure 2.3: The McGill Pain Questionnaire [3]. The questionnaire includes four groups of word descriptors: sensory (1-10), affective (11-15), evaluative (16) and miscellaneous (17-20). The rank value of each descriptor increases from top to bottom. The sum of the rank values is defined as the pain rating index (PRI).

Observation Measure

When the self-report measure cannot work, the therapists or the caretakers of patients could follow some observational measures for pain assessment, which are related to behaviour or activity performances. Attention to observation measures first occurred in assessing pain in infants and young children whose verbal and cognitive skills are not as good as those of older people [143]. To solve the undertreatment of pain in children, researchers observed their particular distress behaviours and found patterns related to pain, including cry/communication, facial expression and body movement [143]. Based on these findings, Voepel-Lewis et al. designed the FLACC, a behavioural scale for assessing pain by observation, which assesses pain according to five types of behaviour: facial expression, leg movement, activity, cry, and consolability [144]. Each type of behaviour contains three levels of scores, and each score matches a particular performance under the behaviour. For example, in the category of cry, the score 0 represents *no cry*, score 1 means *moans or whimpers; occasional complaint* and the score 2 is *crying steadily, screams or sobs, frequent complaints* [143].

Obviously, the difficulty of communication does not only exist in young children; adults with intellectual or development disabilities cannot fluently report pain, also. As a result, some scales for pain assessment were developed for this group of patients. Originally developed for patients with dementia, Warden et al. developed the Pain Assessment in Advanced Dementia (PAINAD) scale, and these scales have been extended to general therapy in pain assessing of elderly patients [145, 146]. Similarly to FLACC, PAINAD is

also based on observation of pain-related behaviours of patients, but it is not surprising that the types of behaviour are not completely consistent with FLACC due to the observed groups. In PAINAD, therapists and caretakers focus on five types of behaviours, including breathing, vocalisation, facial expression, body movement, and consolability [145]. There is still some controversy about the validity of PAINAD, for example, the word descriptors are too generic, and the reliability of the breathing behaviour needs more verification [147, 148]. But some studies have shown that PAINAD could be an adjunct to pain assessment in both patients with dementia and elderly people without cognitive disabilities [146, 149].

As an efficient tool for clinicians, the observation measure has entered more conditions to assess pain, even in sedated, unconscious ICU patients [150]. Although the behaviours of such critically ill patients are hard to observe, the Behavioural Pain Scale (BPS) and the Critical Care Pain Observation Tool (CPOT) were developed for the ICU. Both BPS and CPOT involve three types of behaviour, including facial expression, upper limb movement and compliance with ventilation [151, 152]. According to the meta-analysis, CPOT has better validity than BPS in clinical environments, but CPOT also depends on physiological measures (which will be introduced in Section 2.2.4) [153].

2.2.4 Physiological Assessment

Pain can cause physiological responses in heart rate, blood pressure, respiration, muscle tension, and many other changes associated with stress responses [154]. Therefore, physiological measures can be indirect markers of pain. Especially for patients who lose

consciousness or have very limited motor ability, physiological measures can work in the absence of self-report or observation measures. Furthermore, as objective quantitative measures, physiological signals recorded in different individuals can help standardise pain assessment, which was investigated as the biomarker of brain responses to pain and later became the features of machine learning models (see Section 2.4).

Non-neural Physiological Measure

For discovering the approaches assessing pain with non-neural physiological signals, the primary studies revealed the correlations between physiological changes and pain. This section will introduce four common physiological measures, including heart rate, blood pressure, pupil dilation, and skin conductance.

- **Heart Rate** In pain modulation, the functional interactions between the cardiovascular and pain regulatory systems play a role, so the heart rate and blood pulse are influenced by pain [19]. In [20], Loggia et al. studied how heart rate responds to painful stimulation, and found that heart rate increases along with the intensity of pain stimulation. Otherwise, Loggia et al. also found the change in heart rate has a significant correlation with pain perception at the group level, but not observed significant correlations at the individual level [20]. Heart rate can potentially provide cues of pain in group levels, but may fail in individuals. However, previous research suggested electrocardiography (ECG) may allow predicting pain with the heart rate function. In the recording of electrophysiological signals, heart rate is a main component in ECG, which can be the input of machine learning models for

pain assessment. In applications, the pain assessment algorithms using ECG has presented performances above chance level, e.g., the model developed by Winslow et al. achieved the F1 value of 81.9% [155]

- **Blood Pressure** As another typical physiological measure affected by the interaction between pain and cardiovascular system, blood pressure rises during pain [156]. Furthermore, some evidence showed a negative correlation between blood pressure and pain sensitivity in acute pain [157], but pain sensitivity strengthens with higher blood pressure in chronic pain [158]. With the development of wearable sensors, signals related to blood pressure have become easy to record. Typically, ECG and photoplethysmography (PPG) broadly play the role as the source of blood pressure signals, and the machine learning models based on them have exhibited accuracy above chance level in pain prediction, for example, Winslow et al. developed a model with these signals producing the F1 score of 79.4%, Cao et al. proposed a model using PPG and the maximum accuracy was 81.41% [155, 159].
- **Pupillary Dilation** Since pupillary dilation reflex (PDR) always responds to the painful stimulation, even in anaesthetised patients, researchers investigated it as a potential signature in pain assessment as well [160, 161, 162]. Chapman et al. suggested that the peak amplitude of PDR increased significantly when the painful stimulus has a higher intensity [162].
- **Skin Conductance** Skin conductance is another autonomic response to pain, as well as heart rate [20]. In pain assessment, the the number of fluctuations in skin

conductance per second is measured, which is correlated with the discrete numeric rating of pain [163]. For applications, the skin conductance algometer (SCA) can detect the fact of pain continuously, where the SCA index increases with stronger noxious stimuli [164].

Neural Physiological Measure

Following the anatomy and physiology of pain in Section 2.1.3, pain is objectively detectable from neural signals. In addition, studies based on neural signals can also reveal the neural mechanism in pain processing. As a result, many researchers recently attempted to decode pain from neural signals, especially brain signals [23]. Because EEG will be thoroughly introduced in Section 2.3, EEG is excluded in this section's review. The subjectivity of pain experience can make it controversial about what is detected from neural physiological measures. Since nociception refers to the neural processes of encoding and transmitting harmful stimuli, while pain is the result of such neural processes, the neural physiological measures at least recognise the occurrence of the nociceptive stimuli. This section will introduce four typical techniques for pain assessment. Among them, positron emission tomography (PET) and functional magnetic resonance imaging (fMRI) can provide high spatial resolutions, but their temporal resolutions are limited, and they can only work with professional operations. Magnetoencephalography (MEG) has a very high temporal resolution and a low spatial resolution, but cannot be used at the bedside like EEG. Unlike all non-invasive brain imaging followed, local field potentials (LFPs) are recorded intracranially with invasive leads.

- **Positron Emission Tomography (PET)** PET is a nuclear medical imaging technique, which detects small amounts of posi-tron-emitter-labelled biologic molecules [165]. It has been widely used in neurological research. Toward nonresponsive patients, Boly et al. investigated the perception of pain with PET activation, which found the cerebral correlated with pain in patients in a minimally conscious state (MCS), but a wider distribution occurred in the brain network processing pain in patients in a persistent vegetative state (PVS) [166]. Therefore, PET can be a good tool for pain assessment in non-communicative patients. However, PET could induce the effects of beta decay on the ionisation of induced living tissues, so it is not suggested in many clinical cases [167].
- **Functional Magnetic Resonance Imaging (fMRI)** fMRI detects the blood oxygenation level dependent (BOLD) to visualise brain activities, representing changes in hemoglobin oxygenation states [168]. Using fMRI, the dynamic process of the BOLD change can reflect the activation of different brain regions that respond to an external stimulus [169]. As expressed in Section 2.1.3, the brain's correlations with pain are complex and involve various cortices [101, 170]. Consequently, some work modelled the pain processing mechanism of the brain using fMRI and suggested that the complexity is definitely beyond the range covered by the *pain matrix* [170, 171]. Especially by using machine learning, models with fMRI biomarkers can predict pain accurately; for example, the neurologic pain signature (NPS) can predict pain with an accuracy of 90% – 100% [170, 171].

- **Magnetoencephalography (MEG)** Similar with the main technique used in this study, EEG, MEG measures the magnetic field generated by the electrical activity of the measures in a noninvasive way, which provides high temporal resolution [172]. In pain assessment, MEG has been a prevailing tool for decades [167, 173]. The spectral and temporal measures of the MEG data showed significant correlations with the pain rating [174, 175]. So such measures can work as features in machine learning models. Because the features extracted from MEG are similar to those from EEG, the classical features used for pain assessment will be introduced in Section 2.3.3.
- **Local Field Potential (LFP)** Recently, the frontier techniques which can record intracranial brain signals provided a new solution to assess pain, especially in patients with chronic pain. With LFP recorded with invasive leads, Shirvalkar et al. found that sustained power changes from the orbitofrontal cortex (OFC) are correlated with chronic pain processing, and such power changes can feed the machine learning model for pain prediction [79]. Since such leads can also serve as a stimulator in deep brain stimulation (DBS), this technology has strong potentials in both pain assessment and pain management [118].

2.2.5 Other Novel Approaches in Pain Assessment

With the rapid development of artificial intelligence, some pain assessment approaches are neither behavioural nor physiological directly. These approaches utilised indirect

self-report or observation measures of pain as labels to train the models, but did not use physiological signals as input whose correlations with pain perception can be declared. They can be seen as a kind of behavioural assessment, but the way is not based on direct manual observation.

For example, as a powerful factor in the evaluation of pain using observation, facial expressions have been extensively studied in scaling pain. Currently, by benefiting the algorithms that detect facial expressions in general computer vision (CV) tasks, they can be used to automatically assess pain with self-report pain as labels in model training [176, 177].

Another example is the use of clinical notes in the evaluation of pain during the development of chronic pain. Although it is rare to use natural language processing (NLP) to predict physiological status, Fodeh et al. successfully extracted the features correlated to pain management from a large number of clinical notes, including mention of pain, intensity, quality, etc. The pain assessment classification system using machine learning developed by them achieved an area under the receiver operating characteristic (ROC) curve of 0.94, which can help clinicians monitor and manage patients' pain more efficiently [178].

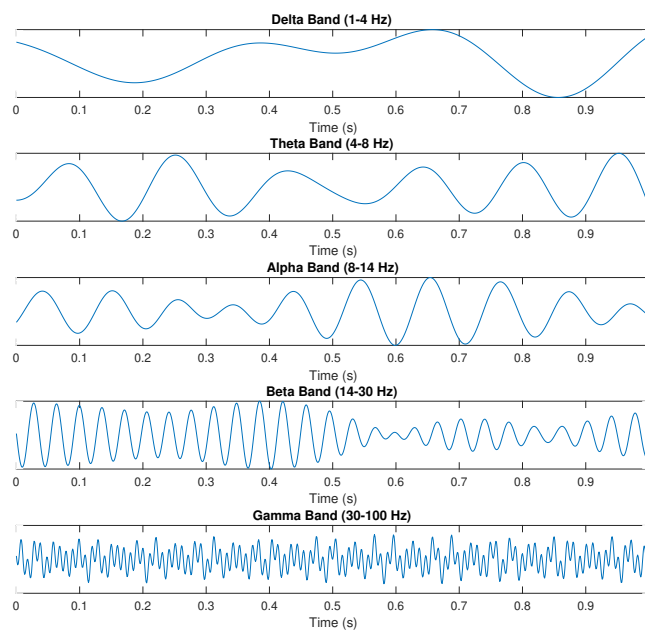


Figure 2.4: Five typical frequency bands which are studied as the brain rhythms from EEG.

2.3 Electroencephalography (EEG) in Pain Assessment

2.3.1 Principles and Advantages of EEG

EEG is a noninvasive neuroimaging technique that detects electrical activity generated by neurons in the brain [179]. When using EEG, electrodes are placed on the scalp according to the 10-20 system to detect electrical signals, which are amplified and recorded [179, 180]. The signals detected by EEG are voltage fluctuations resulting from ionic currents within neurons. Compared to fMRI and PET, EEG has high temporal resolutions, with sampling rates typically from 250 Hz to 1000 Hz until 2023 [181]. According to the Nyquist-Shannon sampling theorem, the sampling rate must be at least twice the

bandwidth of the collected signals, so neuronal oscillations with frequencies under 125 Hz are always dependable with EEG. In the perspective of electrodes, the 32-, 64- and 128-channel EEG system is widely used in research, so it can cover different scalp sites from the frontal to occipital lobes with source localisation [182]. Obviously, these spatial resolutions are lower than non-mobile devices such as fMRI and PET [167]. Hence, the source localisation of EEG signals has spatial limitations, which cannot indicate the activities at the level of neuron clusters [182]. However, the non-invasive and mobile properties of EEG can benefit the daily care of patients at the bedside.

In this study, EEG was the source of brain signals. The selection originated from the requirements of the unresponsive patients' care. First, nonresponsive patients cannot self-report any information about ongoing pain, so using physiological signals is wise to monitor their health issues related to pain. Second, devices must be easy to use at the bedside for daily care, which means the signal recording technique must be both noninvasive and mobile. Moreover, the complexity of the brain regions involved in pain processing requires sufficient spatial resolution. Therefore, EEG is an ideal technique that meets all these requirements, and the research using it can also provide interpretation of neural mechanisms in pain processing.

2.3.2 Brain Rhythms and Electrophysiology of Pain

Brain waves, or neuronal oscillations, are *rhythmic patterns* of neural activity produced by neurons in the CNS [30]. Brain rhythms represent the patterns of brain waves, which are induced by the interaction between the oscillatory electrical activities of neurons,

especially the pyramidal neurons located in the cerebral cortex [183]. The main sources of the EEG signal are the dendritic potentials, typically the post-synaptic potentials occur in the apical dendrites of pyramidal neurons. Across a large population of neurons, the spatial summation of these dendritic potentials generates the electric fields that can be detected by EEG electrodes. Otherwise, the synchronisation of neurons contributes to the EEG signals as well. The synchronisation is facilitated by diverse mechanisms, for example, thalamocortical circuits and local interneuronal networks [183]. These patterns are measured by EEG, for which researchers study mainly how different frequency bands are associated with specific behaviours, perceptions, or cognitive tasks.

Since EEG records the neuronal activities of neuron ensembles on the scalp and the sampling rates limit the valid frequency bands in signal processing, only low-frequency bands mainly occur in the studies of brain rhythms, including delta ($0.5-4Hz$), theta ($4-8Hz$), alpha ($8-12Hz$), beta ($13-30Hz$) and gamma bands ($30-100Hz$) (See Figure 2.4) [30]. In most of the work, the researchers could declare significant correlations between some band and a specific status, e.g., alpha suppression is associated with attentional processes [184, 185], and the theta band increases during the awakening state [186]. The complex pain processing mechanism decides that it covers a wide range of brain rhythms, for which all the typical bands studied contribute to pain processing [173].

Some work suggested that the alpha and gamma bands have the most significant contributions to pain perception [26]. The alpha band is associated with two perspectives in pain assessment, subjective pain rating, and individual pain sensitivity. In the aspect to assess the subjective pain rating, Nir et al. found that alpha-1 ($7-10Hz$) power has a

negative correlation with numeric pain scores (NPSs) [187], and some work suggested that alpha power decreases in the contralateral central scalp when painful stimuli occur [188, 189]. Moreover, some evidence suggested that alpha bands participate in encoding the intensity of pain stimulus in the sensorimotor cortex [119]. The alpha band also presents another importance in measuring individual pain sensitivity. Peak alpha frequency (PAF), the peak frequency in the spectrum of the alpha band, has been investigated as a main biomarker of pain sensitivity [31]. Inspired by the finding of a slower alpha wave during chronic pain [190], researchers studied the correlation between prolonged pain sensitivity and PAF and declared that pain sensitivity increases when PAF is slower [191, 192, 193]. However, with the same data as those used in this research, Valentini et al. proposed that PAF is not the functional biomarker of pain sensation since it does not differ painful stimuli from unpleasant stimuli, but it is still reliable for assessing pain from resting states [32]. In summary, the alpha band is worth utilisation in distinguishing pain from the non-painful states, and its correlation with individual pain sensitivity can help improve the cross-individual model in pain assessment. Hence, this research set the alpha band as the focus for the development of pain assessment approaches.

The main contribution of the gamma band is pain processing, which encodes the intensity of the objective stimulus and the subjective pain [33, 119, 194]. Nickel et al. investigated the encoding mechanism of stimulus intensity and pain intensity, they disclosed that gamma oscillations encode the intensity of pain in the medial prefrontal cortex [119]. Valentini et al. revealed the gamma band as a type of *fingerprint* of pain

sensitivity [194]. As suggested by some classical work, gamma oscillations increase with prolonged pain [188, 195]. This property inspired some work to investigate the gamma oscillation with ongoing chronic pain, which revealed the positive correlation between the gamma oscillation and the intensity of the pain [33]. However, there are concerns about the reliability and robustness of the gamma responses in EEG signals. Particularly, gamma oscillations originating from muscle activity may be erroneously labelled as originating from neural sources [194, 196]. Hence, for this reason, our work did not involve the investigation of gamma band.

In addition to alpha and gamma oscillations, changes in the other low-frequency brain rhythms are also specific to pain processing [26]. Increased delta activity occurs mainly in the posterior parietal region and is distributed throughout the brain except for some occipital areas, which lasts throughout the painful stimulation diffusion period [197, 198, 199]. The contributions of theta and beta bands in pain processing were found mainly in chronic pain studies, where theta and beta oscillations increase in the primary somatosensory and medial prefrontal cortices [33, 200]. In conclusion, low-frequency brain rhythms participate in pain processing in a wide range including theta, delta, alpha and beta bands, so this research utilised them except for the gamma band to discover which EEG-based neural biomarkers can predict pain accurately.

2.3.3 Discovering Neural Biomarker: Neurophysiological Measure from EEG in Pain Assessment

Biomarkers have been defined as *cellular, biochemical or molecular alterations that are measurable in biological media such as human tissues, cells, or fluids* [201]. By extension, the neural biomarker represents the neurophysiological measures that have correlations with specific neural activities. No matter which particular model plays the role of assessing pain with EEG signals, the model acquires neural biomarkers as input features. So the vital objective in the development of pain assessment models is discovering the neural biomarkers specific to pain processing. Furthermore, the neural biomarkers that produce good performance in pain assessment can reverse the interpretability of the neural mechanism in pain processing.

Time-frequency Neural Biomarker of Pain

The majority of pain assessment models utilise the time-frequency representations from the EEG signals [37]. Because the EEG signals originally have two dimensions, including channels and time points, the time-frequency measures are generated mostly along channels, that is, the measures are computed within each channel individually. By using transformations such as the Fourier transform or the wavelet transform, we can obtain the amplitude of EEG signals at particular time points and frequency bands. Therefore, some studies analysed the correlations between these measures and pain perception. Furthermore, many pain assessment algorithms used these measures as features and

performed well. This section reviews some typical time-frequency neural biomarkers in pain assessment.

- **Power Spectral Density** Most temporal neural biomarkers are represented as the power of EEG signals in a specific frequency range. Power spectral density (PSD) is based on the fast Fourier transform (FFT) and represents the distribution of power from particular frequency components [202]. PSD in the band with frequency ranging between f_{min} and f_{max} can be calculated with the formula:

$$\text{PSD} = \frac{1}{2\pi} \int_{f_{min}}^{f_{max}} |FFT(X(t), f)|^2 df \quad (2.1)$$

where $FFT(X(t), f)$ is the spectral power computed from the epoch of the temporal signal series $X(t)$ at frequency f by FFT, in which $X(t)$ is segmented with fixed window length.

There are two outcomes in using PSD as a neural biomarker in pain assessment. Some work used the alpha, beta and gamma bands as PSD sources, and achieved the accuracy above 80% in pain prediction involving pain conditions and resting states [40, 203, 204]. In addition, statistical analysis or machine learning-based analysis can also suggest the relative contributions of different frequency bands and channels [40, 205].

- **Spectrogram** By applying short-time Fourier transform (STFT) to single-trial data from each channel, the EEG spectrogram can be extracted as a neural biomarker with high resolutions in both temporal and spectral domains [206], Figure 2.5

shows an example of the spectrogram. Until now, researchers have investigated some approaches inputting spectrograms into machine learning models for pain assessment, for instance, Tu et al. used the spectrogram to test the differences of the effects of pre- and post-stimulus brain activities' in assessing subjective pain intensity [207], Sun et al. reported good performances of the support vector machine (SVM) in distinguishing pain from non-pain conditions with spectrograms [4]. Another potential of the spectrogram in assessing pain with a machine learning model originates from its nature as an image-like three-dimensional matrix from multiple channels, in which the data can be organised as *time* \times *frequency* \times *channel* matrix matrices. Hence, such features can work with a convolutional neural network like the general computer vision tasks. Although this technical paradigm has not been commonly reported in the development of pain assessment, research in other fields has shown its feasibility [208, 209].

- **Wavelet Spectral Measure** Except for Fourier Transform, wavelet transform (WT) is also widely applied in the extraction of neural biomarkers for pain assessment [210, 211, 212]. WT decomposes the signal into a set of basis functions based on the wavelet function $\Psi(t)$, which can represent the signal in both the temporal and spectral domains [213]. Mathematically, the continuous wavelet transform can be written as

$$CWT_{\Psi}(a, b) = \frac{1}{\sqrt{|a|}} \int_{-\infty}^{\infty} f(t) \Psi^*\left(\frac{t-b}{a}\right) dt \quad (2.2)$$

where $CWT_{\Psi}(a, b)$ is the wavelet coefficient with scale parameter a and translation

parameter b , $\Psi(t)$ is the wavelet function and $f(t)$ is the signal to be decomposed. The work by Hadjileontiadis [212] and Alazrai et al. [211] used the wavelet transform to recognise tonic pain conditions, and both models achieved prediction accuracy close to 90%. Vijayakumar et al. use the Gabor wavelet transform to generate features in the prediction of pain between subjects and achieved the prediction accuracy of 89.45% in the classification among ten classes [214].

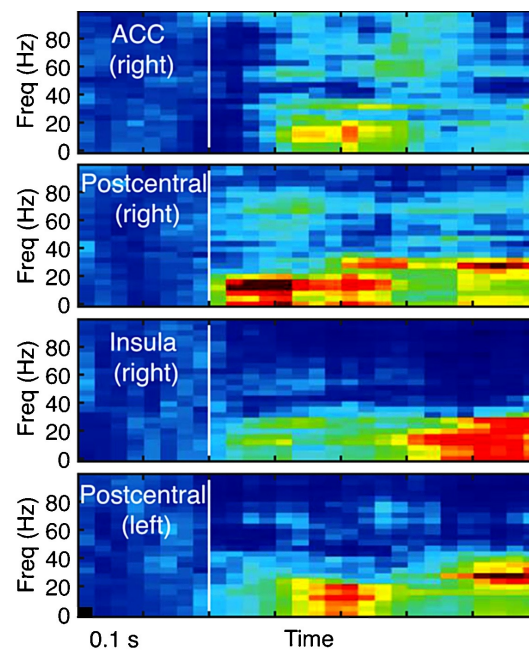


Figure 2.5: An example of spectrogram computed with the EEG signals recorded in different brain regions [4]. The strength of each point represents the amplitude computed with STFT, the x- and y-axis represent the scales of time and frequency. Each spectrogram was averaged across the electrodes in a brain region within the same subject.

Measures of Neural Integration: Functional Connectivity and Cross-Frequency

Coupling

Although time-frequency measures can reflect the characteristics of the temporal and spectral domains in pain processing, they can only show the properties within the same channel or frequency band. Nonetheless, the complexity of pain processing reviewed in Sections 2.1.3 and 2.3.2 is beneficial to be represented by neural biomarkers. In this Ph.D. research, one of the main objectives is how to quantify neural integrations as biomarkers. From this perspective, this work investigated two types of neural integration, functional connectivity of the brain between regions of the brain represented by EEG channels and cross-frequency coupling among neuronal oscillations.

- **Functional Connectivity** Most of work studied the functional connectivity in pain perception with fMRI. These researches proposed several typical patterns of the brain networks associated with pain, for example, the change in functional connectivity between the frontoparietal network and the rostral anterior cingulate cortex/medial prefrontal cortex has a positive correlation with the change in pain rating [215], the functional connectivity of the nucleus accumbens with the prefrontal cortex strengthens during persistence of pain [216]. Recently, some studies *transferred* the paradigm of functional connectivity to the analysis using EEG. In particular, it is difficult for EEG signals to present deep brain activities, such as activities in the nucleus accumbens, so the analysis with EEG was at the level of the scalp [217]. In such a context, de Tommaso et al. investigated the functional

connectivity of EEG in migraine, which revealed the enhancement of the synchronisation entropy between the bilateral temporal-parietal and frontal regions in the patient group [218]. Another work by Topaz et al. demonstrated that functional connectivity of the resting state of EEG is a potential biomarker that distinguishes pain in patients with diabetic polyneuropathy [219].

The literature studying the roles of functional connectivity in pain processing with EEG is still rare, but measures quantifying functional connectivity have been widely reported in a more general field of EEG research. For measuring the functional connectivity of EEG, there are two types of measures according to the general components of the signal, including power- and phase-based measures [8]. Power-based functional connectivity quantifies the relationship of EEG signals between different electrodes or brain regions in the time-frequency domain. Notably, many power-based measures definitely measure the integration from both power and phase [9]. Meanwhile, the phase-based functional connectivity represents the synchronisation of the phase angle or voltage shifts between two electrodes or brain regions. Tables 2.2 and 2.3 list some typical measures of functional connectivity with their specificity. Briefly, with these measures, the correlation between functional connectivity and pain is feasible to study, and they can serve as features in machine learning models (see Section 2.4).

Based on functional connectivity measures, some approaches were developed to predict pain with machine learning. For instance, Modares-Haghighi et al. used

the EEG-based functional connectivity graph from the alpha band with SVM, and obtained the accuracy above 90%. Shamsi et al. predicted pain using the functional connectivity of the gamma band as features with the long short-term memory (LSTM) classifier and produced the accuracy around 80% [220]. The background on machine learning will be reviewed in detail in Section 2.4.

- **Cross-frequency Coupling** Cross-frequency coupling is a measure of the integration between neuronal oscillations, that is the phase or power of a neuronal oscillation at a specific frequency range modulates the phase or power of another neuronal oscillation [221]. In cortical information processing, cross-frequency coupling has important functionality [221]. However, only a limited number of studies analysed the change in cross-frequency coupling in pain processing. Liu et al. revealed the responses of the gamma band to the LFP pain stimulus, which is coupled with the phases of theta and alpha bands in the amygdala and hippocampal regions in the right hemisphere [34]. By localising EEG signals in the somatosensory cortex, Vanneste and De Ridder analysed the differences between chronic pain patients and healthy individuals, and found that the cross-frequency coupling decreases between the alpha and gamma bands, whereas it increases between theta and gamma bands [222]. Similarly as functional connectivity, cross-frequency coupling is quantified as the relationship between two signal series. Therefore, the measures in Tables 2.2 and 2.3 can also represent cross-frequency coupling, but the source of the signal series is supposed to be different neuronal oscillations rather than

brain regions. Although some studies extracted cross-frequency coupling as features to classify different brain states, such as seizure states [223], emotion [224], and sleep stage [225, 226], the work using cross-frequency coupling in pain assessment is still under investigation.

Table 2.2: **Typical Power-based Measures of Neural Integration.** The power-based measures utilise the time-frequency information from signals, which both involve the power- and phase-based properties. In the meanwhile, phase-based measures quantify the synchronisation between signal series by using the phases extracted with the Hilbert transform [8, 9]

Measure	Specificity	Formula
Magnitude Squared Coherence (Coh) [8, 227]	Coh both represents the linear relationships between signal series, which involves both power and phase. But it is sensitive to volume conduction.	$C_{xy} = \frac{S_{xy}(f)}{\sqrt{S_{xx}(f)S_{yy}(f)}}$, where $S_{(xy)}(f)$ represents the cross-correlation between the series x and y [228].
Partial Directed Coherence (PDC)	PDC quantifies the directional relationship between signal series, which ranks the relative strength of casual interactions based on the statistical assumption of normality [229]. In comparison to Coh, it is less sensitive to volume conduction.	$PDC_{xy}(f) = \frac{ A_{xy}(f) }{\sqrt{\sum_{k=1}^p A_{xk}(f) ^2}}$, where A_{xy} is the Fourier transform of the coefficients of the multivariate autoregressive model [230].
Correlation Coefficient (Pearson's; Corr)	Corr measures the linear synchrony or the linear correlation between the power of two series of signals [231, 8].	$r = \frac{\sum_{i=1}^n (X_i - \bar{X})(Y_i - \bar{Y})}{\sqrt{\sum_{i=1}^n (X_i - \bar{X})^2 \sum_{i=1}^n (Y_i - \bar{Y})^2}}$, in which \bar{X} is the mean value of the signal series X .

Table 2.3: **Typical Phase-based Measures of Neural Integration.** The phase-based measures quantify the synchronisation between signal series by using the phases extracted with the Hilbert transform [8, 9]

Measure	Specificity	Formula
Phase Locking Value (PLV)	PLV represents the significant instantaneous phase covariance between two series of signals [232].	$PLV = \left \frac{1}{N} \sum_{n=1}^N e^{i(\phi_{x_n} - \phi_{y_n})} \right ,$ where N is the number of time points, ϕ_{x_n} and ϕ_{y_n} are the phases of the signal series x and y .
Phase Lag Index (PLI)	PLI measures the intensity of the phase angles' distributions pointing toward positive or negative sides of the imaginary axis [233].	$PLI = \left \frac{1}{N} \sum_{n=1}^N \text{sgn}(\phi_{x_n} - \phi_{y_n}) \right ,$ in which ϕ_{x_n} is the same as in PLV, and sgn means the signum function.

2.4 Machine Learning

The development of machine learning makes automatic pain assessment possible. For implementing the machine learning model for pain assessment with EEG, the first step is selecting the appropriate features as input. The features are neurophysiological measures extracted from EEG signals, which were inspired by the principles of neurophysiology of pain in Section 2.1.3. Then, the neural biomarkers in Section 2.3.3 could serve as

features. With neurophysiological measures as input features, the studies always focus on developing particular machine learning algorithms, which can classify the pain and non-pain conditions. Figure 2.6 shows the diagram of how the different components in the pain study inspire the development of a machine learning model for pain assessment. This section introduces the machine learning models utilised in this research and related background.

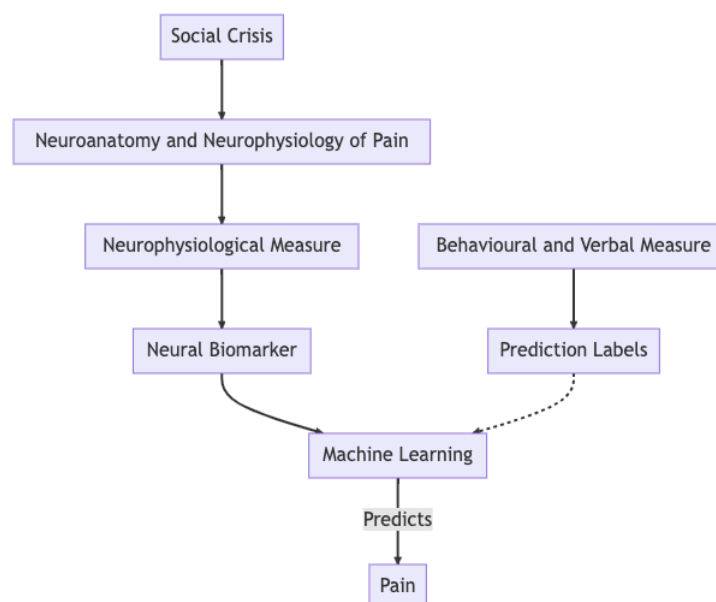


Figure 2.6: **The pipeline of machine learning model's development.** According to the neuroanatomy and neurophysiology of pain, neurophysiological measures were developed. Hence, neurophysiological measures can serve as neural biomarkers inputting the machine learning model as features. In the meantime, the behavioural and verbal measures can play the role of labels in the machine learning model's training. Using an appropriate machine learning model, pain-related states can be predicted.

2.4.1 Machine Learning Algorithm

In recent 20 years, machine learning has emerged as a frontier tool in EEG analysis, boosting both the development of research and clinical applications [234]. Compared to conventional techniques that analyse the correlations between EEG signal change and pain, machine learning algorithms are able to learn from EEG data autonomously, adapt to new information, and make predictions without pilot programming to perform the task. In summary, machine learning enlightens to more accurate diagnosis, real-time monitoring, and personalised treatment in the field of neuroscience [235].

Machine learning can serve the EEG analysis in regression and classification [234]. Since pain assessment is intrinsically subjective, the main use of machine learning in pain assessment until now has been towards classification between pain and non-pain states, or has been extended to cover the intensity of pain stimulus [37, 40]. According to the systematic review by Mari et al. machine learning has been applied to predict pain intensity, classifying pain phenotypes (i.e., distinguishing pain patients from healthy controls), and evaluating the effects of pain treatment [37]. Most algorithms in such literature developed conventional machine learning models, among which SVM is the most common model. Moreover, some recent studies have applied deep learning approaches such as the convolutional neural network (CNN) [44]. In this thesis, I used SVM as the basis for analysing the neural biomarkers of integration, and developed CNN models to improve the performance of pain assessment.

Support Vector Machine

The SVM is a supervised machine learning algorithm, which finds a hyperplane that best separates the data into different classes [236]. Generally, independent of the classes involved in the classification target, the classification can be decomposed as the combination of multiple binary classifications. In a two-dimensional space, the hyperplane is a line, which becomes a plane or a set of planes in a hyperdimensional space. The objective of SVM is to find the hyperplane with the maximum margin that makes the maximum distance between data points of different classes. The mathematical expression of the hyperplane is defined as:

$$\vec{w} \cdot \vec{x} - b = 0 \quad (2.3)$$

where \vec{w} is the weight vector perpendicular to the hyperplane, \vec{x} is the input data points, and b of the bias term. The aim of solving the hyperplane is to maximise the margin M between classes, which is defined as the perpendicular distance from the hyperplane to the closest data point of each class. For a data point (\vec{x}_i, y_i) where y_i represents the class label represented by 1 or -1, the constrain can be expressed as:

$$y_i(\vec{w} \cdot \vec{x}_i - b) \geq M, \forall i \quad (2.4)$$

The SVM's performances can be optimised by adjusting the parameters of its kernel, so that the data in higher-dimensional space could be more linealy separable [237].

As the widely used model in the interdisciplinary research of biomedical engineering, SVM is also a primary candidate as the algorithm to assess pain [37, 238]. In the classific-

ation of the intensity of pain within the subject, SVM models achieved satisfactory results in some work; for example, Vatankhah et al. used the SVM model with time-frequency features that produced the mean accuracy of 95% in binary classification between pain and no pain [239], Misra et al. got the mean accuracy of 89.58% to classify low and high pain [45], and Kimura et al. proposed the model classifying four levels of pain with the accuracy of 79.6% [240].

Convolutional Neural Network

CNN is sensitive to the spatial hierarchies of features, which is a typical deep neural network used primarily in CV [241]. CNN depends on the operation of convolution, which slides a filter or kernel over the input data with dimensions above two and produces a feature map. Therefore, the model can capture local patterns including edges, corners, and textures from the input. The convolution operation for a two-dimensional input X and a filter F is:

$$Z_{ij} = \sum_m \sum_n X_{mn} \cdot F_{i-m, j-n} \quad (2.5)$$

After convolution, a typical CNN architecture is followed by pooling layers for dimension reduction. The features extracted by the convolutional layers finally feed the fully connected layer to produce the final prediction scores, Figure 2.7 presents the progress.

As a technique mostly in need of big data, the available data size in most pain-related research using EEG limited the application of CNN in pain assessment. Since CNN require two-dimensional input, the time-frequency features, i.e., spectrogram, from EEG signals,

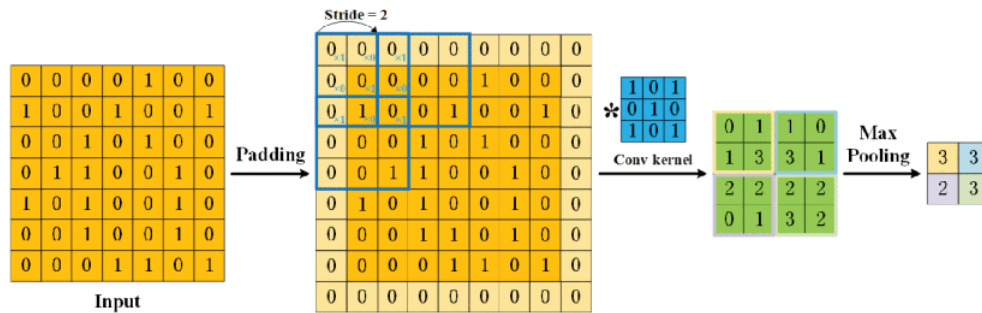


Figure 2.7: **Procedure of a two-dimensional CNN [5]**. After adding the padding for processing the effects of edges, the convolutional kernels were slid on the input, and then the output patterns were processed by max pooling.

are suitable. While using time-frequency samples from EEG to feed the CNN model, the *edges, corners and textures* detected by CNN could be the temporal or spectral patterns. Until now, most EEG-based models to assess pain with CNN used the time-frequency features [44, 242]. Yu et al. extracted time-frequency features from different EEG frequency bands and inputted them into CNN, where the CNN learnt the features specific to pain in different frequency bands, and the accuracy of the result (97.37%) was quite competitive, even compared to the state of the art in binary classification of pain and non-pain [44]. Regarding the classification that involves multiple intensities of pain, Wu et al. proposed a CNN model for the first time, where the features were spatial-spectral-temporal EEG representations of the delta, alpha, and beta bands [242]. In subject-independent and multiclass scenarios, the non-pain state and three pain states can be classified with the accuracy of 92.14% with this model. Nevertheless, although the functional connectivity can be organised as a two-dimensional matrix, where the rows and columns represent

brain regions (i.e., EEG channels in this research), there was no research reporting its use. In this thesis, functional connectivity was used as the input feature to predict pain with CNN models.

2.4.2 Transfer Learning

Toward generalising the pain assessment models to unresponsive patients, this research takes another issue into account. Until now, most automatic pain assessment models were developed in the within-subject scenario, where the subjects' data were involved in the model training when their pain states were to be predicted [37]. Only very few works attempted to assess cross-subject pain predicting pain in subjects without providing labelled data for training [214, 242]. Nevertheless, unresponsive patients cannot provide any pilot information as labels to train the models, so it is essential to develop cross-subject pain assessment algorithms, which can potentially fit the requirement of the caretakers of unresponsive patients at the bedside.

The development of cross-subject pain assessment is a typical application of cross-domain transfer learning, in which each domain represents a subject. Cross-domain transfer learning is a specialised machine learning technique that aims to leverage the knowledge extracted from a domain to improve the performance of the model in another domain, which could be from similar sources, but did not share some important domain-specific characteristics [243].

There are two challenges of cross-subject performance in most scenarios of EEG-based fields, including individual differences and lack of data [46, 244]. Toward the two

bottlenecks, there are paradigms to improve the generalisation of models, respectively: Toward the strong individual differences, matching domains can improve the model's generalisation. One approach of domain matching is adapting the marginal distributions across domains, which aims to minimise the distances between the feature space of different domains [245], or to match the domains with the minimum discrepancy with the target domain [246, 247]. The other issue is the lack of EEG data for machine learning, which can be resolved by reducing data requirements with special machine learning architectures, because they can produce the features with the reduction of individual differences [46]. A solution is the common spatial pattern (CSP), which could filter the EEG data with maximising the variance between different conditions as well as minimising the variance between different subjects [248, 249]. Benefiting from frontier work in deep neural networks, such automatic adaption can be implemented in a more flexible way to produce features toward generating generalised features, which aims to reduce the effects of individual differences while exposing the contributions of features specific to the main task [250].

As reviewed in Sections 2.1.3, 2.2, and 2.3.2, the responses of the brain to pain carry strong individual differences. Hence, the development of the cross-subject pain assessment model could originate from both paradigms of domain matching and frameworks reducing the dependency on data size. Based on the lack of research applying transfer learning strategies in cross-domain pain assessment, this research developed strategies against the discrepancy among different feature domains of subjects. The particular approaches potentially applied for pain assessment will be introduced in Chapter 6.

Chapter 3

Experiment and Signal Pre-processing

This chapter describes the basic information of the participants in the data recording experiment for this research. The experimental design and the signal preprocessing methods applied to the recorded EEG data were expressed as well. This experiment was approved by the Ethics Committee of the University of Essex.

3.1 Participants

All participants in this study were recruited through a selection process, following the dissemination of public advertisement at the University of Essex [32]. 43 healthy participants entered the study (22 females, mean age: 25.36, age range: 20-56). All participants had normal or corrected-to-normal vision and normal hearing. Before the experiment, all participants completed a screening form and were asked to disclose their history of neurological, psychiatric, or pain disorders. This led to the exclusion of two

participants while another five participants were excluded due to procedural and technical issues. Data from 36 participants (which are the same as the data used in [32]) were eventually analysed (19 female, mean age: 24.75, age range: 20-56). Of these, 24 self-identified as white / Caucasian, six as Asian / Pacific Islander, and six as Other.

3.2 Experimental Condition and Procedure

The experimental design consisted of five experimental conditions, including two thermal stimuli conditions (hot [H] and warm [W]), two resting-state conditions (eyes-closed [C] and eyes-open [O]) as baselines, and an auditory condition (sound [S]) as the reference of unpleasantness. This research did not include the S condition in the current analysis since that is designed as an affective reference, and this work did not involve the discrimination of the affective dimension, S condition was excluded from the analysis. I also indicated the potential use of this condition in future research: This study aimed to investigate the approach to predict pain compared with the most basic control conditions. Thus, it will be possible to transfer the methods developed in this work to study psychological unpleasantness in the future.

The electroencephalogram (EEG) was recorded with 62 Ag/AgCl electrodes (Easycap, BrainProducts GmbH, Gilching, Germany), which were placed according to the 10-20 system. The impedance of all electrodes was kept below 10 k Ω and the EEG signal was sampled at 1000 Hz (Synamps RT, Neuroscan, Compumedics). The reference was on the left earlobe and the ground at electrode AFz. Offline, we referenced the data to the

participants right earlobe.

Each condition lasted 5 minutes. The H condition consisted of prolonged immersion of the left hand of the participants, up to the wrist, in a 30-litre tank (RW-3025P, Medline Scientific) with circulating water at an average temperature of 44.5 °C. This temperature was fine-tuned for each participant from the initial setting of 45 °C, which is known to induce a moderate level of pain in healthy individuals [251]. The next paragraph will describe the detailed process to match the unpleasantness associated with the auditory stimulation. The W (non-painful) condition had settings identical to the H condition, except that the temperature was 6 °C lower. The degree of reduction was based on a pilot session (see [32] for further details on the methods). In both resting-state conditions (C and O), the participants did not immerse their hands in the water.

During the experiment, participants were seated 65 cm from a screen, with their left hand placed in the water bath, and their right hand used to control a mouse and a volume adjustment knob. They were asked to focus on the unpleasantness of the sensory stimulation and report it on a visual analogue scale (VAS) with anchors 0 (*no unpleasantness*), 25, 50, 75, and 100 (*intolerable unpleasantness*). The experiment began with a matching phase, in which the bath temperature was initially set at 45 °C. If the participant could not tolerate it, the temperature was reduced by 0.5 °C. On the contrary, if the VAS was rated below 50, the temperature increased by 0.5 °C. After adjusting the temperature, the matching phase was restarted until the participant consistently rated the unpleasantness between 50 and 75. Finally, the painful temperature was determined according to the matching phase, which induced the pain rated between 50 and 75 consistently in the

VAS. During the three sensory stimulation blocks (See Figure 3.1), the participants rated the intensity of unpleasantness with a VAS every 10 seconds. According to the VAS reported during the experiment, the experimenter could confirm the stimulation's validity in its corresponding conditions.

The two 2.5-minute resting state blocks (eyes-open and closed) were recorded before and after heat stimulation. We asked the participants to keep their eyes open during heat stimulation to be able to report the level of pain through VAS. During the thermal stimulation conditions (H and W), the participants kept their eyes open for the whole experiment. Thus, the O condition is more comparable with them than the C condition, because the differences between O and the thermal conditions is the absence of hand immersion in the water and the rating tasks.

3.3 Signal Pre-processing

Before extracting features, the EEG signals were pre-processed to remove artefacts, reduce noise, and reduce volume conduction by re-referencing. This section describes the methods in the signal pre-processing.

3.3.1 Filtering and Artifact Removal

The signal sampling rate was down-sampled from 1000 Hz to 500 Hz. The DC components were then removed with a high-pass filter with a cut-off frequency of 0.5 Hz, and the sinusoidal artefacts related to the power line were removed using a 50-Hz band-stop

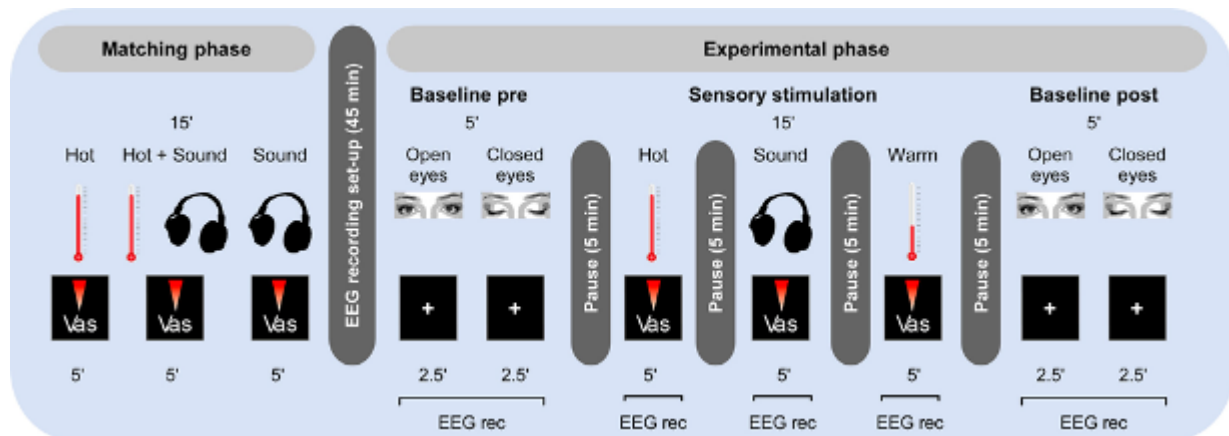


Figure 3.1: The experimental procedure for recording the pain-related EEG signals. During the matching phase, the participants were requested to match the pain rating with the unpleasantness induced by the Dound condition (S). The EEG signals started to be recorded after the matching phase, in which each condition lasted five minutes, and there were two phases of baselines (Eyes-Open [O] and Eyes-Closed [C]) before and after stimulus conditions (Hot [H], Warm [W] and Sound [S]).

filter. Independent component analysis (ICA) was applied to remove artifacts, including eye blinks and muscle movements [252]. By decomposing the EEG signals into simpler independent components, only the EEG components underlying brain activity remained.

3.3.2 Re-referencing

In EEG signals, volume conduction is the effect of electrical potentials recorded a distance from their brain source [253]. The existence of volume conduction created difficulties in the localisation of the EEG source and reduced the reliable spatial resolution in the analysis. Hence, re-referencing algorithms were developed to reduce the volume

conduction.

In this study, current source density (CSD), i.e., the Laplacian transform, played the role of re-referencing. CSD is a measure that locates the sources and sinks of electrical activities in the brain. Mathematically, it is the Laplacian (i.e., the second spatial derivative) of the electric potential V recorded by the EEG electrode. In the Laplacian transform of EEG signals, CSD Φ is expressed in two-dimensional Cartesian coordinates as:

$$\Phi(x, y) = \Delta^2 V(x, y) = \frac{\partial^2 V}{\partial x^2} + \frac{\partial^2 V}{\partial y^2} \quad (3.1)$$

where $\Delta^2 V(x, y)$ is the Laplacian of V at the given point (x, y) . At a electrode C , the Laplacian after transform can be approximated as:

$$\Delta^2 V_C = 4V_C - V_{\text{left}} - V_{\text{right}} - V_{\text{up}} - V_{\text{down}} \quad (3.2)$$

Hence, the CSD represents a more localised representation of the brain activities with the reduction of volume conduction.

Chapter 4

Accurate and Efficient Prediction of

Pain: A Comparative

Electroencephalography Study of

Functional Connectivity and

Cross-Frequency Coupling

In the development of a machine learning model to assess pain, the first step is to declare the ideal neural biomarkers correlated with pain perception. Hence, neural biomarkers can serve as the features that are entered into the machine learning model. Considering the complexity of pain perception, neural biomarkers of integration, including func-

tional connectivity and cross-frequency coupling, are worth investigating. In the analysis of neural biomarkers, there are two requirements for machine learning: accuracy and efficiency. This chapter analysed the neural biomarkers of integration based on their performances in machine learning. This chapter has been submitted as a manuscript to a journal and is under review.

4.1 Introduction

Chronic pain has major health and societal implications worldwide [10, 11]. In clinical practice, pain is diagnosed according to behavioural or verbal expressions [254, 255]. This approach cannot be applied to unresponsive patients, e.g. patients with disorders of consciousness or during anaesthesia. Therefore, the identification of biomarkers from physiological signals is of paramount importance [256]. Blood pressure and heart rate have been suggested as biomarkers in the context of both acute and tonic experimental pain [257, 258, 259]. However, the specificity and generalisability of these biomarkers to chronic pain are uncertain [260, 261]. As a potential alternative, neurophysiological measurements, such as functional magnetic resonance imaging (fMRI) [23] and positron emission tomography (PET) [262], have emerged. Nevertheless, such techniques can be only operated by professionals in hospitals, and the overall operational cost is high. In contrast, electroencephalography (EEG) can be recorded by portable, non-invasive devices at the bedside [193, 263, 264]. Therefore, the EEG is an ideal basis for the development of a neurophysiological pain assessment system, which can benefit a wide

variety of clinical settings.

The brain's response to pain involves a complex integration of neural activities, which consists of cognitive, emotional and motivational processes originating from multiple brain networks and neuronal oscillations [30, 265, 266]. Therefore, by studying neural integration, i.e., the integration among brain regions or oscillations, I may find the neural markers of pain. Past research suggested that two types of integration may be informative of both acute and chronic pain: functional or structural connectivity among brain regions, and cross-frequency coupling (CFC) [23, 267]. In the line of research analysing these integrations, some evidence specific to pain was disclosed in the aspect of physiological analysis. Previous work suggested the role of functional connectivity with fMRI [35], and some other work using local field potentials (LFPs) revealed the cross-frequency coupling between gamma and alpha or theta bands [34]. However, it is still under research about the approach to utilise such integration as neural markers for pain prediction with machine learning [264]. In this study, I investigated such neural integrations using machine learning approaches. The mathematical index quantifying these integrations will be defined as a neural marker of integration.

I first surveyed measures that could effectively quantify the integrations. Past research investigated several aspects of the EEG signal with particular attention to oscillations recorded both during spontaneous ongoing pain in chronic pain patients [33] and during painful stimulation in laboratory volunteers [32, 268]. For example, several studies investigated delta ($\approx 0.5-4$ Hz), theta ($\approx 4-7$ Hz), alpha ($\approx 8-12$ Hz), beta ($\approx 13-30$ Hz), and gamma oscillations (>30 Hz) related to phasic and tonic painful thermal stim-

uli in healthy individuals [30, 269]. Among these frequency ranges, alpha and gamma bands seem the ones having potential as neural markers of pain [189, 268, 270]. Previous work suggested that the gamma oscillations arise from the interaction between excitatory and inhibitory neuronal networks, where GABAergic interneurons synchronise the electric activities among neuronal populations. Thus, the gamma band carries some evidence of the dynamical mechanism of cortical inhibition, which can represent the complexity of pain processing among cortices [271]. Specifically, several studies suggested that event-related synchronisation (ERS) in the gamma range triggered by painful nociceptive stimuli could be the only EEG feature specific to pain perception [272]. This ERS is thought to represent a cortical inhibition which is likely involving several brain structures and maximally expressed at the centro-parietal region of the scalp for phasic [194] and frontal for tonic nociceptive stimulation [189, 273]. However, there are concerns about the reliability and robustness of these responses, particularly on whether this signal is entirely of neural origin or rather an artefact of muscle activity [194, 196]. By contrast, the pain-related modulation observed in the alpha frequency range suffers less from artefactual contamination and has recently been the subject of intense research due to mounting evidence in both clinical and experimental models of pain. Specifically, it was suggested that changes in individual peak alpha frequency (PAF) can predict pain sensitivity. More precisely, scholars suggest that slow alpha frequency at rest is predictive of increased pain experience during painful stimulation [32, 193, 268]. Nevertheless, both the gamma ERS and PAF are spatially confined and may not reflect neural integration across cortical structures [32, 193, 268, 272]. On the contrary, func-

tional connectivity is a measure of the EEG signal which allows accounting for statistical interdependencies between brain signals originating from different regions [274]. Similarly, cross-frequency coupling (CFC) can be conceived as a measure of neural integration across different neuronal oscillations [275].

Based on these previous findings, I aimed to identify neural markers of integration able to inform the machine learning models for pain prediction, and hence reveal the neural integration specific to pain against baseline and sensory conditions. Upon scrutinising previous research, I noticed colleagues most often investigated spectral and spatial information. For example, one approach entailed feeding the machine learning models with the original EEG frequency spectrum or temporal series [276, 277]. Another approach focused on producing novel measures out of the original spectrum or temporal series [40, 278]. The latter inspired our methodology which focused on developing new features of neural integration from EEG functional connectivity and CFC measures.

The diversity of available functional connectivity and CFC measures raised the question of which measures to use. I aimed to answer this question by developing a quantitative assessment of neural integration focused on two features: oscillatory power and phase. In keeping with previous literature, I quantified neural integration as the synchrony between two series from different sources, i.e. channels or frequency bands in EEG signals [279, 280]. The combination of power and phase could lead to three integrative features, namely phase-to-phase, phase-to-power, or power-to-power between different frequency bands or EEG channels. Nevertheless, I restricted our investigation to phase-to-phase and power-to-power synchrony for analysing the independent con-

tributions of phase or power. Phase lag index (PLI) [279], phase locking value (PLV) [281], and inter-site phase clustering (ISPC) [8, 282] are amongst the most used measures of EEG synchrony. These can effectively quantify the phase lags between two phase series, but only ISPC (in its weighted form - with power as the weights), would contain the phase-based and power-based integration [8, 232]. On the other hand, spectral coherence (i.e. square-magnitude coherence) is a common choice to show the integration between two power series. Since spectral coherence quantifies the phase synchrony like the ISPC, either measure was thus the optimal choice to facilitate the comparison of the machine learning performance for both oscillatory EEG phase and power.

After extracting the features, they were fed into support vector machine (SVM) classifiers. The classifiers' prediction accuracy would then reflect how well these features were qualified to index neural activity associated with pain perception. Our study focuses on the alpha band as the origin of functional connectivity for pain prediction, due to its rising popularity as a potential biomarker of pain sensitivity [191]. Moreover, I assessed low-frequency oscillations (i.e. delta, theta and beta bands) in terms of CFC due to their potential aspecific contribution to pain processing [30].

Besides good prediction accuracy, a promising pain prediction system for clinical application would demand high computational efficiency. In general, computational load depends on the number of features, which can be reduced by means of an efficient feature selection process. This is particularly relevant to connectivity analysis which often generates thousands of features. This is an important issue because the clinical/care setting often relies on limited computational resources such as low computational speed

as well as the need of involving the patient's caretakers [283]. Consider the scenario where the detection of pain would be instrumental to the optimal patient's treatment, if the time required for detecting pain is long, the caretakers may not be able to treat the patient in time [284]. In this scenario, both long classification trials, or a large number of integrative features, may contribute to reduce prediction performance. Hence the need to reduce trial length and number of features to optimise the machine performance and achieve higher accuracy in the shortest time and with the least amount of information.

To sum up, I evaluated EEG neural markers of integration, including functional connectivity and CFC, based on their performance, as per prediction accuracy and computational efficiency. The machine learning models aimed to distinguish resting state and thermal pain, as well as thermal pain and innocuous thermal sensation. I first applied a feature selection method on a subset of the data and then trained machine learning models for pairwise classification with controlled numbers of selected features. To expose the neural markers of integration for tonic pain, I contrasted features used to distinguish the thermal pain condition against the baseline resting state and the sensory control condition across accuracy and efficiency of prediction associated with different neural markers of integration, including the inter-channel phase and power functional connectivity at the alpha band and the intra-channel CFC among frequency bands. In addition, I analysed the impact of trial lengths and number of features on both prediction accuracy and computational efficiency. By virtue of these analyses I expected to identify the regions/frequencies of interest apt to be interpreted as neural markers of integration of experimental tonic pain.

4.2 Methodology

4.2.1 EEG pre-processing

To investigate how trial lengths affected prediction accuracy, I segmented the data into 1, 2.5, 5, and 10 sec(s) trials (overlap 50%). The EEG signals were transformed using current source density (CSD) to reduce the signal distortion caused by volume conduction and produce a sharper or more distinct topography [285, 286]. Before feature extraction, the signals were band-pass filtered by a fifth-order Butterworth filter into four frequency bands: delta (0.5-4 Hz), theta (4-7 Hz), alpha (8-12 Hz) and low beta (12.5-16 Hz). Then I applied Hilbert transform to calculate the power and phase of signals (see Figure 4.1a).

4.2.2 Functional connectivity and cross-frequency coupling

I calculated the functional connectivity and the cross-frequency coupling from Laplacian derivative of the scalp sensors (i.e. EEG channels) calculated through CSD. Neural markers of integration were then generated from the calculation of phase (ISPC) or power series (square-magnitude coherence). I investigated functional connectivity only in the alpha band from different channels, and CFC between two frequency bands from each electrode. Thus, I simplified comparisons into functional connectivity vs. CFC, and power vs. phase. Specifically, I measured functional connectivity features as phase or power between two channels, i.e. alpha-phase connectivity (PhaCon) and alpha-power connectivity (PowCon). As to CFC, I measured various pairs of frequency coupling (across

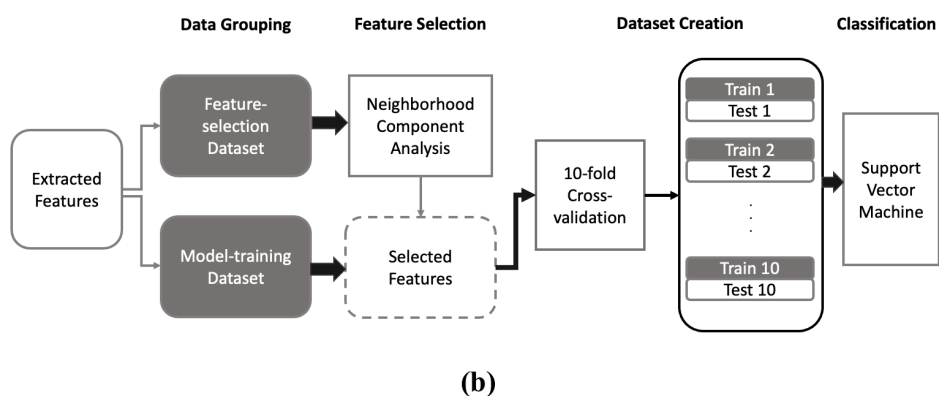
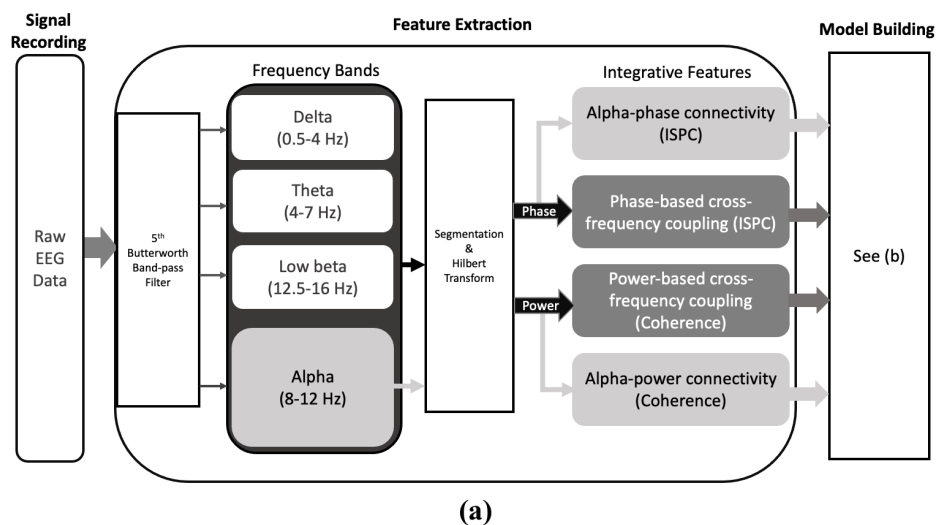


Figure 4.1: **(a) Pre-processing pipeline:** First, delta (0.5-4 Hz), theta (4-7 Hz), alpha (8-12Hz), and low beta (12.5-16 Hz) bands were extracted from the raw EEG data. I then computed power and phase using Hilbert transform. Then, I extracted the neural markers representing functional connectivity or cross-frequency coupling. **(b) Model training and testing pipeline:** I split data into two groups. While one dataset was used for feature selection, the other was used to train and test the classifiers with the selected features using 10-fold cross-validation. Subsequently, feature-selection and model-training datasets would be swapped.

delta, theta, alpha and low-beta bands) per each EEG channel and for both phase and power, i.e. phase-based CFC (PhaCou) and power-based CFC (PowCou).

Inter-site phase clustering

The ISPC describes the distribution of phase differences between two temporal series from different sources, i.e., EEG channels or frequency bands in this study. It is calculated in the following formula:

$$ISPC_{xy} = \left| \frac{1}{n} \sum_{t=1}^n e^{i[\phi_x(t) - \phi_y(t)]} \right| \quad (4.1)$$

where n represents the total number of time points in each data series, ϕ_x and ϕ_y represent the phase angles from two series (i.e. series from two channels for functional connectivity, or two frequency bands for CFC). In short, ISPC is the mean exponential value of the imaginary phase angle differences between the signals from two sources in a particular time window, whose values range from 0 to 1.

Magnitude-squared coherence

Coherence is computed via cross-power spectral density (PSD) between two EEG series from different sources, which reflects the correlation between two series' power distributions:

$$K_{xy} = \frac{S_{xy}}{S_{xx}S_{yy}} \quad (4.2)$$

where S_{xy} represents the cross PSD between data series x and series y , and S_{xx} is the PSD of the signals from series x . With the PSD ratio, the coherence between the signals

x and y can be calculated as:

$$COH_{xy} = |K_{xy}|^2 \quad (4.3)$$

Alternatively, it can be rewritten in a Euler-like format as the weighted ISPC with the analytic magnitudes (e.g. $m_x(t)$ from channel x) as the weights [8]:

$$COH_{xy} = \left| \frac{1}{n} \sum_{t=1}^n |m_x(t)| |m_y(t)| e^{i[\phi_x(t) - \phi_y(t)]} \right| \quad (4.4)$$

Topographical analysis

I calculated the z-scores of the power and phase for the different conditions. These were then used to visualise the current scalp distribution. It is noteworthy that, while the topographical representation of power is straightforward, this is not the case for the visualisation of phase. Because the phase is not a measurement of strength, the mean or median intensity of a region cannot be calculated arithmetically. However, according to the ISPC formula (6.1), this issue can be resolved using the mean Euler-like format of phases across trials calculated as $P_x = \left| \frac{1}{n} \sum_{t=1}^n e^{i[\phi_x(t)]} \right|$ of channel x , which is defined as the *exponential phase* in this study. To analyse the variation of power/phase distribution, I calculated the topography within each frequency band and condition.

I then computed Pearson correlations to test significant differences between pairwise conditions within the same frequency band. Accordingly, the higher the Pearson correlation coefficient the greater the degree of association between two topographies, which reflects a higher similarity in spatial distribution [287].

4.2.3 Machine learning

I trained binary classifiers between all pairwise conditions (with H, W, O and C). I split the pre-processed data into two sets, including one for feature selection and another one with the same size for evaluation. Following feature selection, the set excluded from feature selection went through training and testing of the binary classifiers with 10-fold cross-validation. Then the two sets were swapped, and the same process was executed again.

Feature selection based on neighbourhood component analysis (NCA)

When considering the amount of channels (i.e. 62) and frequency bands (i.e. four) per trial, I could theoretically extract $\sum_{i=1}^{N_{ch}-1} i = 1891$ functional connectivity and $(\sum_{i=1}^{N_f-1} i)N_{ch} = 372$ CFC features, where N_{ch} and N_f are the number of EEG channels and frequency bands. Clearly, this feature-extraction scenario would require significant time expenditure, and numerous features will also increase the necessary amount of trials for model training. Furthermore, with the selected features, the involved brain regions or frequencies can help this study identify regions of interest (ROIs) or frequency bands specific to pain. Hence, I can interpret the mechanism of how these features work by analysing them with respect to the physiological findings.

To select the important features, I used the neighbourhood component analysis (NCA) proposed in [288]. If the distance between two samples in a dataset $T = (\mathbf{x}_i, y_i), i \in [1, N], \mathbf{x}_i \in R^d$ containing N labelled samples, where \mathbf{x}_i are the feature vectors of samples, and $y_i \in \{1, 2, \dots, c\}$ are the class labels representing the classes with the total

number of c in the classification (in this study, $c = 4$), then the distance between two samples \mathbf{x}_i and \mathbf{x}_j is defined as:

$$D_w(\mathbf{x}_i, \mathbf{x}_j) = \sum_{l=1}^d w_l^2 |x_{il} - x_{jl}| \quad (4.5)$$

NCA aims to optimise the weights w_l in order to maximise the leave-one-out nearest neighbour (NN) classification accuracy. The final weights would be referred to as:

$$\mathbf{w} = \arg \max_{w_l} \left(\sum_i \sum_j y_{ij} p_{ij} - \lambda \sum_{l=1}^d w_l^2 \right) \quad (4.6)$$

where p_{ij} is the joint probability of samples \mathbf{x}_i and \mathbf{x}_j , ($y_{ij} = 1$ when $y_i = y_j$, $y_{ij} = 0$), λ is a regularisation parameter tuned via cross-validation. The output \mathbf{w} is the optimised weight vector representing the significance of each feature in classification. I then selected N features with the highest weights from \mathbf{w} used in the classification. I used 10-fold cross-validation for the NN classification within NCA. To determine the features contributing the most in each pairwise classification, six binary classifiers were trained across four conditions. Then I defined the features shared by at least two binary classifiers with one common condition as the representative features of this condition. It follows that the features shared by the three classifiers can be interpreted as the most intrinsic neural integration for one experimental condition. For instance, I defined the important connectivity between channel x and channel y selected from the classifiers O vs H , C vs H , and H vs W , as the representation of class H.

To investigate the impact of the number of features, the features were sorted according to the weights calculated from equation 4.6. I selected one hundred features with the

highest weights from each participant and then the selected features across participants that were kept as candidates potentially involved in training. Across these feature candidates, I summed up the weights of each feature's occurrences as the candidates from all participants. Then the 100 features with the highest accumulated weights were used in primary model training for most research objectives. To analyse the prediction performance with fewer features classification was also performed with 10, 20, 30, ..., 80 and 90 features according to the rank of weights. Finally, I determined the optimal feature number balancing accuracy and efficiency and used this to select the ROIs for physiological analysis.

Classification procedure

Six binary support vector machine (SVM) [289] classifiers (*O vs H*, *O vs W*, *C vs H*, *C vs W*, *O vs C*, and *H vs W*) were trained on the selected features. Then one dataset with 50% trials, previously excluded from the feature selection phase was used as the dataset to quantify the performance of the classifiers. I applied 10-fold cross-validation and quantified both within-condition accuracy for each condition and the mean accuracy across all the conditions.

Computational efficiency

To evaluate the computational efficiency of each feature type, 2000 trials were randomly selected from all trials within each trial length (1, 2.5, 5, and 10 sec). I extracted four types of features from the selected trials and measured the run time during feature ex-

traction and model training, respectively. Finally, I compared the feature extraction and model training time of each feature type to quantify their computational efficiency. The tests were executed with different numbers of features (20, 40, 60, 80 and 100). Because the final goal is to apply the model at the bedside, the efficiency tests were all run on a personal computer (Dell OptiPlex 7050 with Intel Core i7-6700 CPU @ 3.40 GHz, 16.0 GB RAM).

Statistical inference

I performed a linear mixed model analysis of the prediction accuracy and efficiency using the *Linear Model* module in *jamovi* (Version 1.6, The jamovi project (2021), retrieved from <https://www.jamovi.org>). In this analysis, functional connectivity vs. CFC, phase vs. power, and the pairwise comparison in each pair of trial lengths were included as fixed effects. The significance level (α) was set as 0.05, and Holm-Bonferroni correction was applied for post-hoc testing. All the statistical comparisons between functional connectivity and CFC or between phase and power were carried out on the 100-features dataset.

4.3 Results

4.3.1 Prediction accuracy

Table 4.1 reports the within-condition and mean accuracy across all conditions within different feature types. Figure 4.2 shows the binary classification accuracy versus neural

Table 4.1: **Comparisons of sensitivity and accuracy affected by different settings using 100 features in each test.** The prediction sensitivity and accuracy of each setting of trial lengths and feature types were shown in the form of mean sensitivity/accuracy(\pm standard deviation (%)).

Length	Feature	Accuracy of O	Accuracy of C	Accuracy of H	Accuracy of W	Accuracy
1	PhaCon	76.63 \pm 11.57	86.71 \pm 8.28	73.82 \pm 13.13	75.87 \pm 11.65	78.70 \pm 11.76
	PowCon	53.39 \pm 13.63	52.05 \pm 21.88	53.88 \pm 15.82	59.64 \pm 15.20	54.85 \pm 15.57
	PhaCou	74.28 \pm 12.05	86.44 \pm 9.63	72.19 \pm 14.25	74.04 \pm 12.87	77.10 \pm 12.89
	PowCou	61.54 \pm 14.75	72.99 \pm 17.11	61.75 \pm 17.00	64.83 \pm 14.35	65.92 \pm 15.41
2.5	PhaCon	81.83 \pm 11.83	92.30 \pm 7.61	79.29 \pm 13.11	80.71 \pm 12.01	83.63 \pm 12.02
	PowCon	58.58 \pm 18.86	53.71 \pm 26.06	59.03 \pm 16.71	62.37 \pm 16.91	58.34 \pm 17.88
	PhaCou	81.43 \pm 11.87	92.48 \pm 8.32	79.81 \pm 12.89	79.91 \pm 12.48	83.26 \pm 12.32
	PowCou	72.13 \pm 14.65	85.12 \pm 12.63	68.90 \pm 17.00	73.04 \pm 14.69	75.30 \pm 15.13
5	PhaCon	84.78 \pm 13.49	95.04 \pm 7.02	84.35 \pm 12.53	84.47 \pm 12.02	87.07 \pm 11.32
	PowCon	64.92 \pm 19.12	60.49 \pm 28.47	63.98 \pm 16.60	68.59 \pm 16.13	64.29 \pm 18.30
	PhaCou	85.30 \pm 11.75	95.02 \pm 6.97	84.81 \pm 12.67	82.99 \pm 12.48	86.03 \pm 12.00
	PowCou	76.81 \pm 14.69	89.04 \pm 12.55	72.98 \pm 16.99	76.46 \pm 14.87	79.28 \pm 15.10
10	PhaCon	88.42 \pm 12.16	97.69 \pm 6.47	88.72 \pm 11.75	87.53 \pm 11.43	89.23 \pm 11.31
	PowCon	68.24 \pm 19.77	67.55 \pm 27.64	68.84 \pm 17.75	72.19 \pm 16.29	68.28 \pm 18.32
	PhaCou	86.94 \pm 13.09	96.32 \pm 7.52	85.63 \pm 14.84	85.38 \pm 13.53	86.01 \pm 13.46
	PowCou	80.49 \pm 15.57	92.56 \pm 11.87	76.12 \pm 17.22	79.22 \pm 14.74	82.43 \pm 15.26

Table 4.2: **Summary of post-hoc comparisons to the accuracy for the trial lengths and feature types.** Asterisks represent statistical two-tailed significance out of Holm-Bonferroni method were produced ($* < 0.05$, $** < 0.01$, $*** < 0.001$). In the columns, A and B represent the values of the same property to be compared in the post-hoc analysis, where the accuracy produced with the properties of A or B were compared statistically. For example, the first column shows the differences of the accuracy produced by the trials with lengths of 10 and 5 seconds.

		Comparisons between A and B						
		A	B	Difference	SE	t	df	p
(a) Trial Length (s) vs. Trial Length (s)	10	5	0.0215	0.0084	2.57	3	*0.040	
	10	2.5	0.0608	0.0130	4.69	3	*0.040	
	10	1	0.1240	0.0167	7.45	3	*0.018	
	5	2.5	0.0393	0.0078	3.63	3	*0.040	
	5	1	0.1025	0.0121	8.50	3	*0.018	
	2.5	1	0.0632	0.0123	5.14	3	*0.040	
(b) Feature Type vs. Feature Type	PhaCon	PowCon	0.2400	0.0080	30.05	3	***<0.001	
	PhaCon	PhaCou	0.0172	0.0074	2.32	3	0.085	
	PhaCon	PowCou	0.0936	0.0137	6.81	3	*0.018	
	PowCon	PhaCou	-0.2227	0.0126	-17.66	3	**0.002	
	PowCon	PowCou	-0.1463	0.0126	-11.645	3	**0.005	
	PhaCou	PowCou	0.0936	0.0137	6.81	3	*0.037	

markers and trial lengths. Because the main goal is distinguishing pain from non-pain states, I focused on the classification between non-pain resting state and painful thermal stimulation (eyes-open vs hot; 'O vs H'). Thus, the analysis of trial lengths and feature types was based on the binary classification between 'eyes-open' and 'hot' conditions. As the result, Table 4.2 shows the statistical tests between the accuracy produced with different trial lengths or feature types. In conclusion, the linear mixed model revealed that both trial length ($F(3, 9) = 43.3, p < .001$) and feature type ($F(3, 9) = 175.0, p < .001$) significantly affected prediction accuracy.

The effect of feature type

Phase-based features generally performed better than power-based features. The accuracy produced with alpha-phase connectivity is 24.00% higher than alpha-power connectivity ($t(6) = 30.05, ***p < .001$), and phase-based CFC predicted pain with 9.36% higher accuracy than power-based CFC ($t(6) = 6.81, *p = .037$). In summary, alpha-phase connectivity performed best. Considering the only difference between spectral coherence and ISPC is the presence of the signal amplitudes, these comparisons suggest that power weakened the performance of the pain prediction model. Therefore, I analysed Pearson correlation coefficients between conditions using the topography of magnitudes or Euler-like phases as mentioned in Section 4.2.2, to determine whether power or phase carry more differences across conditions (See Figures 4.3 and 4.4). As can be expected, Table 4.3 revealed no significant correlations between power-based and phase-based topography ($|r(62)| < .50$). In the pairwise analysis with each frequency band, the

Pearson correlation coefficients between conditions were $r(62) = .93 \pm .05, ** *p < .001$ for power topography, and $r(62) = .03 \pm .15, p = .423 \pm .322$ for phase topography. This demonstrated higher similarity among topography patterns of power than of phase.

Table 4.3: Summary of comparisons between power and phase z-score topography as represented with Pearson correlations (r-value, p-value). Asterisks represent statistical two-tailed significance (Significance level $\alpha = 0.05$, $**p < 0.01$, $*p < 0.05$).

	Hot	Warm	Eyes-open	Eyes-closed
Delta	(-.49, **.000)	(-.14, .261)	(.05, .705)	(-.32, *.011)
Theta	(-.31, *.013)	(.42, **.001)	(-.05, .715)	(.22, .093)
Alpha	(-.18, .155)	(.14, .275)	(.48, **.000)	(-.41, **.001)
Low Beta	(-.14, .272)	(-.21, .094)	(.10, .436)	(.20, *.048)

The effects of trial length and feature number

Accuracy increased with trial length (Figure 4.2). The mean accuracy was 68.9%, 75.2%, 79.1%, and 81.3% within the trial length of 1, 2.5, 5 and 10 sec respectively. Figure 4.5 displays the relationship between prediction accuracy and the number of selected features used by each classifier. Accuracy generally increased with increasing number of features. Without considering the eyes-closed condition (C), the accuracy increased

Table 4.4: **Summary of pairwise comparisons across power magnitude's z-score topography as represented with Pearson correlations (r-value, p-value).** Asterisks represent statistical two-tailed significance (Significance level $\alpha = 0.05$, *** $p < 0.001$).

	HvsW	HvsO	HvsC	WvsO	WvsC	OvsC
Delta	(.73, ***.000)	(.94, ***.000)	(.92, ***.000)	(.86, ***.000)	(.90, ***.000)	(.99, ***.000)
Theta	(.94, ***.000)	(.99, ***.000)	(.93, ***.000)	(.94, ***.000)	(.94, ***.000)	(.94, ***.000)
Alpha	(.94, ***.000)	(.97, ***.000)	(.92, ***.000)	(.94, ***.000)	(.93, ***.000)	(.94, ***.000)
Low-Beta	(.95, ***.000)	(.96, ***.000)	(.97, ***.000)	(.91, ***.000)	(.92, ***.000)	(.98, ***.000)

Table 4.5: **Summary of pairwise comparisons across exponential phase's z-score topography as represented with Pearson correlations (r-value, p-value).** Asterisks represent statistical two-tailed significance (Significance level $\alpha = 0.05$, * $p < 0.05$).

	HvsW	HvsO	HvsC	WvsO	WvsC	OvsC
Delta	(.21, .101)	(-.08, .541)	(.21, .097)	(-.26, *.044)	(-.24, .057)	(-.01, .960)
Theta	(.07, .592)	(-.03, .802)	(-.20, .110)	(-.01, .921)	(.15, .244)	(.27, *.033)
Alpha	(.23, .074)	(-.02, .874)	(.12, .370)	(.04, .734)	(.09, .466)	(.11, .380)
Low-Beta	(.01, .925)	(.15, .242)	(-.05, .696)	(-.19, .136)	(.13, .305)	(-.10, .446)

more slowly.

4.3.2 Computational efficiency

Figure 4.5 displays the effects of feature number and trial length on computational efficiency, i.e., time cost, in the model training phase. When the number of extracted features is the same, functional connectivity features cost less time - which means they had higher efficiency - than CFC features ($0.0130 \pm 0.0140s$ vs $0.0377 \pm 0.0443s$, $t(196) = 5.281, ** *p < .001$). But there was no significant difference in the computational time cost between the phase- and power-based features ($0.0247 \pm 0.0338s$ vs $0.0260 \pm 0.0364s$, $t(196) = 0.273, p = 0.785$). Both phase-based and power-based features did not show significant correlations between feature number and mean time cost in each trial (see Figure 4.7, $F(9, 190) = 0.0732, p = 1.000$).

4.3.3 Significant neural markers of integration

According to the accuracy and efficiency findings, I then selected the 40 features with the highest classification weights from each feature type (Figure 4.8). The extracted features for each experimental condition (see Section 4.2.3) exposed the most relevant integrations of the condition. Upon qualitative scrutiny of these features, the delta band contributed only toward power-based CFC features. While the other three bands contributed to both CFC feature types. The phase-based CFC features with high contributions were distributed over the occipital region of the scalp, and were only found in resting states, but power-based CFC features displayed effects in the conditions with thermal

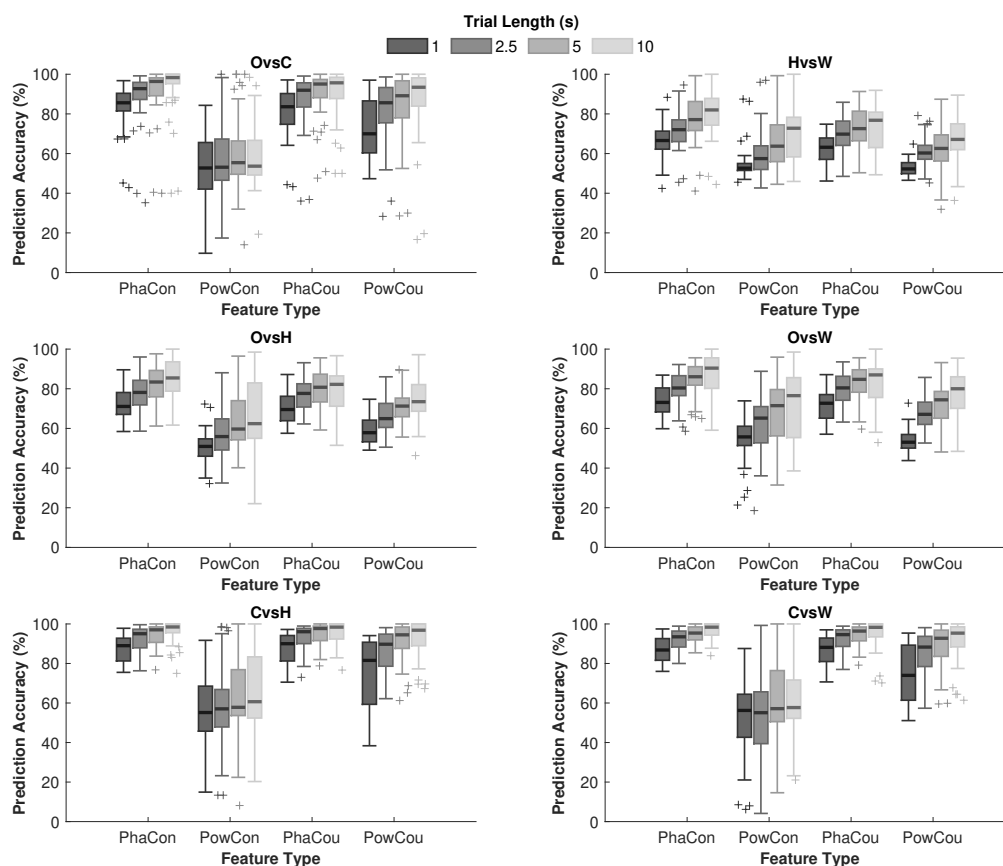


Figure 4.2: **Boxplots of binary classification accuracy versus feature type.** Each plot represents the median of prediction accuracy (y axis) for the 100 features dataset across experimental conditions. The box edges are the 25th and 75th percentiles, the outlines indicate the 95th percentile, the plus sign indicate values out of the confidence interval. The labels 'O' and 'C' represent 'eyes-open' and 'eyes-closed', while 'H' and 'W' mean 'hot' and 'warm'. Alpha-phase connectivity ('PhaCon'), alpha-power connectivity ('PowCon'), phase-based CFC ('PhaCou'), and power-based CFC('PowCou') are displayed on the x axis according to different trial lengths (arranged by different degrees of gray). Each subplot represents one pair of binary classification.

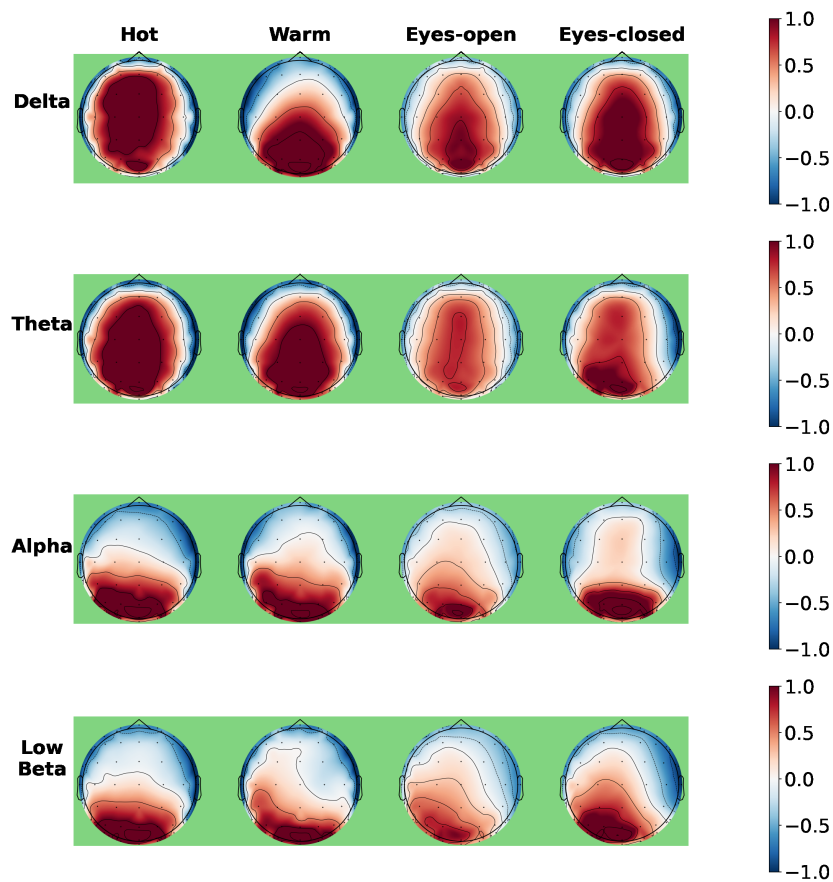


Figure 4.3: **Brain topography of z-scored signal amplitude versus conditions and frequency bands.** Each plot represents the z-scored brain topography of the median signal amplitudes calculated as the square roots of power spectral density (PSD) across pain-related conditions and frequency bands. Each row of plots represents the topography from the same frequency band, and each column of plots represents the same experimental condition. All of the topography does not involve any significant differences from the other one in the same frequency band, the green background represents the topography has significantly high similarity with at least one of the topography within the same band (** $p < .001$).

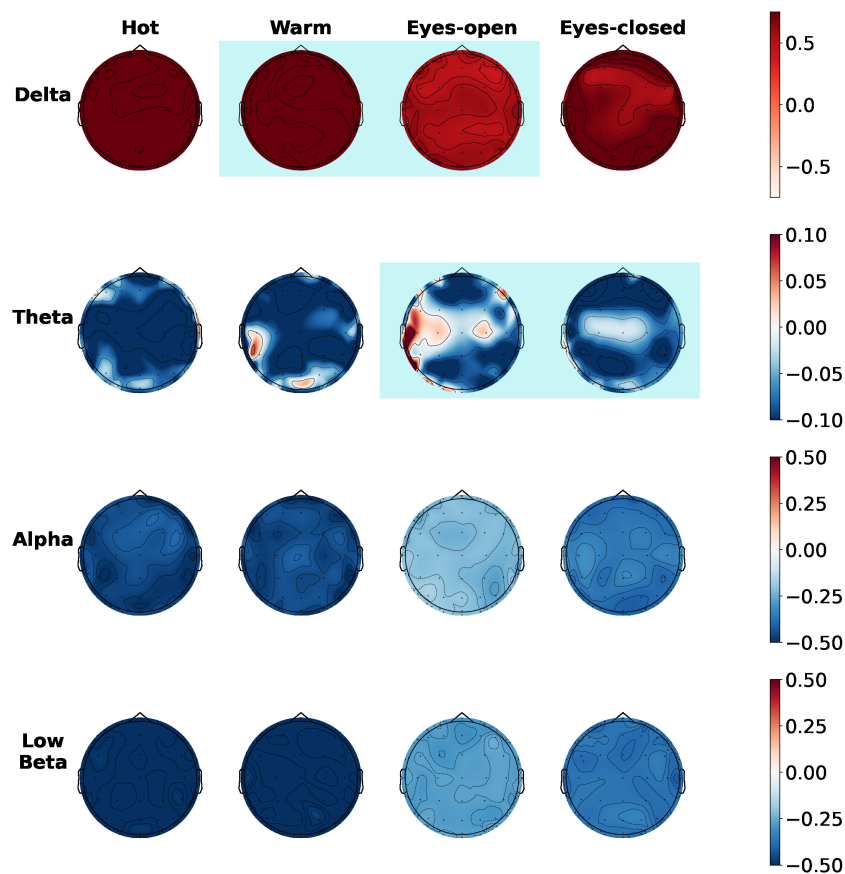


Figure 4.4: **Brain topography of z-scored exponential phase versus conditions and frequency bands.** Each plot represents the z-scored brain topography of the median signal amplitudes calculated as the square roots of power spectral density (PSD) across pain-related conditions and frequency bands. Each row of plots represents the topography from the same frequency band, and each column of plots represents the same experimental condition. The topography with blue backgrounds involves significant similarity to at least one in the same frequency band ($*p < .05$), while the others are significantly different.

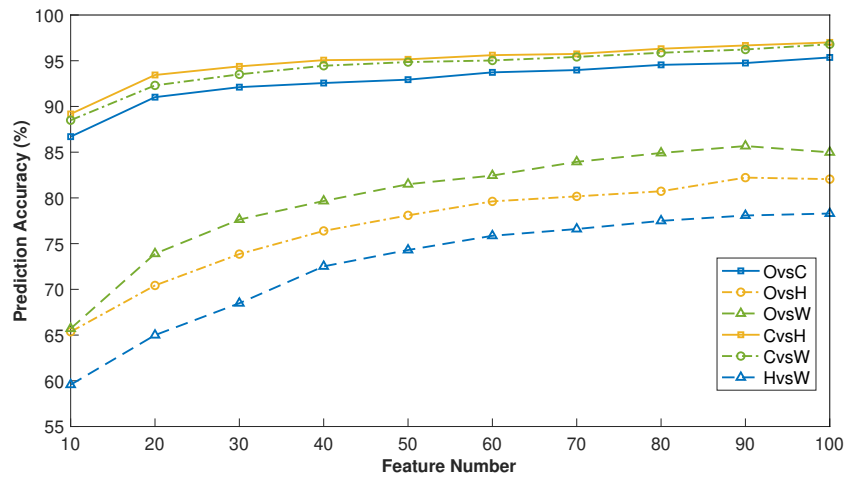


Figure 4.5: **Prediction accuracy of each pairwise classification versus the feature number.**

Each line represents the effects of feature numbers to the prediction accuracy within one pairwise binary classification, in which the tested feature numbers were discrete with a step of 10 between 10 and 100.

stimulus as well (the last two columns of Figure 4.8).

Compared with the three other neural marker types, the most relevant phase-based functional connectivity features were more widely distributed across the scalp (see column 'PhaCon' in Figure 4.8). Specifically, while the PhaCon feature was distributed over the frontal, central and occipital regions, the power-based and CFC features were concentrated in the occipital region. Such difference in distribution pattern likely facilitated a high classification accuracy with phase-based alpha connectivity. This finding led me to select this specific feature to further analyse the planned ROIs for each experimental condition (Figure 4.9). As a result, I identified precise patterns of connectivity for each con-

dition. For example, during tonic pain (H) I identified significant connectivity between electrodes AF8 and F7, thus indicating a role of interhemispheric communication at the level of the frontal region (shown in the intersection between the column and the row of H in Figure 4.9). Importantly, when combined with the connectivity pattern identified for the innocuous condition (W), the classifier can provide discrimination between the two brain states. Moreover, the difference between resting states (O and C) and the innocuous warm condition (W) was localised over the central leads (e.g. C3-CP5), but this difference was absent when comparing the innocuous warm (W) and painful hot (H) condition. Otherwise, the pattern suggested that the model can distinguish the features related to sensation of pain. In the functional connectivity pattern representing the O condition (see Figure 4.9), CZ-CP5 and P1-PO3 both contributed to distinguishing condition O from conditions H and W. Since patterns differed between conditions with and without the thermal stimulus, the connectivity within central and occipital brain regions can be concluded to represent the thermal sensation. Meanwhile, the connectivity between AF8 and F7 occurred when distinguishing pain (condition H) from all the non-painful conditions (i.e., conditions O, C, and W). Thus, such connectivity within the frontal brain regions played a different role from the ones only related to sensation, which can indicate the sensation of pain.

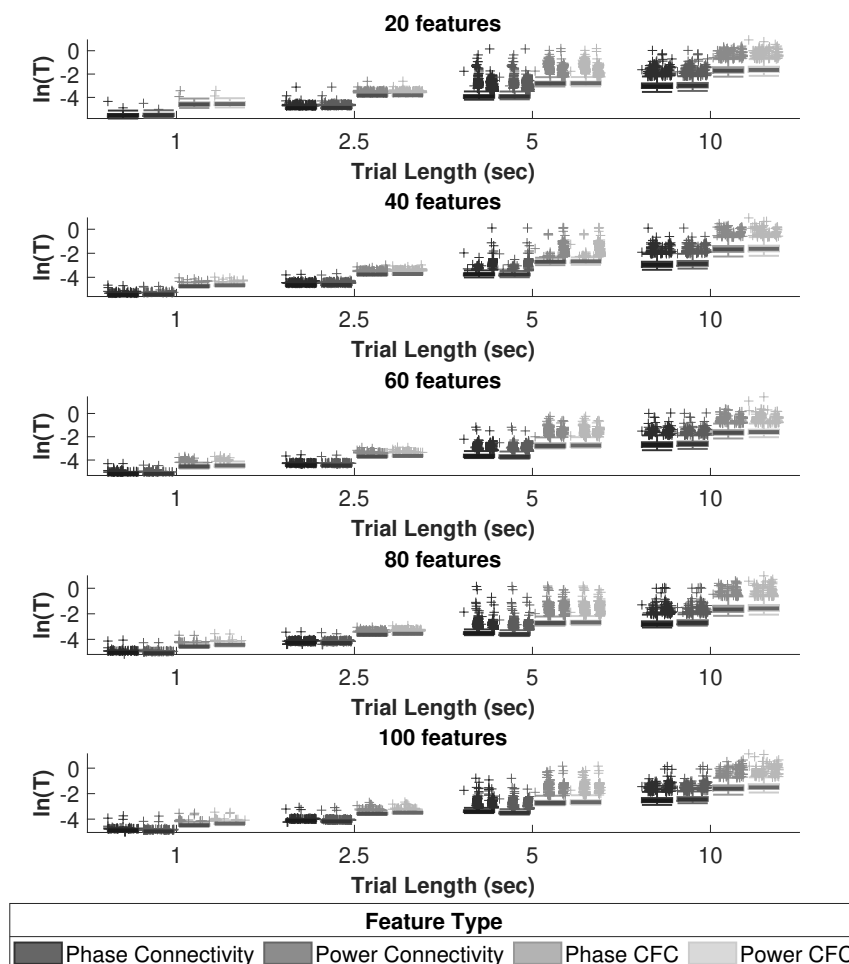


Figure 4.6: **The effects of feature type, trial length and the number of features to the time cost in feature extraction and classification.** The unit of time is the logarithm second $[\ln(T)]$, the box plots show the total running time for extracting features with specific number (i.e. 20, 40, 60, 80, and 100) and type and then predicting the class of each sample with the extracted features. In the boxplot, the central line represents the median value of the time cost's logarithms, and the outlines show the boundary of the 95th percentile, while the markers represent the time costs beyond the confidence interval.

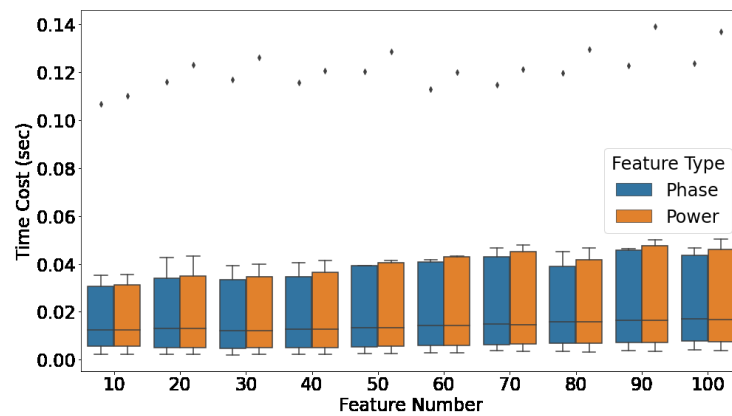


Figure 4.7: **Time cost versus the number of features, the feature types were categorized with phase and power:** The bar-plots show the distribution of time cost in seconds with studied feature numbers. The findings of time cost revealed the absence of significant differences between phase-based and power-based features, thus the time is categorized according to the features' origin, i.e., phase or power. The dots represent the outliers outside 1.5 times the inter-quartile range above the third quartile.

4.4 Discussion

I set out to find the ideal feature for predicting pain with a machine learning model. I compared neural markers representing the integrations of functional connectivity and cross-frequency coupling (CFC), and compared these markers using power-based and phase-based versions. With alpha-phase functional connectivity, the model achieved high accuracy and low time cost (i.e. high efficiency). Importantly, I selected features from the extracted alpha-phase connectivity data using NCA. Feature selection benefits pain prediction in two ways: First, the reduction of the number of features improves the computational efficiency of the model. Second, the ideal features producing good performance can help interpret the mechanism of how the neural markers reflect the brain's responses to pain.

4.4.1 From the *ideal* feature to the *ideal* setting

As shown in Section 4.3.1, the phase-based neural markers can produce significantly higher accuracy than the corresponding power-based features. This begs the question of why power-based features did not lead to good accuracy. Formulas (4.1) and (4.4) show that the magnitude-squared coherence is ISPC with signal amplitudes as weights. Therefore, the independent variable which distinguishes phase- and power-based neural markers is the power magnitude. The results indicated that the power decreases the specificity of each condition. The power distribution contains fewer differences than phase among conditions. Compared with exponential phase distribution (Figure 4.4),

the z-score topography of power magnitude (Figure 4.3) revealed a significantly higher similarity among conditions. Hence, I conclude that the differences in distributions of only phase-based features across conditions were weakened by multiplying the power magnitudes with them, making the conditions vaguer to the classifier.

Nir et al. demonstrated the correlation between alpha power and pain intensity, but our work showed negative effects of alpha power on classification accuracy [290]. That was caused by differences in the measures used, the previous work focused on the change of the power and the peak frequency at the alpha band [31, 32, 193, 290], while I utilised the patterns of the mean level of power within a time trial. Under the context of the previous studies, lower (7-10 Hz) and upper (10-12 Hz) alpha bands had different patterns of desynchronization, and such pattern variation induced the frequency content variability between conditions [290, 291]. The phase-based neural markers of integration indicate the synchronisation of integration, so the desynchronization of the alpha phase can reflect the change of alpha power during pain [292].

From the perspective of settings, I found that prediction accuracy increased with the trial length (Tables 4.1 & 4.2 and Figure 4.2). This finding defies the expectation that segmentation to shorter lengths (e.g. 1 and 2.5 sec) would be conducive to optimised classifiers due to a larger amount of training samples. Fraschini et al. revealed that the measure of functional connectivity, including PLI and amplitude envelope correlation (AEC), became stable with epochs longer than 6 secs, which changed rapidly at the length of 1, 2 and 4 secs [293]. So intrinsically, only such measures produced with trials with appropriate length can represent functional connectivity.

As described, a smaller number of features means lower time cost in feature extraction but also lower accuracy within the studied length range (Figure 4.7). Therefore, I considered the balance between time cost and model performance qualitatively when analysing the effect of feature number. Due to the best performance produced by 10-sec alpha-phase functional connectivity trials, I used them to test the effect of feature number. As shown in Figure 4.5, the accuracy for recognising the C condition was always at a relatively high level (i.e. above 85% in this study), because of the unique pattern of the alpha power in the occipital cortex, that is why I excluded the C condition from the analysis of pairwise classification. For the pairwise classification without the C condition, the prediction accuracy increased more slowly with the feature number above 40. Moreover, time costs in training the model increased with the number of features (see Figures 4.6 and 4.7). Therefore, it is beneficial to keep the feature number as low as possible. Though the generalisation of the number of features needs more evidence, forty can be seen as sufficient in the context of our findings, so I utilised this number for further analysis of the brain ROIs for exposing intrinsic integrations related to pain processing.

I analysed how time cost was affected by the type of neural markers in Figure 4.6. Only one frequency band is required for producing a functional connectivity feature, while two bands are needed for a CFC feature. Therefore, when the number of features is equivalent, the difference of time cost in band-filtering made extracting functional connectivity features quicker than CFC. Hence, due to the better prediction accuracy of phase-based features (Figure 4.2) and the higher computational efficiency (Figure 4.6),

alpha-phase functional connectivity is an ideal neural marker for pain prediction at the bedside with EEG. This feature can both simplify feature extraction and help interpret the neural mechanism behind the engineering application. Even in the comparisons with other work, it showed advantages in the following two aspects. First, in both efficiency and interpretability, though some work produced good performance in pain prediction, they involved multiple types of features, such as the combination of multiple parameters [42], or twelve types of informative features studied [294]. The combination of features made it difficult to explain the mechanism of predicting pain from neurophysiological signals and limited efficiency. The concise form of ISPC can provide higher interpretability, and the use of only one type of feature is ideal in regard to efficiency. Second, though some work also utilised only one type of functional connectivity measure and produced a good performance, ISPC can ease feature extraction. For example, Modares et al. also investigated phase-based connectivity with partial directed coherence based on the multivariate auto-regressive model, which can produce a good performance in the quantification of pain severity as well [295]. Nonetheless, the calculation for extracting ISPC is simpler. Finally, while the potential of the alpha band as the neural marker of pain was revealed before [32, 269], and the correlation of phase-based connectivity to pain was revealed but limited to theta and gamma band [296], our use of ISPC from alpha phase is an effective way to utilise the phase-based functional connectivity in pain assessment.

This work allowed us to identify the neural markers of integration. However, there were some limitations in the experimental design and the testing of parameters. In the

experimental design, the cognitive task to rate the pain with VAS was not involved in the resting states, which may imply far more different brain activations that could have been involved in these states compared with the sensory conditions. Specifically, not only the intrinsic variable contributing to the sensation of pain would contribute to the classification, but the variables related to the cognitive processing in pain rating could also have occurred in the features for the classification. In the parameter testing, the range of trial lengths was too small, i.e., in the same scale of magnitude. Thus, the effects of much more features were not tested. To resolve this limitation, future research should involve the features at different numerical scales, e.g., 10, 100, 1000, and all of the possible features.

This work presented a potential solution to extract biomarkers efficiently, which can possibly work in mobile systems with limited computational resources. Particularly, the developers of healthcare systems can deploy the models based on the alpha-phase functional connectivity to EEG-based mobile systems, whose terminal devices can be mobile phones or laptops. In general, such mobile and low-cost systems can help the patients' caretakers at the bedside. However, the current work can only demonstrate the feasible use of alpha-phase functional connectivity to patients who can report pain as labels. It is still unclear if it can fit the requirements of unresponsive patients - this chapter only discussed the prediction performances trained and evaluated with the same individuals. To fill the gap between the discovery of features and the clinical needs, the follow-up work should first figure out a way to generalise the models based on alpha-phase functional connectivity across different individuals. Particularly, the approach should be able

to assess pain in novel individuals without any labels for training.

4.4.2 Topographical regions of interest in tonic pain prediction

The feature selection I implemented in the current study allowed this work to achieve optimal computational efficiency. This in turn facilitated the identification of the functional connectivity that significantly contributes to pain prediction. I identified a few patterns that may be further investigated in future research, upon qualitative assessment of Figure 4.8. One can identify several features. The most salient difference revolves around the clustering of features within the occipital region vs. a distributed long-ranging connectivity for the alpha-phase features. Nevertheless, other patterns can be identified.

Hot (Pain)

- *Short-range interhemispheric frontal connectivity*

In this study, the crucial task was distinguishing the pain condition (H) from the non-pain conditions. The specific characteristic of the H condition was one connectivity at the frontal region, AF8-F7 (see Figure 4.9). This is in line with previous findings, including the strong correlation between alpha-phase synchrony in the frontal region during pain conditions [297], and the change of alpha power in the frontal region reflecting chronic pain [298].

- *Long-range occipital connectivity*

While the frontal region's functional connectivity was specific to the pain condi-

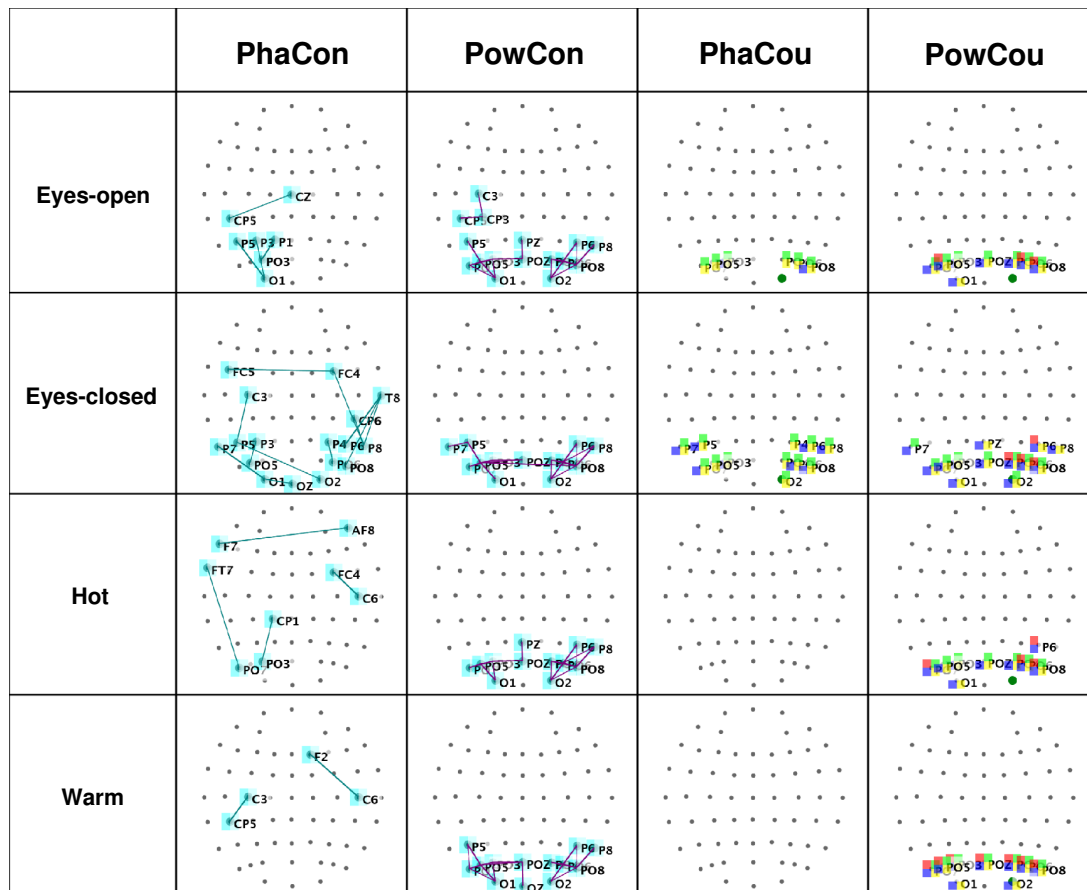


Figure 4.8: **Features showing the characteristics selected from each type of neural marker of integration:** After selecting 40 features with NCA from each type of feature, the ones shared by at least two binary classifiers containing every individual condition were selected to represent the characteristics, the rows represent the conditions, while the column is for the feature type. In the last two columns showing the selected features from coupling features, the color of each square represents the frequency band involved in the CFC at the corresponding channel (red- delta, green- theta, blue- alpha, yellow- low beta).

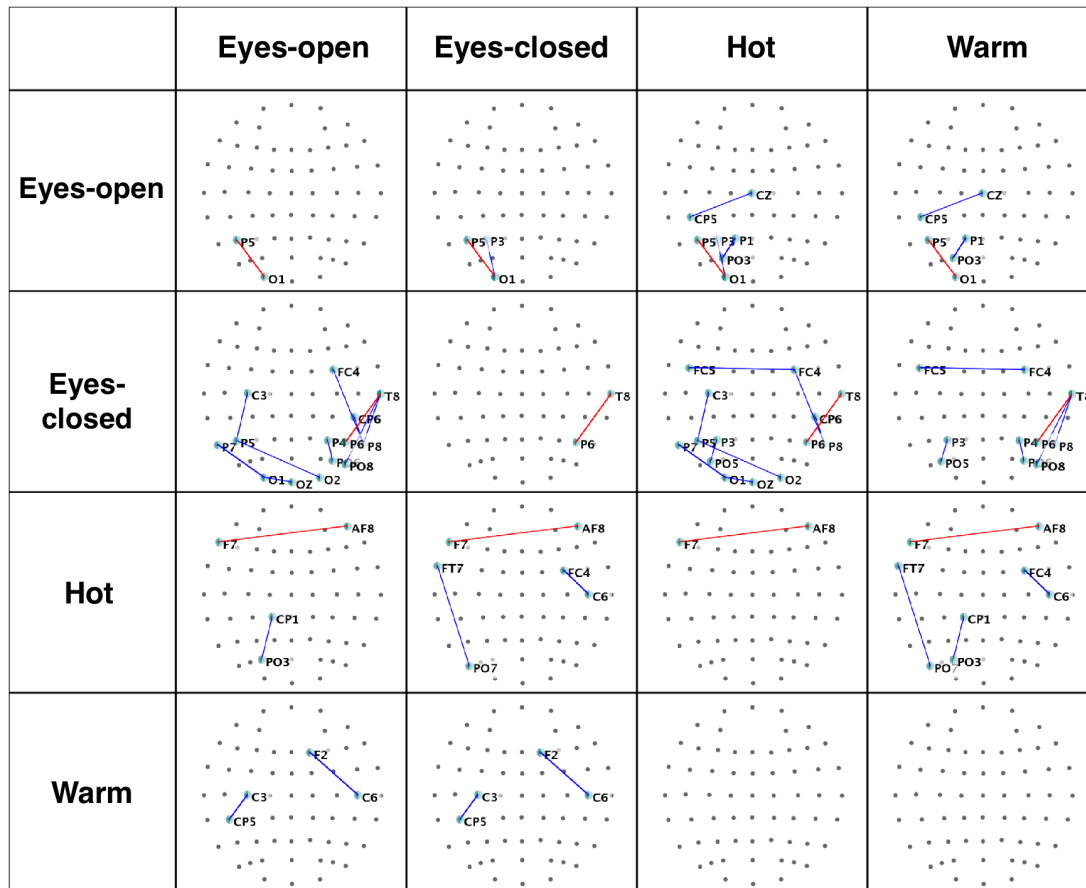


Figure 4.9: Selected features from alpha-phase connectivity features of each condition versus the other conditions. Except for the diagonal from top-left to right-bottom, the row represents each targeting conditions, the column represents the other condition in the corresponding binary classifiers, in which the features are shared by at least two classifiers containing the targeting condition, such features were marked with blue lines in the figure. And the ones on the diagonal show the significant features of every condition, which were shared by all classifiers containing the corresponding condition, which are marked in red.

tion, important features to distinguish resting states from the other conditions were mainly located in the occipital region, e.g., P5-O1 for O (see rows *Eyes-open* and *Eyes-closed* in Figure 4.9). Meanwhile, from the features distinguishing pain and resting states, the connectivity between frontal and occipital regions played a significant role, i.e., FT7-PO7 for H. Such results are consistent with findings focusing on how the alpha-band phase synchrony in frontal and occipital regions is associated with resting states [233]. Hence, the functional connectivity between frontal and occipital regions could be used to determine whether an individual is not experiencing pain.

Warm (Innocuous stimulus)

Though the functional connectivity covering frontal and occipital regions was sufficient to classify the thermal stimulus and resting states, one main challenge in pain prediction is to identify the intensity of pain or innocuous stimulus. In our experiment, I could only investigate pain intensity by classifying the innocuous (W) and painful (H) thermal conditions as two extreme scenarios. Unfortunately, no functional connectivity specific to classifying H and W was found. Nevertheless, by ignoring the nonexistent features shared by all classifiers involving W conditions, some functional connectivity involving the central region was key in the classification between the W condition and resting states (Columns 'Eyes-open' and 'Eyes-closed' in the row 'Warm' in Figure 4.9). The location of these connections, C3-CP5 and F2-C6, suggests the involvement of the somatosensory lobe [299]. The somatosensory lobe is a vital brain region in pain processing and its

activities are specific to pain sensitivity [300, 301, 302].

Considering the significance of frontal and occipital regions, and the central connectivity near the region toward the somatosensory lobe, the correlation between the somatosensory-prefrontal network and tonic pain is consistent with previous findings [280]. Hence, due to both the good performance and widely-distributed ROIs, I analysed ROIs related to tonic pain prediction only focusing on alpha-phase functional connectivity. The results uncovered topological patterns of alpha-phase functional connectivity for further development of the pain prediction model. Functional connectivity from a subset of 32 electrodes shown in Figure 4.9 selected out of 62 electrodes also produced a good performance, which proved fewer electrodes were sufficient for our application [303]. By focusing on the topographical ROIs related to pain processing, I can 'translate' them into neural markers of integration as features to build efficient and accurate online pain prediction models that can be applied at the bedside in the future.

4.5 Conclusions

This work employed machine learning as a tool in a novel analysis, providing quantitative metrics to compare the neural markers of integration. By comparing power-based and phase-based neural markers of integration from EEG for pain prediction, this chapter exposed the importance of phase-based functional connectivity from the alpha band. Briefly, phase-based functional connectivity of the alpha band showed ideal performance in both accuracy ($89.23\% \pm 11.31\%$ from 10-sec trials) and efficiency. This accuracy has

achieved the average binary classification performance around 90% reviewed in [37], which mostly used time-frequency features [207, 210, 211]. Furthermore, the following work using phase-based functional connectivity from the alpha band with convolutional neural network (CNN) produced high accuracy in binary classification around 95%, which further supports the use of this feature for pain prediction [303]. Unlike studies using time-frequency features, the alpha-phase functional connectivity is concise. Consequently, the topography of the neural markers revealed the strong diversity of the alpha phase between conditions, which supported its performance. From the analysis of topographical patterns that contribute to pain processing, we confirmed the role of the connectivity at the frontal lobe in pain conditions and the contributions of the occipital lobe in recognising resting states. To my knowledge, the topographical analysis provided the first explanation of the comparison between phase and power in the prediction of pain. In addition, phase-based functional connectivity provided interpretability of pain processing complexity in spatial integration, which could help the evaluation for clinical applications in the future. A limitation of this study is that the models were trained on the data from each participant individually. Therefore, it is unclear whether the models can predict pain in participants not involved in training. In other words, the generalisation of this feature to unknown participants, for example, transferring the pain assessment model to unresponsive patients, has not been sufficiently studied. Considering the correlation between the alpha band and individual pain sensitivity [304], the functional connectivity of the alpha band could be a key to the generalisation of the pain assessment model. In Chapters 5 and 6, my work focuses on using the EEG alpha band

to improve the generalisation of pain prediction model.

Chapter 5

EEG-based Cross-Subject Pain

Prediction I: EEG-Based Pain

Assessment Model Using Convolutional Neural Networks

Following the findings on the ideal performance of phase-based functional connectivity from the alpha band in Chapter 4, the functional connectivity features input the CNN model for pain prediction. The work in this chapter evaluates the performances of the CNN model in cross-subject pain prediction. Most of the materials in this chapter have been published in [303] and [305].

5.1 Introduction

Finding the optimal feature is always the first step in building a machine learning model, and Chapter 4 has disclosed the alpha-phase functional connectivity as the ideal feature in pain assessment. Although the SVM model evaluated in Chapter 4 could classify the pain condition and resting states with good accuracy, its performance in predicting pain from more general non-painful states, e.g., the sensation of innocuous thermal stimulus, was still under improvement. Furthermore, it was still unclear whether the SVM model can predict pain in the novel user, from whom the data were not involved in the model training. Therefore, when recalling the requirements of unresponsive patients' caretakers at the bedside and in clinical need, more attempts are still necessary to make the model more generalisable. In simple terms, if the SVM has poor generalisability, this research is supposed to propose another solution to generalise the model to novel users. Taking into account the unique patterns of functional connectivity under different conditions (see Figure 4.9), in this work we aimed to develop a novel classifier for pain prediction, and its performance was evaluated in both within-subject and cross-subject tests.

As reviewed in Section 2.4.2, although many machine learning models achieved good performance by training and predicting pain in the same individual, cross-subject pain prediction models were rarely reported [37, 214, 306]. Intrinsicly, cross-subject pain assessment is a typical cross-domain transfer learning task, and each domain represents a subject. In research of cross-domain transfer learning, many effective and robust models have been proposed [47, 243]. These models have been widely used in many fields of

AI, including CV and NLP [47, 307]. However, unfortunately, not only specific to pain assessment, individual variation is a main obstacle to generalising models classifying brain states using EEG to novel subjects [308]. Neural responses to pain have strong individual differences, thus it is difficult to expose nonspecific characteristics to individuals, which means that pain assessment is even quite a challenging aim among the development of transfer learning models based on EEG [31].

In the discovery of neural biomarkers correlated with individual specificity, Schulz et al. revealed that individual sensitivity to pain is correlated with alpha ($8 - 10Hz$) and gamma ($\leq 80Hz$) oscillations, both of which presented significant cross-individual variation statistically [39]. More particularly, some recent studies suggested that the PAF is a powerful predictive index of pain sensitivity [32, 191]. On the basis of these findings, I proposed that the functional connectivity from the alpha band may also carry specificity to individual differences in pain processing. Therefore, the model can be sensitive to both the pain-related features and the individual-related features, which can allow it to expose the intrinsic features specific to pain perception. Therefore, alpha-phase functional connectivity is still the neural biomarker to predict pain in this chapter.

Not only did this research take the vague generalisation of SVM into account, but it also considered applying transfer learning architectures to improve the generalisability of the pain assessment model with limited data. Accordingly, most transfer learning frameworks were designed based on deep learning algorithms [47]. For example, the AutoTransfer framework can transfer models trained with biosignals to novel domains [309]. In the field of EEG, adversarial learning has shown the potential to improve

cross-domain transfer learning [310]. Another fact is the lack of deep learning's use in pain prediction [37], so for the further use in the development of the pain assessment framework in transfer learning, the deep learning model became the centre of this work.

Among deep learning models that assess pain, Yu et al. reported a high classification accuracy of pain states with CNN models above 95% [44]. Nonetheless, it is still unknown whether such CNN algorithm, which is effective within the same subject, can generalise to novel subjects. This gap aroused the idea to develop a deep learning model for pain assessment which can process features that indicate individual specificity. As a technique that can extract spatial patterns from two-dimensional data, this study reorganised functional connectivity features into two-dimensional matrices and input them into CNN classifier for pain assessment [311].

While using machine learning to classify biomedical signals, there are always concerns about the interpretability of the models [312, 313, 314]. Since the models developed in this work are directed toward use in unresponsive patients, it became even more rigorous to prove whether the features exposed by the CNN model are specific to pain processing or not. For CNN, Gradient-weighted Class Activation Mapping (Grad-CAM) can detect and visualise regions with high contributions extracted by hidden layers in CNN [315]. Grad-CAM generates coarse localisation maps with the gradients of a class inputting the final hidden layer in a CNN architecture. Therefore, the patterns of the important regions in the input image are highlighted. In sum, it exposes the important regions for classification in the input two-dimensional data, especially images. Particularly, the activated patterns of functional connectivity detected in this work can suggest

the integrations between which brain regions are specific to pain perception.

In addition, before exploring the capability of CNN model to detect individual-related features, the association between alpha-phase connectivity and individual specificity needs to be declared. Traditionally, gender and age differences in the perceptual experience of pain were reported [316, 317]. Therefore, it is a good option to group subjects using functional connectivity of the alpha phase as input, which can evaluate whether output groups correlate with particular properties or original identification of subjects [318]. If significant correlations occur in some property or identification, I could propose that the alpha-phase functional connectivity is also a neural biomarker for subject recognition. Therefore, the prediction scores for each cluster produced by the classifier might be a measure of similarity between subjects [319]. Then the *most similar domain* (i.e., *the subject in this study*) to the novel subject can be selected to train the model, which predicts pain-related conditions in the novel subject [320, 321]. This strategy is selective transfer learning; it can be a candidate to resolve the challenge of cross-subject pain assessment.

In summary, the models in this chapter aim to overcome the limitations caused by individual differences in pain processing. First, a CNN model was designed to predict pain, whose performance in both within-subject and cross-subject tests is evaluated, and the performance baseline from the SVM model in Chapter 4 is compared with the novel model. And after the models' evaluation, I analysed the activation patterns of functional connectivity with high contributions from the CNN model, then the patterns can interpret the model's performances according to the neurophysiology of pain perception. Second,

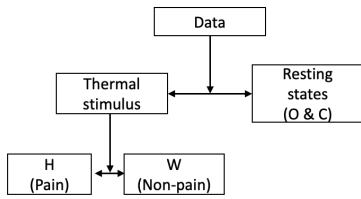
subjects were clustered according to alpha phase functional connectivity, and another CNN model was designed to recognise subjects for selective transfer learning.

5.2 Methodology

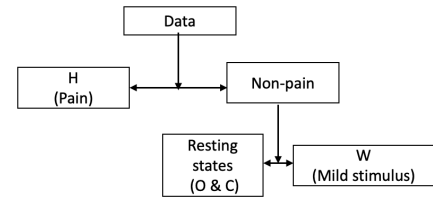
5.2.1 Experimental Conditions

The data was recorded in the experiment described in Chapter 3. The condition inducing psychological unpleasantness (S) is excluded from the analysis in this chapter. The painful thermal stimulus (H), innocuous thermal stimulus (W), eye-open resting state (O), and eye-closed resting state (C) were involved in the training and evaluation of the machine learning models in this chapter. In the part of selective transfer learning, this chapter only focusses on the main target of classifying conditions O and H in the analysis.

The primary aim of pain prediction is to distinguish pain from non-pain conditions. Therefore, this study utilised binary classification which ultimately combines the conditions into the nodes in binary decision trees. We propose two paradigms of the decision trees: 1) distinguish resting states from thermal stimulus (both pain and innocuous non-pain conditions) (see Fig. 5.1a); 2) recognise pain from non-pain states (both resting states and innocuous thermal stimulus) (see Fig. 5.1b). This thesis still focuses on the objective of recognising the main affective experience of pain (i.e., unpleasantness), and ignores the main sensory experience of pain (i.e., intensity). Hence, this chapter followed the rationale of Decision Tree 2. However, future research must also engage with Decision Tree 1 as to fully map the features associated with the experience of pain. As a



(a) Decision tree 1



(b) Decision tree 2

Figure 5.1: Two types of decision trees in pain prediction: (a) classifying if the thermal stimulus was induced before distinguishing the intensity of the thermal stimulus, (b) targeting at recognising the pain, then classifying the non-pain conditions, respectively.

result, we trained and tested the binary classification in each branch of the decision tree presented in Table 5.5.

5.2.2 Data Re-organisation

Based on the important functional connectivity revealed in Figure 4.9 of Chapter 4, 31 channels remained in this work, including FP2, AF3, AF8, F6, F7, FC4, FC5, C2, C3, C6, Cz, CP1, CP2, CP3, CP4, CP5, CP6, FT7, T8, P3, P5, P6, P7, P8, PO5, PO6, PO7, PO8, O1, Oz, O2 (see Figure 5.2). Due to a mistake in data pre-processing, FC5 was duplicated incorrectly in this research.

After filtering the data into the alpha band ($8 - 12Hz$), phase-based functional connectivity was generated with Formula 4.1 as ISPC. Based on the findings in Chapter 4, the data were then split into 5-second epochs with 90% overlap between neighbouring epochs. When the ISPC was calculated between each pairwise channel from a trial, the

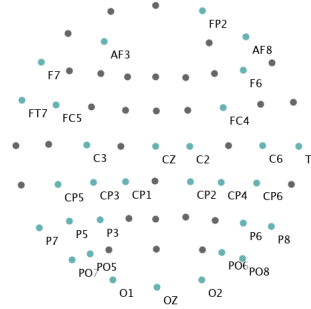


Figure 5.2: **The map of EEG channels used for feature extraction this this chapter.** The highlighted channels with labels were used for generating features in this chapter and Chapter 6.

ISPCs were assigned as an element in a matrix representing the functional connectivity of this trial. Therefore, we obtained the ISPC data set $X = \{(x_{ab}, y_s, y_p)\}_{a=b=32}^N$ that contains N samples, where each 32×32 feature matrix x_{ab} contains the ISPC value between the channels a and b , i.e., $x_{ab} = ISPC_{ab}$ where $x_{ab} \in [0, 1]$, y_s are the subject labels and y_p represent the pain-related conditions (that is, H, W, O, and C). When features were inputted into the SVM model, the features were transformed into one-dimensional vectors without duplication. The transformed dataset is $X'_t = \{(x_{a*b}, y_s, y_p)\}_{a,b=1}^N$, where $a < b$, in which each input sample has 496 elements. Figure 5.3 shows an example of the re-organised ISPC matrix.

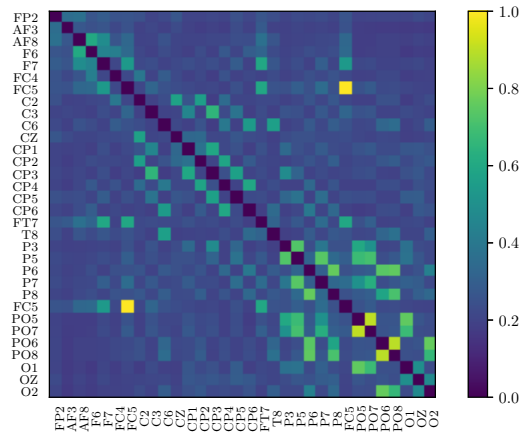


Figure 5.3: An example of the re-organised ISPC feature matrix. Each sample of an ISPC matrix was a 32×32 square matrix, in which the columns and rows represented the EEG channels, and the orders of channels were consistent.

5.2.3 Machine Learning

Support Vector Machine

This chapter used the same SVM model as the classifier used in Chapter 4. The features x_{a*b}^r that input the SVM models, and the labels for training and testing were the pain conditions y_p . This study used the performances produced by the SVM model as baselines in the evaluation.

Model for Pain Prediction

Table 5.1 and the combination of Tables 5.2 and 5.3 display the CNN classifiers' architectures for pain prediction. The input was the two-dimensional dataset x_{ab}^r and the labels are the pain conditions y_p . Since the elements in a two-dimensional ISPC matrix range

Table 5.1: Architecture of the CNN model: Three basic structures (layers 1-9) were applied, in which the activation function of each convolutional hidden layer was a rectified linear unit (ReLU) function. The 2D sizes in brackets involved in 'Size/Parameter' represent the kernel size of the corresponding layer, and the parameter multiplied with the kernel size in each hidden layer is the number of filters.

No.	Layer	Size/Parameter	Output
1	2D Convolution 1	$(7 \times 7) \times 128$	$(32 \times 32) \times 128$
2	2D Max-pooling 1	(3×3)	$(10 \times 10) \times 128$
3	Batch Normalisation 1	-	$(10 \times 10) \times 128$
4	2D Convolution 2	$(5 \times 5) \times 64$	$(10 \times 10) \times 64$
5	2D Max-pooling 2	(3×3)	$(3 \times 3) \times 64$
6	Batch Normalisation 2	-	$(3 \times 3) \times 64$
7	2D Convolution 3	$(3 \times 3) \times 32$	$(3 \times 3) \times 32$
8	2D Max-pooling 3	(3×3)	$(1 \times 1) \times 32$
9	Batch Normalisation 3	-	$(1 \times 1) \times 32$
10	2D Dropout	0.2	$(1 \times 1) \times 32$
11	Flatten 1	-	32
12	Fully Connected 1	100	100
13	Activation (ReLU)	-	100
14	Flatten 2	-	100
15	Activation (sigmoid)	-	100
16	Fully Connected 2	2	2
17	Softmax	-	2

between 0 and 1, the ISPC matrix is an ideal input to a CNN model. Consequently, no further processing of x_{ab}^r was essential before training the CNN model. In the end, the softmax layer produced the prediction of pain conditions for each sample.

Model for Subject Recognition

To test if the alpha-phase functional connectivity correlates with the identification or general properties of subjects, this work applied k-means clustering to quantify the similarity among subjects [318]. The clustering algorithm is for partitioning N samples into k clusters, in which the sum of the squared distances from each sample to the centroid of its cluster is minimised. In this work, I initiated the number of clusters as 36, the number of subjects. Mathematically, the initial centroids k were randomly generated in a k-means clustering. Then the features of the i -th sample x_i were assigned to the nearest centroid μ_j and associated with the j -th cluster, for which the algorithm computed the distance between x_i and μ_j as the Euclidean distance:

$$C(i) = \arg \min_j \|x_i - \mu_j\|^2 \quad (5.1)$$

After the assignment step, the centroid μ_j of the cluster was updated as the mean of all points x_i currently in the cluster with the formula:

$$\mu_j = \frac{1}{|C_j|} \sum_{x_i \in C_j} x_i \quad (5.2)$$

When the centroids converged to stop changing significantly, the samples in each fixed cluster were seen as similar samples. Therefore, when most samples from the same subject were clustered in the same cluster, I could propose that the alpha-phase functional

Table 5.2: The encoder's architecture for feature extraction

No.	Layer	Size/Parameter	Output
1	2D Convolution 1	$(7 \times 7) \times 128$	$(26 \times 26) \times 128$
2	Batch Normalisation 1	128	$(26 \times 26) \times 128$
3	2D Convolution 2	$(5 \times 5) \times 64$	$(22 \times 22) \times 64$
4	Batch Normalisation 2	64	$(22 \times 22) \times 64$
5	2D Convolution 3	$(3 \times 3) \times 32$	$(20 \times 20) \times 32$
6	Batch Normalisation 3	32	$(20 \times 20) \times 32$

connectivity is a biomarker of subject identification.

If the alpha-phase functional connectivity can be the biomarker to cluster the subjects' identification, I could assume that a classifier can recognise the subject with it. If not, the performance of such a classifier can also suggest whether there is a possibility to use the alpha-phase functional connectivity predicting pain. Inspired by the adversarial learning model to classify EEG signals [310], the subject recognition model shared the same architecture as the pain prediction model in Section 5.2.3. But the activation functions were different. Therefore, it can be a preparation for the further development of the transfer learning model (which will be covered in Chapter 6).

Table 5.3: The architecture for the classifying pain and non-pain conditions

No.	Layer	Size/Parameter	Output
7-1	2D Dropout	0.2	$(20 \times 20) \times 32$
8-1	Flatten 1	-	12800
9-1	Fully Connected 1	100	100
10-1	Activation (ReLU)	-	100
11-1	Flatten 2	-	100
12-1	Activation (sigmoid)	-	100
13-1	Fully Connected 2	2	2
14-1	Softmax	-	2

Model Training and Testing

This study used Adam optimiser in the training, and the learning rate was 10^{-3} . The decay rates were established with $\beta_1 = 0.9$ and $\beta_2 = 0.99$, the L2 penalty was 0.01. The batch size was 256 and 100 epochs were trained in each classification. In the validation, the pain assessment models were the architecture in Table 5.1 or the concatenation of the encoder in Table 5.2 and the architecture in Table 5.3, and the subject recognition models contained the encoder in Table 5.2 and the layers in Table 5.4. To simplify the model, all the pooling layers were removed in the models of selective transfer learning and subject recognition in Table 5.2 compared to the architecture in Table 5.1.

Table 5.4: The architecture for recognising individuals (Number of subjects: N)

No.	Layer	Size/Parameter	Output
8-2	Flatten 1	-	12800
9-2	Fully Connected 1	N	N
10-2	Softmax	-	N

- Subject Recognition

- *All-mixed*: The basic dataset involved the data from all subjects. For controlling its comparability with the LOO training, the 36-fold cross-validation split the data into a training and a testing set, with the ratio of 35:1 in each cross-validation fold.
- *LOO training*: With excluding one subject in each test, 36 independent models were trained and validated with only the data of 35 included subjects. Similarly, 80% data from the included subjects participated in the training, and the other 20% were the testing set.

- Pain Prediction For each training set, 7500 epochs per each class were randomly selected from the training data to balance the training set in the binary classification. If one binary class contained the mixture of several conditions, for example, pain (H) vs. non-pain (mixture of W, O and C), the consistent number of epochs was selected for each class (i.e. 2500 epochs from W, O and C respectively). In all runs of model evaluation, I applied 10-fold cross-validation, and the accuracy of each classification output was used

as the metric of model performance.

- *Within-subject assessment*: In each test, the subject-wise data from one subject is used to train and test the model, which means 36 independent models with the same architecture were covered. Data from each subject were divided into training and test sets with a ratio of 4 : 1.
- *Subject-mixed*: To make the size of the data equivalent to further LOO tests, a 36-fold cross-validation was applied to the dataset where the data of all subjects mixed.
- *LOO testing*: In each test, a subject was excluded. And the model was trained on the basis of the data from 35 included subjects. Then the model predicted the labels of the data from the excluded subject, whose accuracy is the basis for quantifying the model's performance.

Cumulative Evidence and Performance Validation

At the bedside, the patient's caretakers always ask for a balance between the precision and immediacy of the pain assessment [283]. Based on this background, this study tested the accuracy of the prediction with cumulative evidence. Since the duration of the trial was five seconds and the overlap ratio was 90%, the duration of time involved in an epoch increased by 0.5 seconds with another trial included in the evaluation. This work tested the effects of trial numbers between 2 and 109 (with the time duration between 5.5 and 60.5 seconds, respectively).

Two strategies of cumulative evidence were used in the prediction of pain in this study. One of them is based on the mean prediction scores of each class in the involved trials. The other strategy is a voting mechanism that produced the prediction as the most frequent class among all trial-based predictions. Figure 5.4 is an example involving five trials with the application of these cumulative evidence strategies.

The mean accuracy between all *testing sets* in each validation mode represented the performance of the models studied: a) In the leave-one-out (LOO) validation of pain prediction, each testing set contained data from one excluded subject. This model also involved the analysis of the maximum accuracy produced by the cumulative evidence. b) In the subject-mixed validation, each testing set consisted of the a fold of the cross-validation.

Selective Transfer Learning

Assuming that the subject recognition model could predict the identification of subjects, when a subject is excluded in training the subject recognition model, the prediction of excluded samples can reflect which subjects are similar to the excluded one from the included subjects in the training. By training the pain prediction model with a similar subject, the pain-related conditions of the excluded subject might be predicted.

This strategy is selective transfer learning, and Figure 5.5 shows the pipeline. In each leave-one-out (LOO) test, the subject recognition model was trained with 35 subjects excluding one subject. Then the most frequent output label k predicted with the samples of the excluded subject j was selected as the subject most similar to the subject j . Sub-

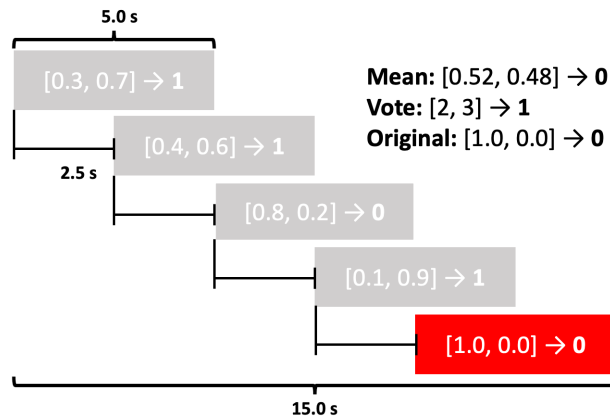


Figure 5.4: An example of the cumulative evidence involving 5 trials. (The values are only examples instead of real predictions) The red trial represents the target to be predicted. Two classes are represented by labels 0 and 1, x is the prediction score of class 0 and y is the prediction score of class 1. The prediction labels are shown at top right from two strategies. The original prediction is only produced with the target trial itself.

sequently, a subject-wise pain prediction model was trained with only data from the most similar subject k , and predicted pain-related conditions in the subject j excluded from the subject recognition model training.

5.2.4 Grad-CAM

Grad-CAM identified the activated regions within the functional connectivity in the pairwise binary classification of all conditions [315]. The main idea of Grad-CAM is to use the gradients of the target class (score) with respect to the feature map of a convolutional hidden layer, so the important regions in the feature map can be exposed. After computing the gradients of the target class score S_c of the feature map A of a hidden

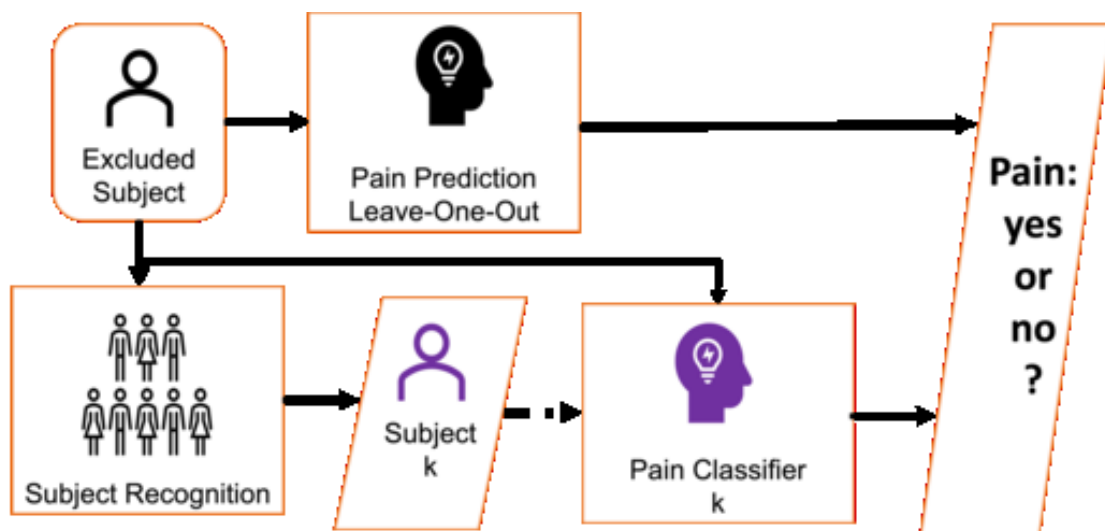


Figure 5.5: **The pipeline of selective transfer learning.** The testing set of both models on the figure is all the data of the excluded subject. The subject recognition model predicted the subject most similar to the excluded subject. The pain prediction model then predicted the pain-related labels, where the subject-wise pain prediction model was trained with the data from the excluded subject (i.e., Pain Classifier k).

layer. The gradients $\frac{\partial S_c}{\partial A^k}$ represent how much the output class score changes with a small change in the k-th feature map. Then the global average pooling is applied to the feature map A to compute the weight a_c^k in class c as:

$$a_c^k = \frac{1}{Z} \sum_i \sum_j \frac{\partial S_c}{\partial A_{ij}^k} \quad (5.3)$$

Finally, the Grad-CAM L_c is produced as the weighted sum of the feature maps, followed by a ReLU activation:

$$L^c = \text{ReLU} \left(\sum_k \alpha_k^c A^k \right) \quad (5.4)$$

The CNN model accepted the mean ISPC matrix from each condition to detect the corresponding feature maps generated by the last hidden convolutional layer (layer 7 in Table 5.1). For generating the patterns, the mean matrix of each condition is input into each binary classifier containing this condition, and the pattern of each class within the binary classification was produced, respectively. Then we matched the feature map to fit the original size of the input and summed them up to reveal the activated regions, thus the functional connectivity with main contributions in pain assessment can be demonstrated. Finally, we computed the absolute arithmetic differences between the activated patterns of two conditions from each pairwise binary classification, which informed convincing functional connectivity differentiating the two conditions.

Table 5.5: Performance of binary classification with CNN and SVM models: (1) 'All': the models were trained with the data from all subjects. (2) 'LOO': Each training excluded a subject, here shows the accuracy of predicting the pain-related labels of the excluded subject's data.

	CNN		SVM	
	All	LOO	All	LOO
Pain(H) vs Non-pain(W+O+C)	94.37%	61.55%	49.12%	38.59%
H vs O	94.16%	61.01%	49.49%	44.58%
Pain (H) vs Resting states (RS)				
H vs C	98.85%	77.20%	52.00%	23.52%
H vs RS (O+C)	96.85%	63.87%	53.60%	34.18%
W vs O	98.35%	57.64%	50.61%	43.60%
Warm (W) vs Resting states (RS)				
W vs C	97.76%	72.54%	51.15%	28.96%
W vs RS (O+C)	95.25%	63.94%	49.15%	33.41%
H vs W	94.43%	52.21%	50.80%	51.05%

5.3 Results

5.3.1 Basic Cross-Subject Pain Prediction

Table 5.5 presents the performance of the CNN and SVM models, which were acquired in each binary classification declared in the decision trees in Figure 5.1. When using the mixed data of all subjects, the CNN model produced satisfactory accuracy (mean: 96.25%, accuracy between H and O: 94.16%), which is a bright signal when the SVM model cannot work against individual differences (mean accuracy: 50.74%, accuracy between H and O: 49.49%). The CNN model also worked better than the SVM model to classify the painful and non-painful thermal stimulus (H vs W), in which the accuracy was 94.42% > 50.80%. So it could contribute to the generalisation in discriminating pain intensity among individuals. Moreover, it was even better than the accuracy of the SVM model within the subject in Chapter 4, where the mean accuracy was 82.55%.

In the perspective of LOO tests, the performances of the CNN model were less satisfactory (mean accuracy: 63.69%, accuracy between H and O: 61.01%). However, it is still better than the SVM model benchmark (mean accuracy: 37.24%, accuracy between H and O: 44.58%). So the model has the potential to be improved for generalising it across subjects.

The within-subject evaluation of the CNN model produced the mean accuracy of 92.76%, which was higher than the baseline produced with SVM in Chapter 4 (86.03%) with the same length of trials. But the limited performance of LOO suggested the poor generalisability of the CNN model. Therefore, the influences of cumulative evidence were

analysed. Figure 5.6a shows the curve of accuracy that changes along the time length in the cumulative evidence, which increases significantly within the studied range. Not only it is feasible to use one minute in pain prediction as the highest accuracy shown in this evaluation, but also the mean level of cumulative evidence achieved a higher level than the original prediction around just 30 seconds .

Table 5.6: **Accuracy produced in different testing modes in the classification between conditions O and H.** Three columns represent three different testing modes in the study without pooling layers. (1) Within-subject (WS): the models were trained and tested with the data from the same subject. (2) Leave-one-out (LOO): in each test, the model training excluded the subject in the corresponding row. (3) Mean accuracy of cumulative evidence (Mean CE): The accuracy was from the results applied with cumulative evidence, where the mean values across all the studied time length represented the average level produced by cumulative evidence. The bold value in each row represented the larger value between the accuracy from LOO and Mean CE.

Subject No.	WS	LOO	Max CE
0	86.81%	57.74%	58.89%
1	90.83%	63.95%	74.86%
2	89.84%	63.21%	86.76%
3	96.34%	56.39%	55.80%
4	75.82%	63.27%	76.17%
5	99.33%	47.78%	43.36%
6	84.67%	66.30%	78.66%

7	95.95%	52.76%	55.32%
8	99.11%	45.58%	48.03%
9	80.50%	51.86%	53.97%
10	89.58%	52.41%	55.44%
11	79.69%	59.14%	61.52%
12	83.55%	61.80%	64.62%
13	97.56%	56.01%	64.00%
14	94.67%	57.95%	55.44%
15	98.73%	68.84%	92.93%
16	96.82%	58.61%	68.97%
17	97.68%	57.86%	70.64%
18	89.85%	60.25%	68.10%
19	93.68%	48.22%	53.40%
20	98.76%	49.63%	52.50%
21	99.69%	49.09%	48.36%
22	95.28%	55.24%	63.75%
23	95.98%	54.44%	53.69%
24	99.22%	56.40%	60.53%
25	97.09%	44.55%	36.75%
26	95.18%	58.60%	65.95%
27	95.19%	69.56%	82.82%

28	91.35%	52.90%	53.95%
29	95.60%	54.82%	56.62%
30	95.13%	76.92%	90.53%
31	85.03%	67.84%	69.41%
32	95.18%	53.89%	55.46%
33	97.07%	67.51%	84.73%
34	87.17%	56.87%	58.57%
35	95.47%	68.04%	90.30%
Mean	92.76%	57.95%	64.19%
Standard Deviation	6.12%	7.35%	13.79%

5.3.2 Subject Recognition

Clustering of Subjects with Functional Connectivity

By clustering phase-based functional connectivity samples from the alpha band using the k-means algorithm, the samples were clustered into 36 clusters. Among the 36 subjects participating in this research, more than 90% samples of 30 subjects appeared in the same group, respectively. Hence, I proposed that the alpha-phase functional connectivity has correlations with the individual specificity, which can be the features predicting the identification of subjects.

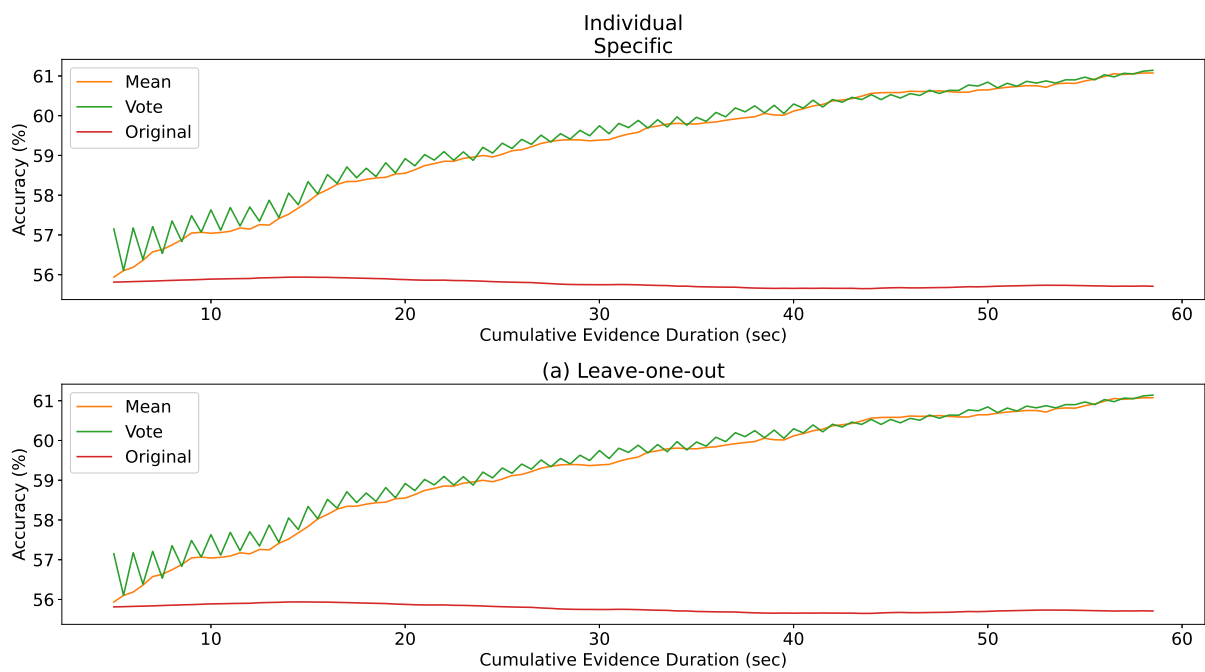


Figure 5.6: **The curves of mean accuracy versus the time duration of classification between conditions O and H with cumulative evidence.** The curves represent the mean accuracy across excluded subjects from the two paradigms based on cumulative evidence, and the original curves represent the accuracy produced by only the target trial in the corresponding test.

Table 5.7: Accuracy produced by the individual recognition and pain assessment models under different validation modes. For the tests about generalisation, including the leave-one-out (LOO) and selective transfer learning (STL) tests, it showed the original accuracy without cumulative evidence, and the maximum accuracy produced by mean and voting mechanisms of cumulative evidence.

Model	Validation	Mean Accuracy (%)	Max Individual Accuracy (%)
Individual recognition	All-mixed	99.63 ± 0.23	
	Leave-one-out	99.55 ± 0.22	
Pain Prediction	Within-subject	92.76 ± 6.12	100.00
	Subject-mixed	96.52 ± 1.02	
	LOO (original)	57.81 ± 7.48	73.33
	LOO (max., mean)	69.56 ± 14.72	100.00
	LOO (max., vote)	69.75 ± 14.59	99.43
	STL (original)	53.73 ± 10.59	79.50
	STL (max., mean)	58.41 ± 15.32	100.00
	STL (max., vote)	58.83 ± 14.92	100.00

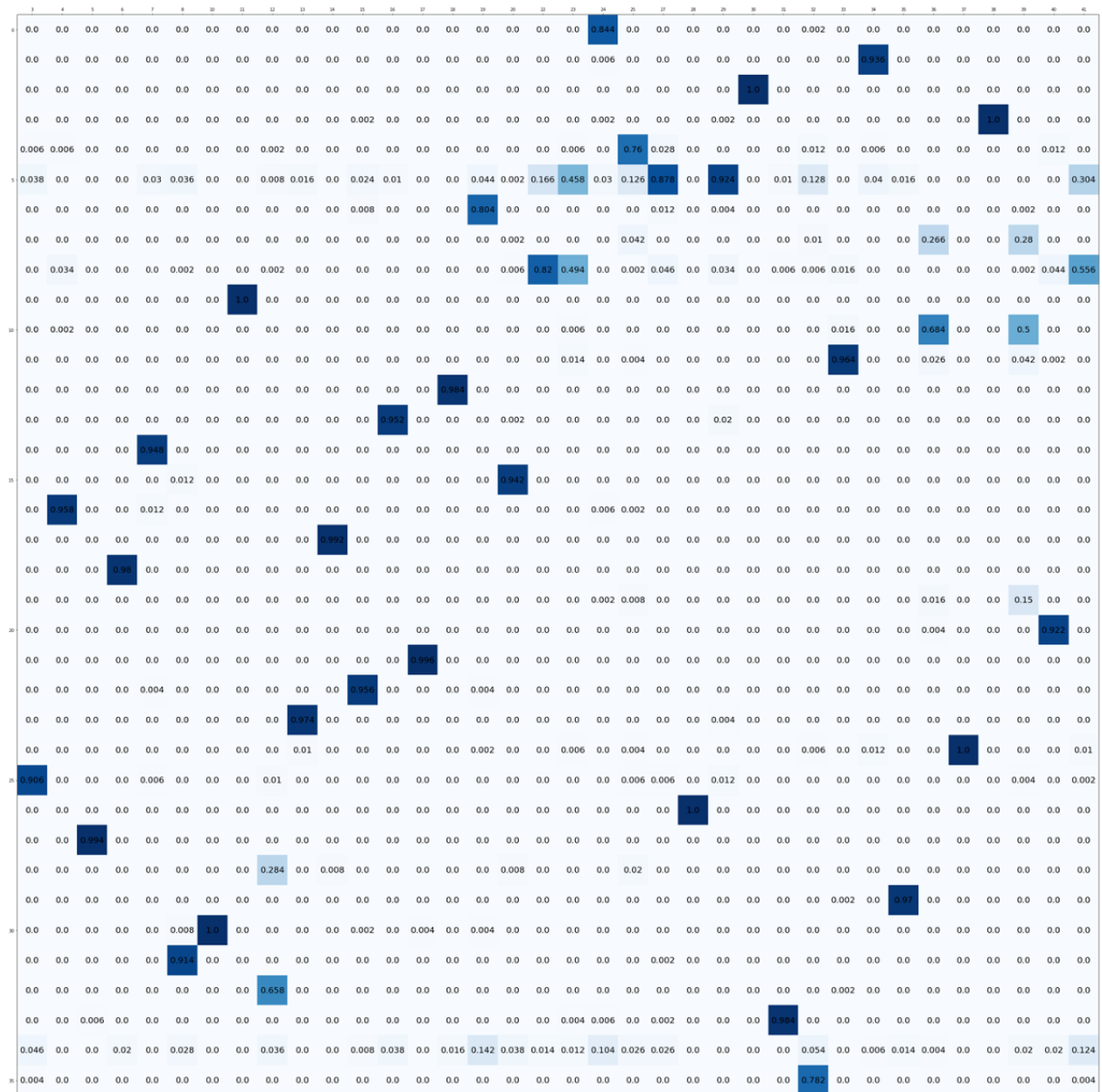


Figure 5.7: The clustering result of all subjects based on the alpha-phase functional connectivity. The column represents the true subject s , and the row represents the clustered group's number c . The value on each cell represents the ratio of samples clustered into group c belonging to the subject s .

Performance of CNN model for Subject Recognition

Table 5.7 showed the nearly perfect performance of the CNN model to recognise the subjects, it is consistent with the clustering result and the theoretical correlation between individual pain sensitivity and the alpha band. With the mean accuracy above 99% in both training with all 36 subjects or 35 subjects in the LOO dataset, the development of the selective transfer learning model can potentially rely on this pain recognition model to select a subject similar to the to-be-predicted subject.

5.3.3 Selective Transfer Learning

I implemented the selected transfer learning paradigm as expressed in Section 5.2.3 and Figure 5.5. Figure 5.8 displays the ratio of predicted subject IDs, in which the subject taking the highest proportion was selected as the *most similar subject* for subject-wise model training. However, when the subject involved in model training was selected according to the subject recognition model (Figure 5.6b), the accuracy was always lower than the LOO test based on the models trained with the 35 subjects except the tested one (Figure 5.6a). Table 5.7 also showed the performance metrics of the LOO and selective transfer learning tests.

5.3.4 Activated Functional Connectivity

Figure 5.9 displays the differences between the activation patterns of Grad-CAM. The main aim of this analysis is to detect the features in charge to recognise the H condition (shown in the first column). According to the activation feature maps, the patterns

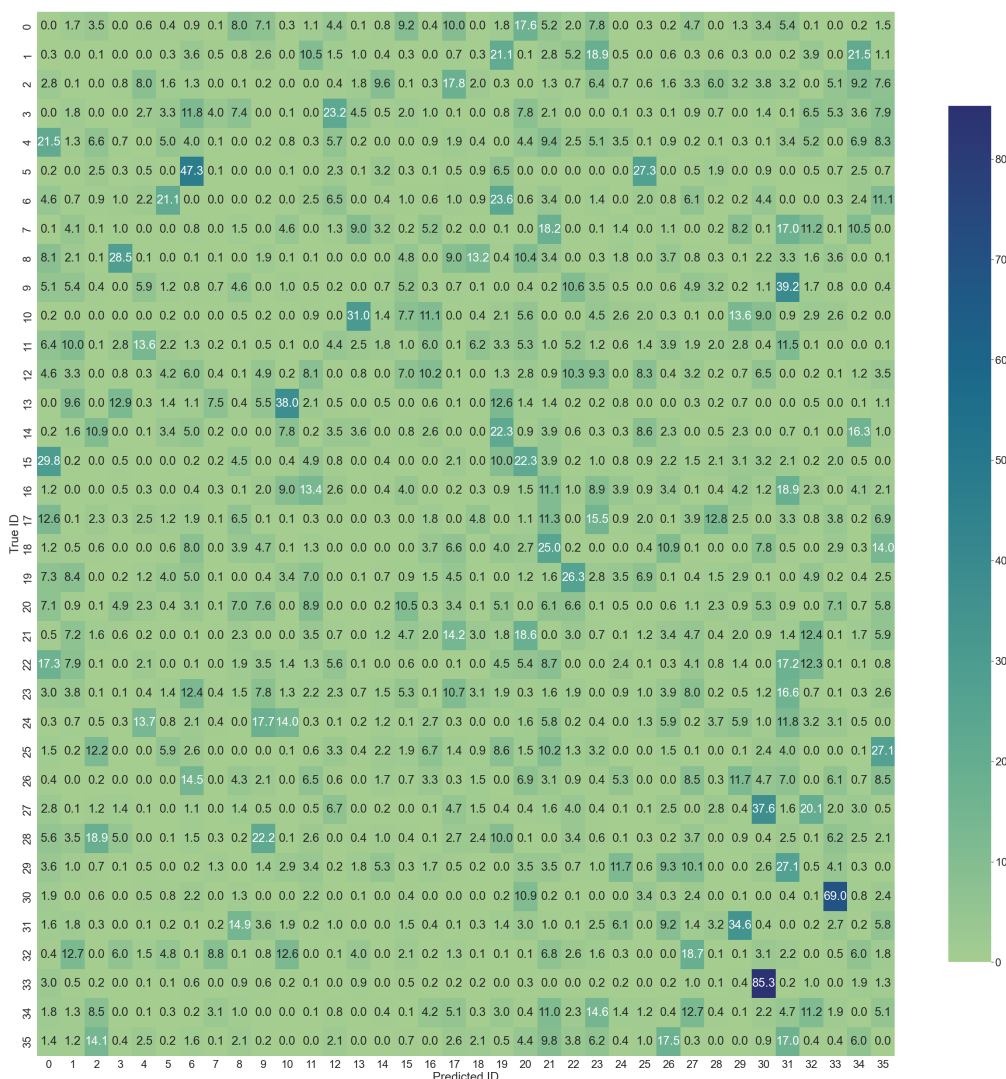


Figure 5.8: The proportion of subject ID predicted with the data from the subject whose pain labels were predicted. The rows represent the subjects to be tested, whose pain-related labels were predicted. The columns represent the predicted subject IDs produced by the subject recognition model, the ones with the highest ratio were selected as the most similar subjects to the ones in the rows. The models were then trained with each *most similar subject* to predict pain in the respective subject in the rows.

related to the H condition distributed over the central-parietal and central-occipital regions of the scalp. Furthermore, central-central, frontal-parietal, and parietal-parietal functional connectivity offered some evidence to distinguish the conditions of W and O ('W vs O' in Figure 5.9), in which their contributions were significantly weaker than the specific functional connectivity of pain. And it is not surprising that there were also compelling patterns for recognising the C condition, suggesting that the model can extract the features intrinsic to some neurophysiological characteristic unrelated to the cognitive tasks in rating pain.

5.4 Discussion

5.4.1 Improvement of Generalisation in Pain Assessment Model

When a subject can provide training labels, that is, involved in the training phase, the prediction performances in within-subject and subject-mixed tests had ideal accuracy in pain prediction. More particularly, the model can differentiate between pain and resting states or between pain and an innocuous sensation. Moreover, the performances equated to the benchmark of the work using several multiple components to generate features.

The SVM model worked well in within-subject pain prediction (see Chapter 4), but it was not sensitive to the features related to the individual differences, which produced accuracy around the chance level (Table 5.5). This limitation might originate from the principle of SVM, which focuses on finding a single and optimal hyperplane, which separates the classes using the average margins. Nonetheless, when the data involves strong

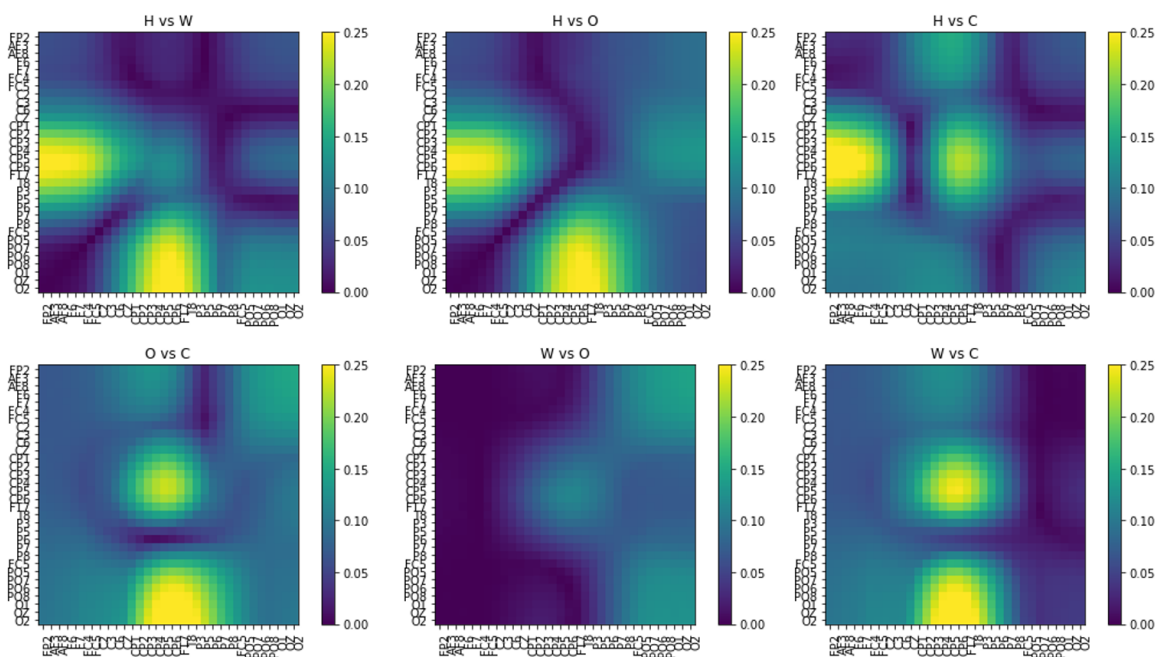


Figure 5.9: The absolute values of arithmetic differences among the activated patterns out of layer 7 in Table 5.1 between each pair of conditions. These differences can show the cogent regions reflecting the connectivity capable of significantly classifying the corresponding conditions: Hot [H], Warm [W], Eyes-open [O], and Eyes-closed [C].

individual differences, SVM might perform poorly since it does not accommodate variability in data distribution across domains that is individuals in this work. Therefore, the fixed, singular decision boundary generated by SVM may not reflect the separations among individual characteristics accurately. Compared to the SVM model, the subject-mixed performance of the CNN model tended to defeat the negative effects of individual differences. And the LOO results in Tables 5.5 and 5.7 also revealed the potential to generalise the CNN model to the novel subject not involved in model training, but the feasibility is still limited in accordance with the accuracy. So the model cannot be applied to unresponsive patients. Such a limitation most probably resulted from the strong individual variation of the brain's responses to pain. Despite that PAF is sensitive to account for individual variation [191], the approach to utilise functional connectivity of the alpha band requires more attempts to predict pain in the novel subject.

Although this study did not produce an ideal accuracy in predicting pain between subjects, cumulative evidence optimised performance ($64.19\% > 54.96\%$). According to Table 5.5, 8 of 36 subjects achieved a mean accuracy above 75% with cumulative evidence, and most of them were better than the accuracy produced without cumulative evidence. Table 5.7 demonstrated that some subjects can even obtain the maximum accuracy of 100% with a long cumulative duration. Despite the mean accuracy being worse than the benchmark (89.45% in [214]), the large standard deviation (13.79%) indicated the effects of individual differences. The difference between the mean and maximum accuracy in the cumulative evidence also denoted the effects associated with individual variation.

However, selective transfer learning tested in this work did not assign the potential of alpha-phase functional connectivity in cross-subject pain prediction as expected. This may be caused by differences in the number of subjects. In general, the sensitivity of machine learning models to target classes is specific to the number of samples in training, where more data can make it easier for the classifier to detect specific features of each class [322]. Nevertheless, the data included in the selective transfer learning training set was nearly $1/35$ of the data in training the LOO model. One strategy to capitalise on similar subjects to predict pain in a novel individual may entail increasing the number of samples within a generative adversarial network (GAN) [323], or building an adversarial learning model that will contrast a pain assessment network and an individual recognition network [324]. More simply, the model can measure the similarity between subjects to select the most similar subject (s), for example, the Kullback-Leibler divergence (KL divergence) [325]. With such measures, the pain prediction model can follow any efficient framework, not only limited by deep learning methods.

Cross-subject pain prediction models typically used time-frequency features within specific channels or frequency bands, but did not use enough measures of neural integrations, such as functional connectivity. Furthermore, most of the previous models extracted features from several frequency bands and used multiple types of features [214, 306, 326]. Accordingly, the advantage of the CNN model proposed in this work was obvious that it was concise and efficient. Taking into account the requirements of efficiency, the use of phase-based functional connectivity from the alpha band made it concise and efficient. Therefore, it is worth further investigation in the development of

applications at the bedside.

5.4.2 Functional Connectivity of Interests in Pain Assessment Revealed by Deep Learning

One of the main highlights of this work is the interpretability based on Grad-CAM, Figure 5.9 intuitively exhibited the activation patterns of the feature maps classifying different conditions. This analysis can support the reliability of the models developed in this study, which can help its promotion in clinical environments.

As the activated pattern shared by all binary classifications involving the H condition, functional connectivity between the frontal and central brain regions contributed to pain processing. In pain processing, neural signals are processed mainly in the somatosensory and frontoparietal regions, and the central brain region is around the somatosensory cortex located in the parietal lobe according to the general localisation [327, 328]. Some research even demonstrated that functional connectivity between these two regions modulates pain attention [327]. Therefore, the importance of frontal-central connectivity can match the neurophysiology of somatosensation and somatic pain [329, 330].

There were also patterns that distinguish pain without considering the changes in cognitive tasks, i.e. H vs W and H vs O in Figure 5.9. This pattern concentrated on the connectivity between the central and occipital brain regions. Beyond the importance of the somatosensory cortex in pain processing, some work disclosed that activities in the occipital lobe vary between pain states and resting states [331]. Synthesising the

findings in Figure 4.9 and these activation maps, occipital regions are supposed to be the focus in pain prediction, especially for recognising the resting states.

However, I have to consider the limitations reflected by Figure 5.9. The main limitation of the CNN model developed in this Chapter is the large size of padding, thus the output of hidden layers did not have *high resolutions*. More intrinsically, the Grad-CAM patterns can only represent the functional connectivity at the level of cortex roughly, which cannot show the connectivity between smaller regions. One typical example is the Grad-CAM pattern discriminating the conditions of O and W, where the activated regions were not clear enough. Hence, the features related to sensations shown in Chapter 4 were not recognised by this CNN model. Although the features in the classifications of *H vs O* and *H vs W* can show this model's performances in pain prediction, this study still needs improvement in the architecture to be more sensitive to the shorter-range connectivity. In Chapter 6, the model will be improved in this aspect.

5.5 Conclusions

The CNN model proposed in this work is satisfactory for pain assessment when it is trained with the data from the subject to be predicted. In terms of accuracy, it was better than the SVM model in Chapter 4 and achieved the same level as the benchmark in this field. In particular, it has a significant advantage of conciseness, which uses only one type of feature and offers good interpretability.

Compared with the accuracy of the pain prediction from the SVM model, the CNN

model proposed in this chapter showed a tendency against individual variation in subject-mixed tests. However, the model's sensitivity to individual differences relied on the data involved in the training set, thus casting a shadow on the model's capability to predict pain on novel subjects providing no data for training. The ideal performance of the subject recognition model demonstrated that alpha-phase functional connectivity can also be the neural biomarker of subject identification. Therefore, this neural biomarker can work in a suitable way to reduce the effects of individual differences. However, selective transfer learning with *the most similar subject* to the novel subjects did not work as expected in this work, which may be due to lack of data. In conclusion, further work should be conducted, the feasible approaches contain finding the measures of similarity among subjects, and developing transfer learning frameworks to defeat the contributions of individual-specific features.

Chapter 6

EEG-based Cross-Subject Pain

Prediction II: EEG-Based Transfer

Learning Approaches for Pain

Assessment

The work in Chapter 5 proposed a CNN model that can predict pain accurately, but did not work as expected in cross-subject pain prediction. Following the CNN model using the phase-based functional connectivity from the alpha band, I discovered the effects of transfer learning frameworks in improving the performance of pain prediction in this chapter. Furthermore, the Grad-CAM analysis revealed the reason for the difficulty in cross-subject pain assessment.

6.1 Introduction

As a marker of tissue damage in health management, monitoring pain is always essential, especially for patients' caretakers. Nevertheless, until now, the number of models is still limited to assess pain using EEG in the individuals not involved in training [37]. Therefore, it is still unfeasible to monitor pain in unresponsive patients. Although our work in Chapter 5 involved some attempts to improve the generalisation of the pain prediction model, the proposed CNN model still cannot adapt the need for cross-subject pain prediction. To resolve the obstacles that transfer the pain prediction models to novel subjects, this chapter used novel transfer learning approaches to evaluate their generalisation.

Not limited by the purpose of pain assessment, transfer learning models are being developed for most EEG-based research [308]. Inherently, the EEG-based cross-subject machine learning model is a type of cross-domain transfer learning, where a subject represents a domain. Two main challenges obstruct the application of transfer learning in EEG-based research, individual differences and insufficient data [46]. To resolve the limitation induced by individual variation, there are two perspectives worth paying attention to. First, following the paradigm of cross-domain transfer learning, the model could align the domains by decreasing the discrepancies among the samples of different domains, which is based on measures of cross-domain differences, such as the distance in Euclidean space or the maximum mean discrepancy (MMD) [332, 333]. The other solution is to explore the characteristics that carry individual specificity, which mainly

originate from physiological findings. In this research, Chapter 5 has investigated the potential of phase-based functional connectivity from the alpha band as a marker of individual differences according to the relationship between PAF and pain sensitivity [32, 191]. Following the findings in Chapters 4 and 5, I still utilised the alpha-phase functional connectivity as features in CNN model to develop transfer learning models.

Another main challenge in pain assessment is the small size of the data and the lack of standardisation. Different from the frontier development of *big data* and even the popular large language model (LLM), the current trend of applying machine learning to neurophysiological signals still uses small data primarily [46]. In studies based on EEG, this lack of data is not surprising. In the recording of EEG signals, the majority of experiments are still conducted by professionals in laboratories with wired devices, and time and economic cost also limit efficiency [334]. Moreover, the differences in experimental design, devices, and environments also made the standardisation of the datasets challenging. There are two main paradigms to process the lack of data. One is based on data augmentation, for example, using GAN to generate simulated EEG data [323, 335]. In this work, I selected another solution, using transfer learning frameworks that could reduce the contributions of specific features to individual differences, and it can also reduce the requirement of data size.

With the consideration of individual differences and the limited amount of data, our work is finding a possible solution to utilise deep learning frameworks for transfer learning applied to the small dataset. As a preparation for this part of the work, the CNN models in Chapter 5 shared the same architecture of convolutional layers for both pain

prediction and subject recognition. Therefore, in this chapter, I adapt the CNN architecture developed previously to the transfer learning frameworks. The purpose for using the transfer learning models was to expose the feature components specific to pain prediction, as well as to reduce the effects of individual-specific components.

Thus, I selected two frameworks which can achieve this target empirically. One of them is a partial fine-tuning model with feature extraction. The partial fine-tuning strategy is widely used in zero-shot or few-shot transfer learning [336]. This approach pre-trained some layers with a primary target (i.e., subject recognition), which is classifying the subjects in this work. But the pre-training phase aimed to lower the sensitivity of the model to the subject-specific characteristics by increasing the training loss. Therefore, the features related to the primary target can be *blurred*. Then the pre-trained layers were frozen, and some additional layers joined the architecture. By training the newly joined layers toward the main target, i.e., pain prediction, the model would finally expose the features correlated with pain processing.

The other transfer learning framework implemented in this work was an adversarial learning model. Adversarial learning used a shared encoder of two classifiers, which were the equivalent convolutional layers in Chapter 5. Bethge proved its feasibility with cross-domain transfer learning tasks to classify EEG signals, so it could be an ideal candidate for this study [310]. The two classifiers had different optimisation targets: one is decreasing the loss in pain prediction so that the features can be more sensitive to pain perception's specificity; the other could be either increasing or decreasing the loss in subject recognition which depends on the performances.

Beyond transfer learning frameworks designed to extract intrinsic features, this work also involved evaluating the domain matching strategy. Transfer component Analysis (TCA) learns *transfer components* which can project the features from different domains into the Hilbert space with the least cross-domain discrepancy [243]. In this study, the kernel of the Hilbert space was produced based on the condition excluded in the classification, and the data included in the classification were transformed with the learnt kernel. The transformed samples then input the two transfer learning frameworks as features, which were compared with the original results from the transfer learning framework.

Whether these frameworks worked as expected or not, the quest for interpretability still exists in the analysis. Like in Chapter 5, Grad-CAM still played a role in analysing activation feature maps in both subject recognition and pain prediction. Therefore, I can declare the important brain regions involved in functional connectivity for both targets as the patterns shown in Chapters 4 and 5, which could show key features to reduce the effects of individual differences [315]. Moreover, I discuss the possibility to select similar subjects with a single measure. A post hoc analysis was conducted to the correlation between the Kullback-Leibler (KL) divergence and the accuracy of subject-wise pain prediction, which was between each pair of domains [337].

In summary, this chapter focusses on the development of cross-subject transfer learning models in pain prediction. For testing the generalisability between all pairwise subjects, I also trained 36 subject-wise CNN models with the data from each subject and then tested them on all the other subjects. The performances of two proposed transfer learning frameworks were analysed and compared with the original model and the

subject-wise models. With the same pipeline, this work also studied the effects of TCA. Synthesising these results, Grad-CAM suggested the interpretability of the models' performances and the existent challenges revealed in this research.

6.2 Methodology

6.2.1 Experiment and Signal Pre-processing

This chapter still uses the data recorded in the experiment in Chapter 3, and the signal pre-processing was consistent with Section 3.3. Channel selection was equivalent to Chapter 5, where 31 channels were used.

6.2.2 Feature Extraction

From Chapter 4, the phase-based functional connectivity in the alpha band was proven as ideal features for pain prediction, which can be measured as inter-site phase clustering (ISPC) [8, 232]:

$$\phi_a(t) = \arctan \left(\frac{\mathcal{H}(s_a(t))}{s_a(t)} \right) \quad (6.1)$$

$$ISPC_{mn} = \left| \frac{1}{n} \sum_{t=1}^n e^{i[\phi_m(t) - \phi_n(t)]} \right| \quad (6.2)$$

where $\mathcal{H}(s_i(t))$ is the Hilbert transform of the signal series $s_a(t)$ at EEG channel i , $\phi_a(t)$ is the phase series of channel i produced from the Hilbert transform. In formula 6.2, the differences of phases between the channels m and n (i.e., $\phi_m(t)$ and $\phi_n(t)$) were measured, and the modulus of their mean values $ISPC_{mn} \in \mathbb{R}$ represents the phase

synchrony between two channels during the trial time range.

6.2.3 Dataset Generation

The dataset was inherited from Section 5.2.2. No matter whether using TCA to align the data among different subjects, it is always necessary to use a few samples to extract the features specific to the individual specificity. So I first cut the dataset X into two parts: X_{pre} from the third minute of each condition of the resting state was extracted from all subjects involved in model training for domain alignment between subjects using TCA. The other data remained as X_{main} , which was used to train the networks for pain prediction.

6.2.4 Model Training and Validation

Classification Tasks

Aiming at transfer learning, the transfer learning frameworks in Section 6.3 always involved two parts: one to process individual variation and the main architectures for predicting pain as another part. Respectively, there are two classification targets in our research: individual recognition for evaluating whether the network can extract the features related to individual specificity and pain prediction as the main purpose.

Before pre-training the network layers specific to individual variation, especially in the pre-training of fine-tuning and adversarial learning models, this study evaluated if they can detect the individual-specific features, i.e., classify the individual accurately. Therefore, the network can be sensitive to individual specificity before extracting pain-

related features. As mentioned above in Section 6.3.1, to extract individual-specific characteristics, this study assumed that only the resting state data or the pain data can be reliably recorded from novel users (e.g., unresponsive patients). Furthermore, the size of data used for pre-training was always limited.

The main task of this research is to predict the pain from the unlabelled domains. For testing the models' performances in transfer learning, here used leave-one-out (LOO) tests for every subject in the dataset. In each LOO test of the individual independent models, X_{main} was split into X_S from the 35 included subjects and X_T from the one excluded subject. In the individual-dependent tests with all the models studied, X_S contained the data of one subject in each test. Data from X_S was used to train the models and the models' performances were evaluated with the tests on X_T .

However, I was also curious about the potential of each individual to predict another individual's pain. Such an idea can make it possible to only use the 'ideal' subjects to predict the pain in the target subject. Hence, a subject-wise test was run in the basic CNN model (see Section 6.3.1) to discover the 'ability' of each subject to predict pain from the other one. In this test, the data of each subject was used to train a CNN model. With the 36 resulting independent models, their performances to predict pain from each other subject, respectively, were tested.

Cumulative Evidence

Our previous work in Chapter 5 suggested that the prediction accuracy of each single trial was limited, but the accumulation of evidence can significantly increase the accuracy.

In this study, cumulative evidence was applied to predict pain-related conditions. For evidence accumulation, I first obtained the predictions of n successive samples' prediction score vectors $\mathbf{z} = \{z_i\}_n$. Then the mean values was obtained across the n score vectors and found the maximum score index in the mean value vector.

$$y_n = \arg \max_i \left\{ \frac{1}{n} z_i \right\} \quad (6.3)$$

where z_i are the i -th scores from each score vector. Therefore, the model can predict the label of the n -th sample as y_n . Obviously, when the trials participating in evidence accumulation are more, the available testing trials will be fewer. Therefore, in recording each condition of each participant, though this work tested 90% of the full length (i.e., 270s from 300s) as the length for cumulative evidence, this study analysed the mean accuracy produced by all the accumulation of evidence results to represent its effect.

Training and Evaluation

In the experiments of this research, the main target is distinguishing the pain condition from the non-painful conditions. Since the subjects' eyes were kept open during the induction of thermal stimulus, this study used the condition of eyes-open (O) representing the resting state. Hence, there are three pairwise binary classifications to test, including O vs H, O vs W, and H vs W. Otherwise, the study tested the performance of the three-classification involving O, H, and W.

In training, Adam Optimiser with the learning rate of 10^{-3} was applied and the decay rates were between $\beta_1 = 0.9$ and $\beta_2 = 0.99$, and the L2 penalty was 0.01. The batch

size was set as 256. I trained the model with epochs of 100. All experiments ran with PyTorch 1.12 on NVidia RTX2080 or GTX1080Ti GPUs.

This study calculated the accuracy (ACC) to evaluate the performance of the transfer learning models. The metric is defined as:

$$ACC = \frac{\sum_{i=1}^K C_{ii}}{N} \quad (6.4)$$

where C_{ij} denotes the number of samples of class i classified as class j in the confusion matrix, and N is the total number of samples.

6.3 Framework

Toward transfer learning, our main objective is to train the models with data from the labelled domains and to generalise the models to unlabelled domains, where the domains represent individuals in this research. Given a domain $\mathbb{D} = \{\mathbf{X}, \mathbb{P}^{\mathbf{X}}\}$, it consists of two components, the feature space X and the probability distribution of the feature space $\mathbb{P}^{\mathbf{X}}$ [47]. Respectively, this work proposed the transfer learning frameworks to extract specific pain features with X , and used TCA to align the probability distributions $\mathbb{P}^{\mathbf{X}}$ in collaboration with the transfer learning frameworks.

Transfer Component Analysis (TCA)

The key purpose of TCA is to find the map $\phi(\mathbf{x})$ that minimises the maximum mean discrepancy (MMD) between two distributions $\mathbb{P}^{\phi((\mathbf{x}_S))}$ and $\mathbb{P}^{\phi((\mathbf{x}_T))}$. In this way, the empirical

distance between two transformed distributions represented by MMD can be written as:

$$\text{MMD}(\mathbf{x}_S, \mathbf{x}_T) = \frac{1}{n_S} \sum_{i=1}^{n_S} \phi(\mathbf{x}_{Si}) - \frac{1}{n_T} \sum_{i=1}^{n_T} \phi(\mathbf{x}_{Ti}) \quad (6.5)$$

\mathcal{H}

where each feature instance \mathbf{x}_i is mapped to the Hilbert space \mathcal{H} associated with the kernel $k(x_i, x_j) = \phi(x_i)^T \phi(x_j)$, n_S and n_T are the numbers of instances from source and target domains used for finding the map $\phi(\mathbf{x})$. Before applying TCA to get the transform map, Formula 6.5 can be written as:

$$\text{MMD}(\mathbf{x}_S, \mathbf{x}_T) = \text{tr}(\mathbf{K}\mathbf{L}) \quad (6.6)$$

$$\mathbf{K} = \begin{bmatrix} \mathbf{K}_{S,S} & \mathbf{K}_{S,T} \\ \mathbf{K}_{S,T} & \mathbf{K}_{T,T} \end{bmatrix} \in \mathbb{R}^{(n_S+n_T) \times (n_S+n_T)} \quad (6.7)$$

$$\mathbf{L} = [l_{ij}], l_{ij} = \begin{cases} \frac{1}{n_S^2} & x_i, x_j \in \mathbf{x}_S \\ \frac{1}{n_T^2} & x_i, x_j \in \mathbf{x}_T \\ -\frac{1}{n_S n_T} & \text{otherwise} \end{cases} \quad (6.8)$$

Then the optimisation problem is to reformulated as learning $\mathbf{W} \in \mathbb{R}^{(n_S+n_T) \times m}$ which satisfies

$$\begin{aligned} \min_{\mathbf{W}} \text{tr}(\tilde{\mathbf{K}}\mathbf{W}\mathbf{W}^T\tilde{\mathbf{K}}\mathbf{L}) + \lambda \text{tr}(\mathbf{W}^T\mathbf{W}) \\ \text{s.t. } \mathbf{W}^T\tilde{\mathbf{K}}\mathbf{H}\tilde{\mathbf{K}}\mathbf{W} = \mathbf{I} \end{aligned} \quad (6.9)$$

where $\mathbf{H} = \mathbf{I}_{n_S+n_T} - \frac{1}{n_S+n_T}\mathbf{1}\mathbf{1}^T$ is the centring matrix, and the kernel matrix \mathbf{K} is decomposed as $\mathbf{K} = \tilde{\mathbf{K}}\mathbf{W}\mathbf{W}^T\tilde{\mathbf{K}}$. Hence, the m leading eigenvectors of $(\tilde{\mathbf{K}}\mathbf{L}\tilde{\mathbf{K}} + \lambda\mathbf{I})^{-1}\tilde{\mathbf{K}}\mathbf{H}\tilde{\mathbf{K}}$ are the matrix solution of the TCA transformation map \mathbf{W} . Then the TCA transformation is $\phi(\mathbf{x}) = \mathbf{W}\mathbf{K}$, which aligned the data from the source and target domains.

In potential applications, it is not practical to use all data from the target domains as reference to learn $\phi(\mathbf{x})$. Considering the clinical environment applied to unresponsive patients, I could assume that patients are mainly in the resting states [338]. Therefore, this work only used data between 120 and 180 seconds in each 300-second EEG recording of each condition of a subject as a reference for learning \mathbf{W} , which is more stable than the first minute of the recording according to the previous analysis [339].

For fitting the transformed data to the same frameworks which were evaluated with the original features, the size of the transformation results was equivalent to the original matrix. Because the functional connectivity matrix is symmetric along the diagonal, the non-repeating half of each matrix (size: 496) was flattened as the basis to generate the kernel matrix \mathbf{K} . With the kernel generated with the data outside the reference range, this chapter used \mathbf{W} with 496 eigenvalues for the transformation learnt from the reference data to project the data into the latent space aligning the data. Finally, the transformed data were reorganised into symmetrical 32×32 matrices along the diagonal.

In simple, the input feature size was always consistent in both the tests with the original data and the TCA-transformed data, i.e., the features \mathbf{x} are:

$$\mathbf{x}_{32 \times 32} = \begin{cases} \mathbf{x}_{\text{orig}} & \text{Original} \\ \phi(\mathbf{x}_{\text{orig}}) & \text{TCA} \end{cases} \quad (6.10)$$

in which \mathbf{x}_{orig} represents the original phase-based functional connectivity features from the alpha band, and $\phi(\mathbf{x})$ is the transformation function of TCA.

6.3.1 Neural Network Model

Based on the work in Chapter 6, this chapter improved the CNN model for pain assessment with phase-based functional connectivity from the alpha band and evaluated its performance in individual recognition. In this study, the effects of domain alignment using TCA were also compared with the original features using the same model. By utilising the model's ability in extracting features specific to the individual specificity, I tried to build the transfer learning models toward reducing the negative influences of the individual variation, including a fine-tuning framework and an adversarial learning framework. Figure. 6.1 showed the architectures of the frameworks.

Convolutional Neural Network (CNN)

Chapter 5 proposed a CNN model with good performance in the evaluation of pain within the subject using phase-based functional connectivity from the alpha band as features (see Chapter 5 as a reference). Due to the small size of the input (32×32), I removed the pooling layers in the architecture in the pilot work of this research. This part of the work kept using this architecture and tested its performance in subject-wise transfer learning, in which the 36 independent models were trained with each subject, respectively, and tested every model's performance in each other subject. Therefore, I can find the potential of using particular subjects to predict the pain of a novel subject.

To recognise pain-related conditions and individuals, there were two different architecture designs for classification, but they shared the same encoder. The shared encoder is also the basis of two transfer learning models in Sections 6.3.1 and 6.3.1. The encoder's

architecture contains three hidden layers followed by three batch normalisation layers, respectively (see Table 5.2). Following the encoder, the architectures differed between the two classification tasks. The one for pain assessment (pain-classifier) contained a dropout layer, a ReLU activation function layer, a sigmoid layer, two fully connected layers and a softmax layer. While the one (domain-classifier) for individual recognition was quite simple, which only consisted of a fully connected layer and a softmax layer. For training the model, the objective can be described as:

$$\min_{\theta} \mathcal{L}(Y, \hat{Y}(\theta)) = \min_{\theta} \left\{ -\frac{1}{N} \sum_{j=1}^N \sum_{i=1}^C y_{ij} \log(\hat{y}_{ij}(\theta)) \right\} \quad (6.11)$$

in which θ represents the model parameters, Y represents the true labels, and $\hat{Y}(\theta)$ represents the predicted probabilities produced by the model with parameters θ .

Partial Fine-tuning Training

In Chapter 5, I found that the basic CNN model produced an ideal performance in individual recognition. Therefore, it was assumed that the encoder is sensitive to individual-specific features. Inspired by such sensitivity, a transfer learning model was built with a fine-tuning mechanism. In this architecture, two encoders with architectures that share the basic encoder parameters in Table 5.2 were concatenated. The first encoder aimed to classify the domains, i.e., subject identification in this study, which were frozen after training with the domain-classifier following it. Therefore, the first encoder learnt the representation of individual specificity from the input features. Simply, the training is towards Formula 6.11 with the subject labels y_s as the true labels and aims to minimise the loss. Then the other encoder (fine-tuning encoder) was concatenated to the first encoder,

which is followed by a pain classifier architecture. The second encoder was trained with the output of the first encoder as input, in order to minimise loss with pain labels y_p as targets. In detail, the input to the second encoder has carried the representations of individual specificity, then the second encoder could learn the pain-related representations with a control of the individual differences' interferences.

During training the fine-tuning model, I split the training set in two ways. The first pipeline uses all the data in the training set for both encoders. However, it is not practical to use all the data to train the individual-specific encoder in applications. So the second pipeline used the same data as the reference data (data between the 120th to 180th seconds) in TCA for pre-training the first encoder, and the fine-tuning encoder was trained with the rest of the training set.

Adversarial Learning Training

Adversarial learning has been proven to be a powerful tool to eliminate the effects of domain variation in transfer learning [324]. A typical adversarial learning application is a generative adversarial network (GAN), which learns deep representations using a discriminator, and its generator can produce novel instances with the representation learnt by the discriminator in a confrontation [340]. But my use of adversarial model is not completely the same as GAN, which mainly used the confrontation between two characteristics represented by the same data, hence the features correlated to one characteristic, i.e., pain or not, can be exposed. The work in Chapter 5 proved that the encoder architecture in Table 5.2 can learn the features related to pain and individual specificity.

Hence, I attempted to use this encoder to develop the adversarial learning model for cross-subject transfer learning.

The encoder and the corresponding architectures for the classification of two targets were consistent with those in Section 6.3.1. The learning objective was to maximise the loss of domain classification, as well as minimise the loss of pain prediction. The objective can be written as:

$$\min_{\theta} \mathcal{L}(Y_p, \hat{Y}_p(\theta)) - \lambda \mathcal{L}(Y_s, \hat{Y}_s(\theta)) \quad (6.12)$$

Here I chose $\lambda = \log(C_p + 1) / \log(C_s + 1)$ for scaling the loss of domain classification into a similar level to the loss of pain prediction, where C_s and C_p are the numbers of subject and pain-related labels respectively.

However, in adversarial learning, the encoder did not have pilot knowledge about the characteristics that represent the domain specificity. Therefore, it is risky to maximise the loss of domain directly. To resolve such an issue, a pre-training experiment was conducted beyond the tests on the whole training set. This study continued using the stable data from seconds 120 to 180 to pre-train the encoder with the domain classifier to produce the TCA-transformed data and applied the same test.

6.3.2 Pattern Analysis

Cross-domain Kullback-Leibler Divergence

This research used the Kullback-Leibler divergence (KL divergence) to measure the similarity between different domains (i.e., subjects) [341]. By analysing the KL divergence

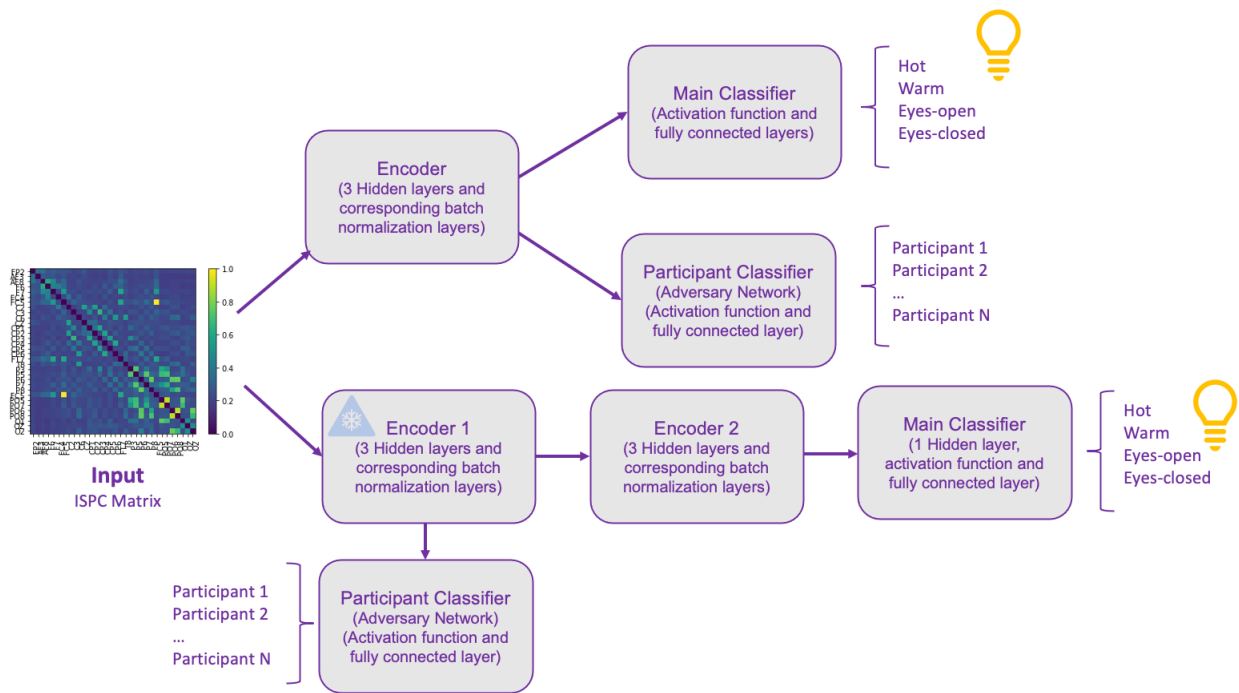


Figure 6.1: **Architecture of transfer learning frameworks.** Two transfer learning frameworks processed the input of ISPC matrices. Both frameworks aimed to minimise the loss in training the pain prediction model. (a) The upper is the adversarial learning framework. An encoder was shared by two classifiers, and two networks were trained at the same time. (b) The lower one is the partial fine-tuning framework. This framework trained encoder 1 to recognise subjects ahead. Then encoder 2 was added to frozen encoder 1 and trained toward pain prediction.

and the subject-wise accuracy, this study investigated the assumption of the correlation between the similarity and the potential of cross-domain transfer learning.

Before getting the KL divergence between two domains, the distribution of the ISPC values of the functional connectivity was first obtained between all pairs of electrodes. From the subject k , I got the ISPC distribution P_{ij}^k of functional connectivity between electrodes i and j . Then the connectivity-wise KL divergence can be represented as:

$$D_{KL}(P_{ij}^m \parallel P_{ij}^n) = \sum_{x \in \mathcal{X}} P_{ij}^m(x) \log\left(\frac{P_{ij}^m(x)}{P_{ij}^n(x)}\right) \quad (6.13)$$

where \mathcal{X} is the sample space of ISPC. Then this work used the mean KL divergence across all the connectivity between two domains (i.e., subjects in this research) to represent the divergence from domains m to n :

$$D_{KL}(P^m \parallel P^n) = \frac{1}{\sum_{i=1}^{N-1}} \sum_i^N \sum_j^N D_{KL}(P_{ij}^m \parallel P_{ij}^n) \quad (6.14)$$

where N is the number of electrodes ($N = 32$ here), the mean KL-divergence across all channels between two domains represented the difference/similarity between them. The smaller KL divergence between two domains shows that they are more similar, and vice versa. Because the measure of similarity should be independent of the classified targets in the application, this work measured the cross-domain KL divergence based on the eyes-closed (C) condition for analysis.

Grad-CAM Feature Analysis

This chapter used the same Grad-CAM algorithm as what was used in Chapter 5. But the progress in generating the activation patterns was different. Unlike the mean ISPC

matrix used in Chapter 5, 5000 samples of each condition were randomly selected, and the Grad-CAM patterns were generated from all the classifiers involving the condition. Finally, the mean Grad-CAM pattern from each classifier represented the Grad-CAM pattern in the respective classification. The patterns were generated from the convolutional layers of the basic CNN model and the classifier that predicts pain in adversarial learning.

6.4 Results

6.4.1 Performances of Transfer Learning Frameworks

Performances of Subject-wise Pain Prediction Model

The limitation in Chapter 5 suggested the absence of robust strategy to select the similar subjects to a novel subject. Hence, this chapter utilised the subject-wise pain prediction models using the basic CNN architecture, which provided the upper boundary of subject-wise transfer learning's accuracy in each subject. In other words, it could suggest the generalisability of each subject. For this purpose, Figure 6.2 showed the mean accuracy of the subject-wise pain prediction from cumulative evidence in the classification between conditions O and H, and the columns Subject (max) in Table 6.1 displayed the maximum accuracy in subject-wise accuracy of each subject. In binary classifications between resting states and thermal stimulus (between O and H / W), the majority of subject-wise accuracy was achieved 75%, including 25/36 for *O vs H* and 30/36 for *O vs W*. As found in previous chapters, the classification of thermal stimulus was always challenging. But the mean accuracy of subject-wise prediction between H and W was

	O vs H				O vs W				H vs W				O vs H vs W			
	Basic	Fine-Tuning	Adversarial	Subject (max)	Basic	Fine-Tuning	Adversarial	Subject (max)	Basic	Fine-Tuning	Adversarial	Subject (max)	Basic	Fine-Tuning	Adversarial	Subject (max)
0	58.89%	57.44%	58.84%	74.28%	64.42%	78.40%	64.57%	71.26%	52.13%	52.12%	52.72%	76.70%	38.18%	38.39%	37.04%	57.66%
1	74.86%	85.55%	72.33%	91.89%	69.30%	85.90%	69.09%	88.97%	71.94%	52.25%	62.87%	70.01%	57.97%	59.37%	68.09%	62.10%
2	86.76%	83.67%	59.92%	83.38%	76.40%	68.95%	59.16%	86.73%	59.65%	57.97%	48.24%	63.32%	48.25%	46.58%	43.35%	51.62%
3	55.80%	66.78%	46.13%	81.15%	53.96%	59.85%	62.18%	75.30%	49.06%	54.81%	62.73%	65.63%	34.81%	49.69%	38.64%	44.37%
4	76.17%	73.14%	94.19%	74.29%	57.33%	43.63%	53.04%	83.70%	48.55%	50.48%	61.82%	62.26%	33.74%	45.75%	54.37%	52.18%
5	43.36%	42.34%	45.86%	79.22%	61.08%	55.01%	69.09%	90.70%	48.96%	49.06%	49.38%	71.79%	52.29%	38.91%	37.32%	58.93%
6	78.66%	72.60%	77.15%	75.94%	71.01%	65.67%	64.30%	91.33%	51.97%	53.31%	57.84%	74.12%	65.21%	49.86%	57.16%	57.08%
7	55.32%	44.87%	49.62%	73.53%	52.55%	23.18%	44.92%	76.67%	42.34%	59.23%	77.86%	80.40%	50.53%	40.15%	31.13%	50.56%
8	48.03%	64.68%	54.62%	67.25%	33.03%	34.70%	46.98%	83.97%	51.88%	61.51%	54.98%	77.22%	33.78%	26.62%	20.36%	48.54%
9	53.97%	52.77%	49.81%	86.12%	67.38%	66.61%	77.70%	83.10%	55.34%	45.67%	46.34%	76.56%	27.37%	45.97%	38.98%	62.07%
10	55.44%	43.87%	59.39%	67.54%	44.40%	56.49%	64.37%	81.23%	57.11%	54.39%	54.74%	68.94%	33.80%	46.78%	39.58%	48.04%
11	61.52%	71.63%	48.00%	82.64%	91.85%	83.99%	76.57%	95.85%	70.38%	75.43%	85.24%	84.00%	40.70%	61.28%	58.70%	66.47%
12	64.62%	81.95%	83.51%	90.08%	36.21%	54.55%	51.08%	87.00%	69.09%	58.38%	63.95%	73.63%	62.62%	45.96%	40.92%	64.57%
13	64.00%	73.62%	64.52%	86.37%	79.97%	59.22%	59.86%	97.62%	47.47%	47.47%	47.58%	81.18%	35.84%	61.79%	63.09%	65.49%
14	55.44%	61.08%	60.64%	67.88%	43.51%	64.72%	52.37%	71.79%	53.21%	53.61%	69.17%	71.57%	28.71%	36.63%	49.53%	53.94%
15	92.93%	72.98%	93.80%	94.07%	45.73%	77.55%	70.20%	93.74%	50.26%	68.67%	53.67%	88.37%	63.79%	55.95%	56.76%	69.11%
16	68.97%	70.96%	87.54%	91.66%	76.37%	76.86%	84.59%	89.07%	67.22%	66.76%	56.34%	80.10%	72.96%	41.42%	53.96%	66.66%
17	70.64%	57.29%	62.56%	74.49%	58.59%	62.93%	62.69%	68.45%	49.89%	61.21%	61.92%	66.86%	42.89%	46.46%	43.77%	47.72%
18	68.10%	79.96%	67.74%	85.57%	60.65%	66.30%	60.65%	87.69%	52.93%	54.26%	55.33%	75.72%	43.63%	42.15%	45.82%	58.72%
19	53.40%	21.01%	63.23%	71.18%	60.16%	62.76%	65.08%	79.87%	48.35%	50.00%	51.31%	55.63%	37.50%	43.26%	40.59%	51.09%
20	52.50%	50.54%	55.52%	72.98%	51.38%	36.51%	19.81%	100.00%	1.36%	3.16%	36.06%	100.00%	28.41%	49.76%	0.00%	74.90%
21	48.36%	62.15%	63.62%	82.88%	59.21%	57.83%	42.55%	76.52%	49.48%	56.35%	48.28%	64.84%	37.51%	38.03%	34.41%	50.56%
22	63.75%	62.74%	62.67%	76.67%	60.56%	57.76%	67.07%	65.58%	63.02%	50.81%	57.34%	84.91%	35.12%	44.64%	38.43%	43.01%
23	53.69%	70.07%	67.66%	76.16%	73.24%	76.52%	80.42%	85.84%	48.42%	49.62%	48.52%	66.16%	37.71%	38.56%	39.11%	46.86%
24	60.53%	47.95%	61.98%	82.74%	27.12%	54.94%	15.41%	84.78%	38.83%	59.87%	46.24%	72.47%	18.42%	31.09%	31.51%	58.22%
25	36.75%	51.00%	56.03%	79.22%	56.33%	69.11%	59.69%	87.16%	62.44%	56.73%	48.76%	74.32%	35.41%	54.36%	46.48%	53.87%
26	65.95%	61.41%	56.38%	80.23%	51.67%	53.15%	57.85%	73.29%	51.44%	57.34%	45.64%	72.26%	42.89%	42.18%	45.32%	54.55%
27	82.82%	82.54%	64.01%	78.17%	75.67%	57.44%	74.31%	87.80%	45.02%	50.55%	55.30%	65.77%	57.15%	30.25%	47.75%	64.33%
28	53.95%	69.42%	78.76%	76.23%	61.09%	71.41%	64.33%	77.25%	51.18%	50.04%	53.29%	80.07%	49.41%	52.17%	43.66%	63.19%
29	56.62%	62.81%	44.77%	73.97%	62.76%	52.41%	61.02%	85.12%	32.12%	46.74%	36.00%	71.93%	28.91%	36.83%	39.74%	53.90%
30	90.53%	89.21%	85.69%	90.25%	91.11%	82.94%	74.89%	89.28%	0.81%	0.00%	22.96%	57.00%	13.70%	27.92%	21.27%	53.08%
31	69.41%	62.64%	74.97%	84.81%	60.98%	62.47%	69.17%	75.12%	56.82%	43.73%	56.68%	65.45%	46.85%	42.25%	44.25%	52.83%
32	55.46%	58.39%	53.24%	71.80%	55.99%	55.70%	55.77%	64.26%	41.10%	48.93%	48.59%	62.19%	33.24%	34.78%	29.86%	41.92%
33	84.73%	84.43%	76.41%	89.20%	81.37%	65.86%	75.40%	76.35%	40.07%	18.05%	43.41%	75.79%	40.30%	45.96%	42.46%	56.40%
34	58.57%	46.34%	57.09%	77.70%	82.36%	77.44%	70.00%	82.12%	53.81%	55.94%	52.59%	71.10%	43.13%	59.45%	57.87%	56.78%
35	90.30%	69.46%	52.51%	84.21%	86.41%	85.48%	80.39%	87.82%	62.71%	79.85%	62.86%	73.40%	39.80%	56.30%	73.11%	66.56%
Max	92.93%	89.21%	94.19%	94.07%	91.85%	85.90%	84.59%	100.00%	71.94%	79.85%	85.24%	100.00%	72.96%	61.79%	73.11%	74.90%
Mean	64.19%	64.15%	64.19%	79.88%	62.25%	62.90%	61.85%	82.84%	49.90%	51.51%	53.79%	72.82%	41.46%	44.65%	43.18%	56.33%
SD	13.79%	14.57%	13.24%	7.17%	15.34%	14.11%	14.62%	8.62%	14.74%	15.57%	11.07%	8.73%	12.71%	9.04%	13.60%	7.76%

Table 6.1: The subject-based mean accuracy out of cumulative evidence. This table shows the mean accuracy produced with the cumulative evidence in each subject. Conditions of warm (H), warm (W), and eyes open (O) were involved in the analysis. Under each classification, the first three columns represent the accuracy of the basic CNN model (Basic), adversarial learning (Adversarial), and partial fine-tuning (Fine-tuning) frameworks. The bold values highlight the maximum accuracy produced among the three frameworks. The last column in each classification represents the maximum accuracy of the subject-wise pain prediction.

72.82%, which was acceptable. In the multiclass classification containing the three conditions studied, 29/36 subjects had the accuracy above 70%. Therefore, most subjects had at least one similar subject from the dataset, which can be the basis to train the pain prediction model to be generalised to them.

Performances of Transfer Learning Frameworks

Figure 6.3 presented the change of loss during training, all the training phase toward pain prediction converged to slight changes, and the loss of subject recognition in the adversarial learning framework increased as expected. In the same way as the results in Figure 5.6, the curve of cumulative evidence effect on the accuracy in Figure 6.4 increased significantly with the time length universally. Hence, the models have learnt some features related to the target labels.

However, the adversarial and partial fine-tuning frameworks did not optimise the generalisation of the pain prediction model very widely. According to Table 6.1, among 288 tests of 36 subjects \times 4 classification targets using transfer learning frameworks, only 27 of them achieved higher accuracy than the corresponding subject-wise prediction. Compared to the accuracy produced by the basic CNN model in Chapter 5, more than half of the tests (160) performed better. The large standard deviations hinted at the strong individual differences in the feasibility of different frameworks. I also ran a non-parametric Friedman test on the accuracy from all the subjects in all classifications, which covered the basic CNN model, partial fine-tuning and adversarial learning frameworks. The p-values in the Durbin-Canover pairwise comparisons did not show significant dif-

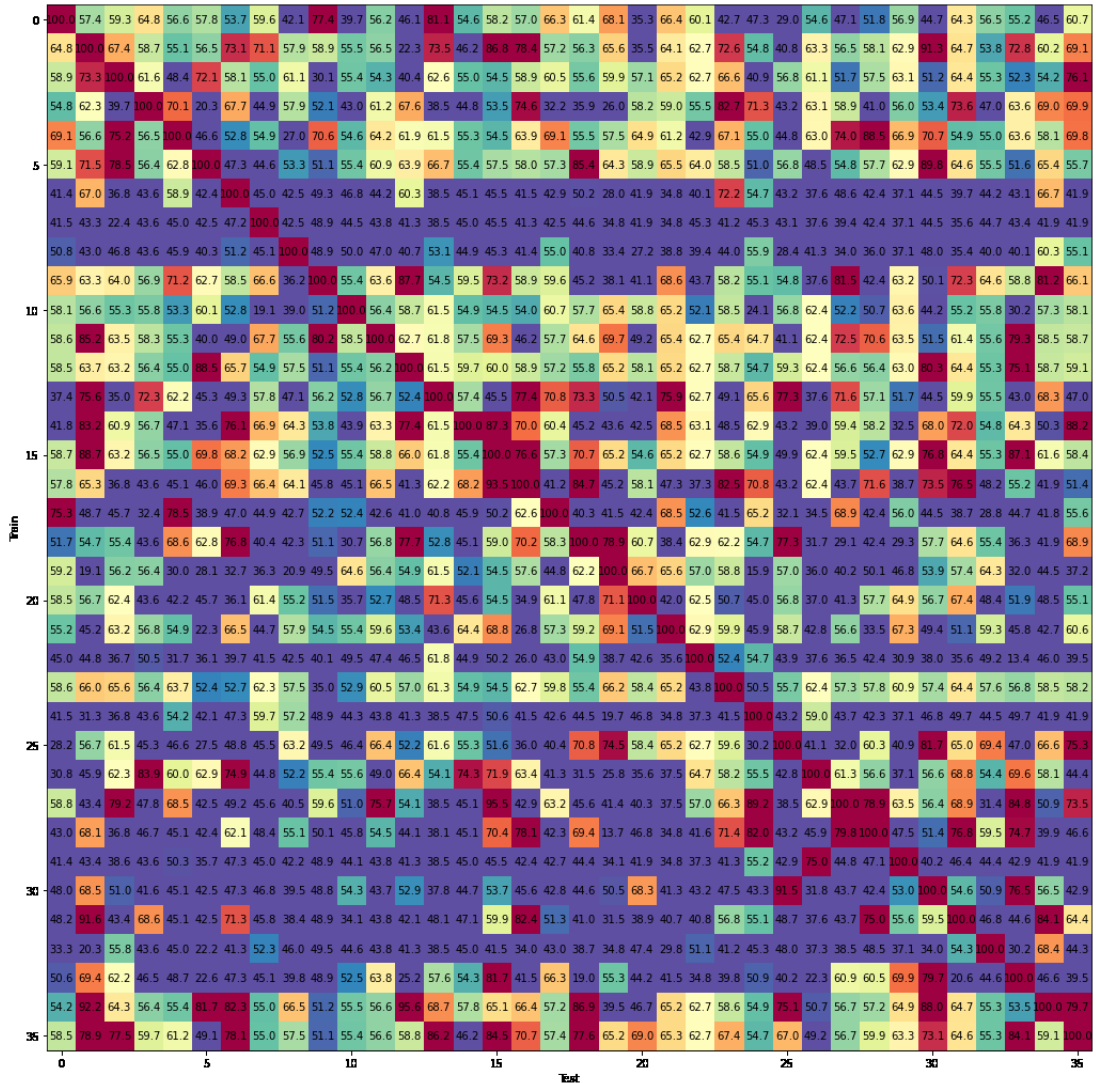


Figure 6.2: The accuracy of subject-wise pain prediction models trained and tested with each pairwise subjects. (Classification between O and H) Each row represents a subject x involved in training a subject-wise model, and each column represents the subject y whose pain-related labels were predicted with the model trained with x , the accuracy of pain prediction is shown as the value in (x, y) . In particular, the values on the diagonal should be ignored.

ferences ($p > 0.05$) between these models. The p-values were 0.195 between the basic model and the partial fine-tuning framework, and 0.105 between the basic model and the adversarial learning framework. The performances' differences between two transfer learning frameworks were very limited statistically, whose pairwise comparison p-value was 0.745 [342].

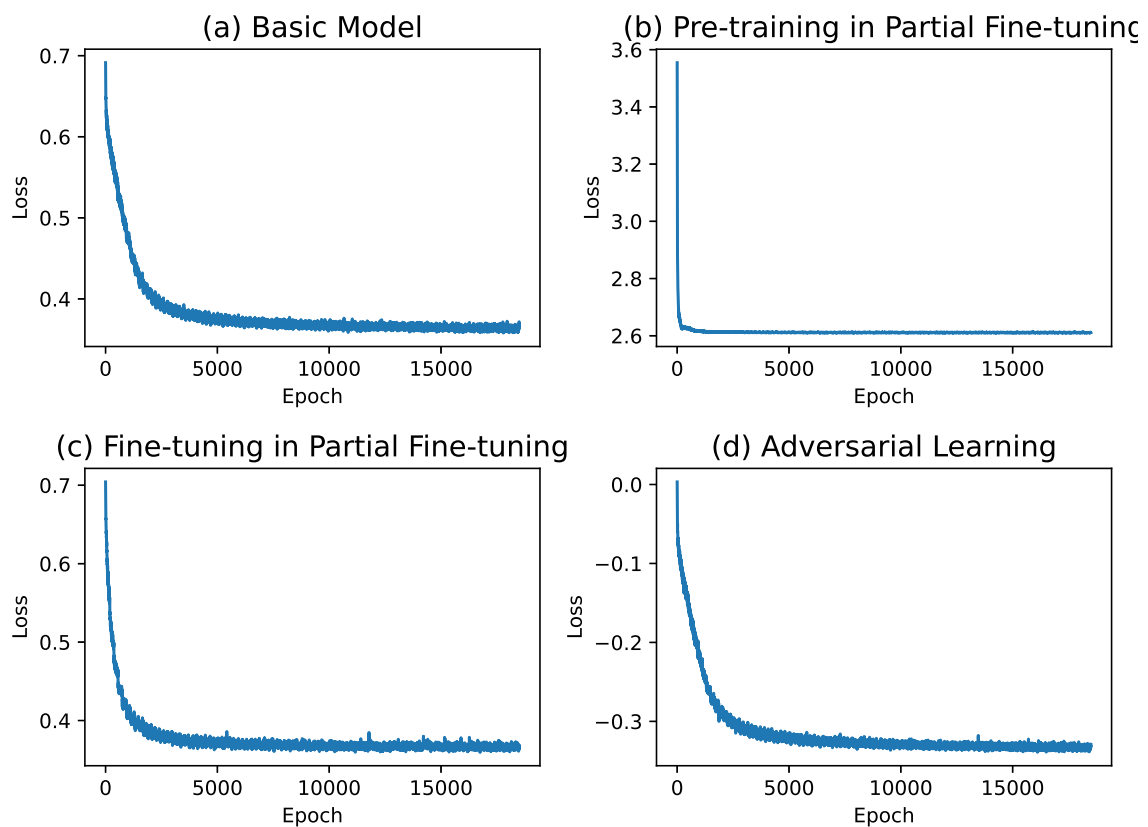


Figure 6.3: Mean loss curves of training different frameworks across 36 LOO tests respectively. The curves were made with the classification between O and H.

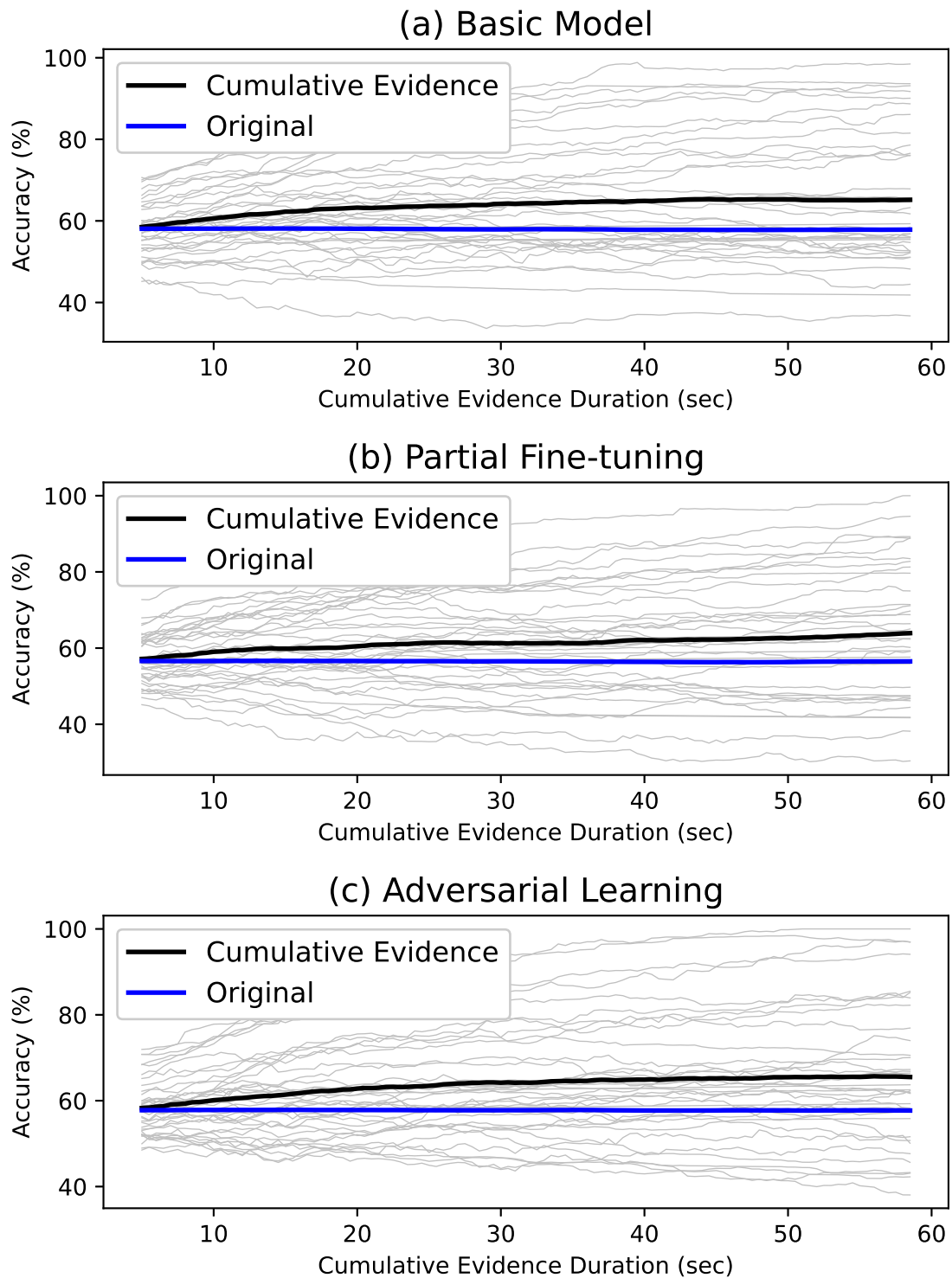


Figure 6.4: **The effects of time length involved in cumulative evidence.** The bold curves represent the mean curves of cumulative evidence's effects on accuracy across the all the LOO tests, and the grey curve represents the accuracy curve of cumulative evidence from each LOO test.

Effects of Transfer Component Analysis (TCA)

By using two resting states as references to obtain the kernel separately, TCA transformed the data samples into the Hilbert space where the distances were minimised. Table 6.2 presents the performance of tests based on the original ISPC matrices and the tests applied with TCA. Unfortunately, TCA even weakened performance in pain prediction in most settings.

6.4.2 Correlation between Similarity Measure and Accuracy

Figure 6.5 shows the mean KL divergence across the same channels of pairs of subjects. For analysing their correlation with the subject-wise accuracy, a linear regression was executed. Figure 6.6 showed the significant negative correlation between KL divergence and subject-wise precision ($***p < .001$). Therefore, the KL divergence is potentially a measure of the similarity between subjects from this post hoc analysis.

6.4.3 Grad-CAM Pattern

Since the architecture of the subject recognition model was adapted to adversarial learning and partial fine-tuning frameworks, the study generated its activation regions of the feature maps with Grad-CAM (see Figure 6.7). The main specificity of this pattern is the wide distribution of functional connectivity of importance. Despite the wide distribution, functional connectivity within the frontal brain region (FP2-AF3) showed an exceptional contribution.

Figure 6.8 is the set of Grad-CAM patterns in different classifications. The main char-

		Non-TCA		TCA			
				O-based		C-based	
		Mean	Std	Mean	Std	Mean	Std
O vs H	Basic	64.19%	13.79%	64.50%	13.70%	62.28%	13.49%
	Fine-Tuning	64.15%	14.57%	59.50%	13.80%	63.78%	12.93%
	Adversarial	64.19%	13.24%	65.30%	12.30%	65.38%	14.66%
	Subject (max)	79.88%	7.17%	76.40%	9.30%	78.37%	10.12%
O vs W	Basic	62.25%	15.34%	65.40%	11.80%	62.15%	13.20%
	Fine-Tuning	62.90%	14.11%	59.50%	11.40%	60.32%	13.55%
	Adversarial	61.85%	14.62%	61.00%	14.30%	66.71%	13.63%
	Subject (max)	82.84%	8.62%	75.20%	11.30%	75.28%	11.70%
H vs W	Basic	49.90%	14.74%	52.40%	9.14%	52.28%	13.79%
	Fine-Tuning	51.51%	15.57%	52.00%	9.42%	52.55%	11.95%
	Adversarial	53.79%	11.07%	51.60%	8.70%	52.08%	10.19%
	Subject (max)	72.82%	8.73%	72.50%	10.60%	72.15%	9.28%
O vs H vs W	Basic	41.46%	12.71%	43.10%	9.59%	43.75%	10.53%
	Fine-Tuning	44.65%	9.04%	36.70%	9.59%	39.98%	8.64%
	Adversarial	43.18%	13.60%	40.80%	8.04%	42.93%	10.88%
	Subject (max)	56.33%	7.76%	53.50%	7.69%	54.93%	6.36%

Table 6.2: Performances produced by different models without and with TCA. The bold values show the maximum mean accuracy in each row.

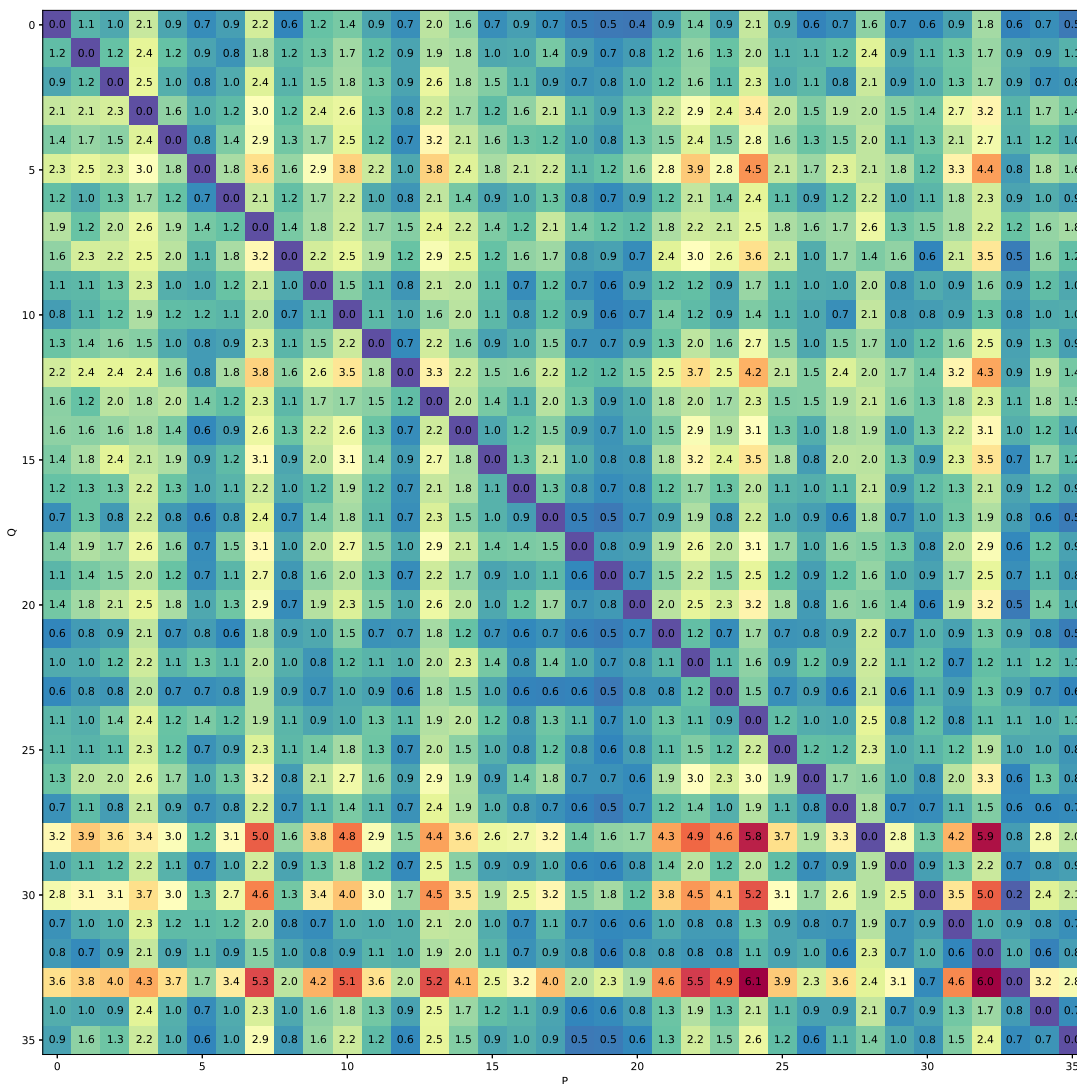


Figure 6.5: The mean KL divergence between the distributions of ISPC values between the same channel of pairwise subjects. Since KL divergence is not symmetrical, P and Q represent subjects' IDs, where the KL divergence was computed with $D_{KL} = \sum P(x) \log(P(x)/Q(x))$. Each KL divergence was computed as the mean values of the KL-divergences acquired from the same channel from subjects P and Q respectively. The values of KL divergence represent the directed similarity from P to Q .

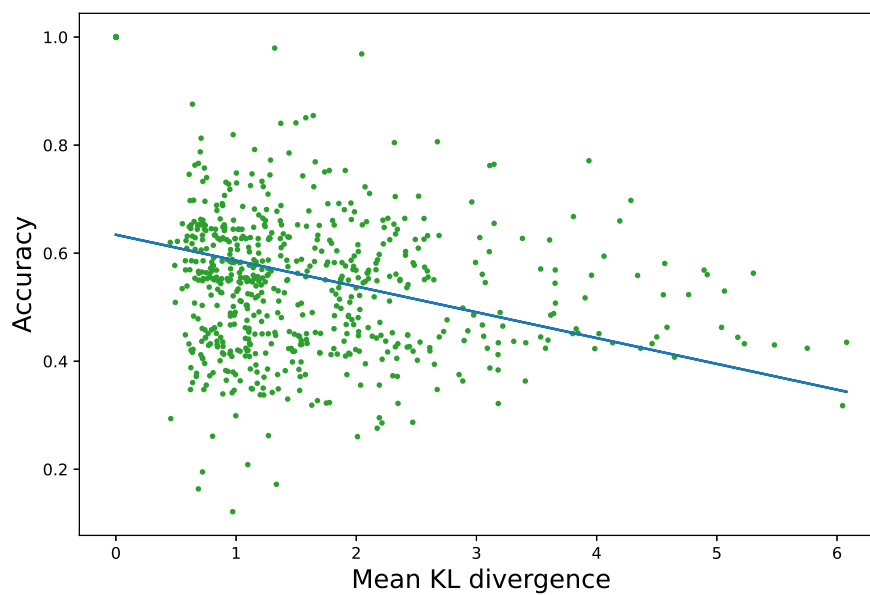


Figure 6.6: The scatter plot of KL divergence versus the subject-wise accuracy, with a fitted linear regression line $y_{acc} = -0.0478x_{KL} + 0.6341$; $R^2 = 0.0992$, $***p < .001$.

acteristic of all of these patterns is the extraordinary functional connectivity inside the frontal brain region. The consistency of the vital functional connectivity of subject recognition and pain prediction is evidence of the poor performances in Section 6.4.1. Another significant pattern of functional connectivity occurred between the central and occipital regions, especially whilst classifying the painful and innocuous thermal stimulus. In a more universal view, most functional connectivity contributed significantly to pain prediction, except for long-distance connectivity between the frontal and occipital regions.

6.5 Discussion and Conclusion

The abundant attempts in developing transfer learning models did not provide ideal results as assumptions. However, the loss curves (6.3) proved that the networks learnt some features correlated with pain, so the analysis aims to dig into the Grad-CAM patterns to demonstrate the possible interpretability.

Before reviewing the differences and similarities between the feature patterns of subject recognition and pain prediction, I tend to discuss a counterintuitive difference, the activation regions revealed in Figures 5.9 and 6.8a. The models producing them had similar architectures and were trained toward the same target, classifying pain and non-pain conditions. So in principle, they are supposed to have similar activation patterns. However, functional connectivity between the frontal and central regions had high contributions in Figure 5.9, which existed but was not so exceptional in Figure 6.8a. Fur-

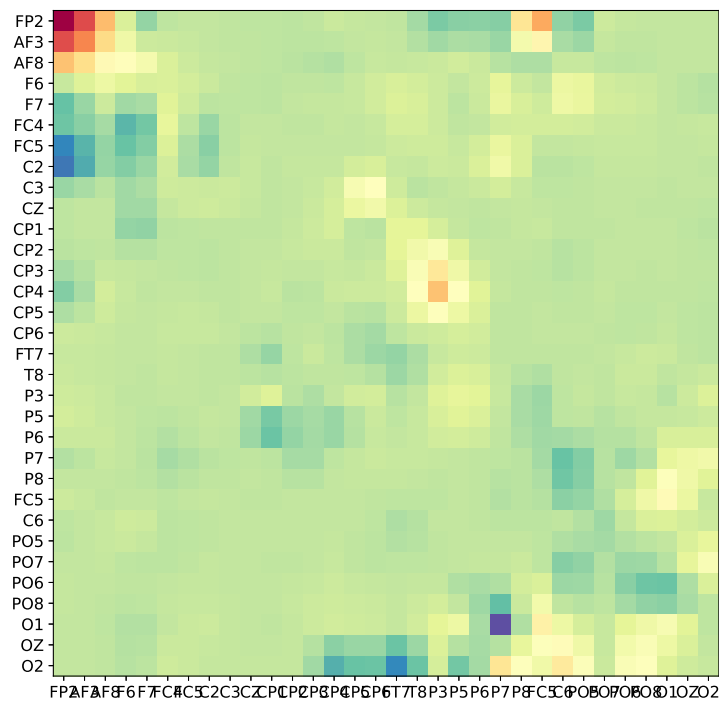
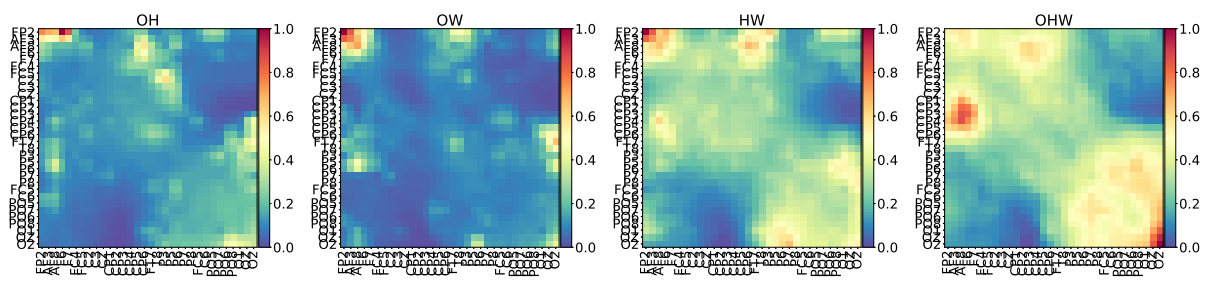
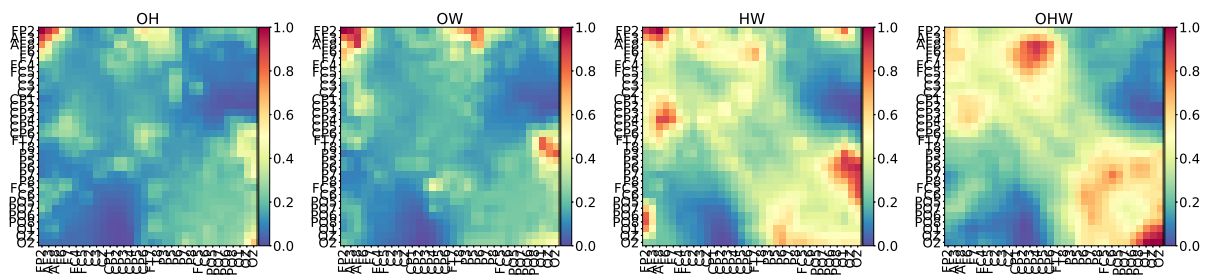


Figure 6.7: **Grad-CAM feature maps produced in the model recognising subjects.** The map was generated based on the subject recognition model in Chapter 5, which was the basis of the subject recognition models in adversarial learning and partial fine-tuning frameworks.



(a) Basic CNN model



(b) Adversarial learning network toward pain prediction

Figure 6.8: **The Grad-CAM feature maps of the models predicting pain.** The activation patterns were produced from the last hidden convolutional layer in each architecture, the strength of each region represents the contributions in pain prediction.

thermore, the importance of functional connectivity within the frontal brain region was not shown in Figure 5.9. Such differences possibly resulted from the use of max pooling layers. When comparing the architecture of the convolutional layers in Tables 5.1 and 5.2, the output sizes of the last hidden layers in two-dimensional space were 3×3 and 20×20 . In Chapter 5, I used the max pooling layers following the hidden layers, which can extract the local features and reduce the size of features to increase computational efficiency. Although the accuracy showed in Chapter 5 was acceptable, the Grad-CAM patterns suggested that the use of max pooling wasted lots of local features, for instance, the output feature dimension was 3×3 , which represented the brain regions quite roughly. This weakness could make the model ignore the features specific to individual characteristics. Thus, it may weaken the generalisation of the CNN model. In simple, max pooling down-samples the input in CNN by selecting the maximum value from a group of values in a local region with the specific size, it *blurred* the spatial details in the patterns [343]. Therefore, some important details were blurred or even ignored with max-pooling, such as small-ranging connectivity within the frontal region. And the widely distributed property can be exposed easily, for example, the connectivity between frontal and central brain regions. After removing the max-pooling layers, more details can be kept in the functional connectivity patterns. Thus, the output from the Grad-CAM analysis can reveal more localised, short-range activation regions.

Observing the feature patterns shown in Figure 6.7, the main characteristic is the extensive distribution of activation. In the fMRI-based study, Hoeppli et al. did not detect that brain activation was significantly correlated with individual differences in pain

processing [344], but Lin et al. reported individual differences in activities in the somatosensory cortex (S1), supplementary motor area (SMA), medial prefrontal cortex (mPFC) and insula, as well as some evidence of the contributions of ACC and thalamus [207, 345]. Although these findings were intuitively opposite each other, both provided potential explanations for the wide distribution of functional connectivity that affects subject recognition. In conclusion, the spatial features of neurophysiological signals, typically functional connectivity, are always distributed very broadly. Hence, it is challenging to decompose them from the features specific to pain processing.

Interestingly, the main similarity is concentrated in the frontal region between the activation patterns specific to individual differences and pain processing. Regarding the strong contribution of the frontal region to subject recognition, some work found the change in prefrontal cortex activities as the marker of individual differences, including activation of the medial and ventral lateral prefrontal regions that varied the processing of pain-related cognition between individuals [346], and differences in prefrontal cortex activation intensity presented individual differences in the effects of perceived controllability on pain perception [347]. In the prediction of cross-subject pain, the work by Lin et al. suggested that mPFC was both a region that predicted pain with negative correlation and responded to pain with individual differences [345]. This declaration can be proven by the activation patterns in all sub-figures of Figure 6.8. It was consistent with the finding about the contributions of the prefrontal cortex to pain processing, for example, the right lateral frontal cortex had distinct activation dynamics responding to the pain stimulus [348, 349]. Therefore, the similarity of the frontal region's roles caused

barriers in detecting the features associated with both targets.

The similarity of the frontal regions' contributions to both pain-related and individual specificity also provided possible reason for TCA's negative effects. The main purpose of TCA is *aligning* the data across domains, so that the individual-specific characteristics can be reduced. Nonetheless, during subtracting the components specific to individual differences, key representations of pain-related features were also reduced.

This work also uncovered the functionality of the occipital lobe more deeply. In previous studies, the occipital lobe was suggested as an important region for detecting resting states [331]. In this chapter, the central-occipital functional connectivity strengthened in the classification between conditions H and W, even compared with the distinction of thermal stimulus from the resting state. Therefore, the occipital lobe might also be a marker of an innocent stimulus, but evidence of such effects was rarely reported. One possible explanation is that activities in the left occipital lobe are associated with violated expectations, which could be induced by thermal stimulus regardless of intensity [350].

Deep learning is widely focused on transfer learning research, but it is not necessary to improve generalisation in a specific task, i.e., pain assessment in this work [47]. However, with an appropriate measure of domain similarity, selective transfer learning can be implemented in a very concise way [325]. The correlation between KL divergence and subject-wise pain prediction accuracy in Section 6.4.2 showed the potential to select *similar subjects* to a novel subject. Hence, the pain prediction model could be trained with similar subjects selected, even using concise models such as SVM.

The novel models in this chapter did not produce ideal accuracy as expected, but

the analysis of Grad-CAM patterns demonstrated the possible origin of challenges in generalising the pain prediction model across subjects. The wide overlap of important functional connectivity, remarkable within the frontal region, hardened the decomposition of features specific to individual differences from features related to pain. Therefore, more efforts are needed to develop transfer learning frameworks and corresponding hyperparameter optimisation [351]. Another potential solution is utilising the measure of domain similarities to determine the similar subjects to the novel subject as the basis of model training. This study advised the feasibility of the KL divergence as an objective for selective transfer learning. Recent work by Valentini et al. suggested that the increase in gamma oscillations carried a significant correlation with individual variation; inspired me that combination between phase-based functional connectivity from the alpha band and the features generated based on the gamma band to improve the generalisation of the model for pain prediction [194].

Chapter 7

Conclusion

This chapter summarises the contributions of this thesis in a global view, which follows the flow from feature discovery to model development. Further discussions declare the existing limitations, which have not been resolved in the current study, and propose the potential future work associated with them.

7.1 Main Contributions

In summary, this work found the neural marker of integration to represent the complexity of pain, and developed machine learning models with such neural markers as features. The current research aimed to implement machine learning models for pain assessment in an *extreme* way: Different from the classical thoughts to use multiple features for pain assessment, this research involved the input features from only one type of neural marker specific to pain processing.

From the systematic research, I revealed the good performance of phase-based functional connectivity from the alpha band in both prediction accuracy and computational efficiency. Since the final objective of developing the pain assessment model was to apply it in unresponsive patients, the model demands cross-subject generalisation. Using alpha-phase functional connectivity, this study proposed a CNN model to assess pain, whose architecture can process both the specificity of pain perception and individual differences. Remarkably, this research used Grad-CAM to reveal the interpretability of the features extracted by the CNN model from the perspective of physiology. Accordingly, all of questions in Section 1.2 were answered systematically.

In general, this research contributed to the requirements of patients' daily care at the bedside in two aspects. First, it can be implemented both in terms of hardware and software. The mobility of EEG devices makes signal acquisition easy, while the execution of our machine learning algorithm does not require abundant computational resources. Second, this work disclosed some useful strategies to improve the pain assessment model's generalisation. Based on our paradigms, future models may more quickly fit in novel patients.

7.1.1 Phase-based Functional Connectivity from the Alpha Band:

Ideal Neural Marker of Integration for Pain Prediction

This research demonstrated the phase-based functional connectivity from the alpha band as an neural marker of pain, with which the appropriate machine learn-

ing models (e.g, the SVM model in Chapter 4) can accurately and efficiently predict pain. Although brain's responses to pain are complex, the neural integrations among different brain regions or neuronal oscillations were not investigated sufficiently as a neural marker. This work considered measures of two major neural integrations, functional connectivity and cross-frequency coupling, and studied the effects of phase and power from EEG signals to predict pain. For rigorous comparability between the measures, this work innovatively employed ISPC and the Euler-like form of spectral coherence to quantify the phase- and power-based neural integrations. By inputting functional connectivity from the alpha band and cross-frequency coupling from four low-frequency bands, the phase-based functional connectivity from the alpha band presented outstanding performances in both accuracy and efficiency. Furthermore, the topography of phase and power in different bands was analysed, which spatially revealed the significant differences of exponential phases' distribution among conditions within a frequency band, and suggested the reverse performances of the power topography. Thus, I obtained the quantitative reason why phase-based neural markers can discriminate the pain and non-pain conditions better than the power-based ones.

In addition, this work analysed the effects of trial length and the number of features in pain prediction based on alpha-phase functional connectivity. The result of four tested the effects of trial lengths (1, 2.5, 5, 10 seconds), when the length was 5 or 10 seconds in this work, the accuracy was significantly better and tended to be stable. Therefore, stable trial lengths were applied in the further development of pain prediction models in the following sections. It was consistent with the stability of phase-based quantification

of neural integration [293]. Regarding the number of features, this research did not find a significantly optimised number of important features between 10 and 100, but 40 features can be a *threshold* of converging accuracy. Following this finding, NCA selected 40 features in each pairwise classification and found the important functional connectivity to recognise each pain-related condition. As a main finding, functional connectivity within the frontal brain region (AF8-F7) was vital for predicting pain.

7.1.2 Discovery of Deep Learning: Convolutional Neural Network for Cross-subject Pain Assessment

This study proposed a novel CNN architecture for pain prediction, which can recognise the subject identification with the same feature as well. Benefiting from the rapid development of deep learning, I proposed a concise architecture of a CNN model. This model had two advantages. First, to solve the challenge of generalising pain prediction models across subjects, this model was sensitive to the individual specificity of the subjects involved in training. Compared with the poor performance of the SVM model using the same feature, it suggested its potential to be the fundamental of the cross-subject pain prediction model. Second, by using this CNN architecture, subjects can still be recognised accurately with alpha-phase functional connectivity. Hence, this combination of model and neural marker can also help expose individual-specific features suitable for transfer learning.

Three transfer learning strategies were tested to evaluate the performance of

cross-subject pain assessment. For cross-subject pain prediction, this research evaluated three transfer learning strategies to test if they could produce better results than the basic CNN model, including selective transfer learning, adversarial learning, and partial fine-tuning transfer learning. Moreover, the CNN model was also a suitable model for being the components in transfer learning models. In selective transfer learning, though the CNN model can select subjects similar to novel subjects excluded from training, the subject-wise pain prediction model did not produce a better performance than the basic model. In the use of adversarial learning and partial fine-tuning frameworks, the loss curves suggested that they could learn some features associated with pain perception. Nevertheless, they did not perform significantly better than the basic model.

7.1.3 Physiological Interpretability of the Features Extracted by CNN Model

A highlight of this research is using Grad-CAM to analyse the features exposed by CNN, which interpreted the physiological principles of the model's working mechanism. The activation patterns generated by Grad-CAM from the CNN model matched the important functional connectivity with the findings of brain regions' activities in pain perception. Taking into account the importance of the somatosensory cortex in pain processing, functional connectivity that involves the parietal region near the location of the somatosensory cortex played an important role. To be highlighted, the functional connectivity within the frontal region was of importance in all deep learning frameworks in

this research. It is consistent with the findings of fMRI on the change of frontal activities in pain perception, as well as the analysis in Section 7.1.2 about the important functional connectivity between electrodes AF8 and F7.

Grad-CAM analysis also helped interpret the poor performance of adversarial learning and partial fine-tuning frameworks. The activation pattern to recognise the strong activation shared by subjects within the frontal lobe. Moreover, its activation feature map of functional connectivity covered most of the brain regions. Therefore, it is still difficult to decompose the features specific to individual differences in pain processing for the pain assessment model.

7.2 Limitations and Future Work

Although this thesis presented a potential approach to assess pain from EEG data. However, the amount of data collected in laboratory environments limited the models' performance. The development of more powerful transfer learning algorithms needs more work as well. In addition, this thesis did not evaluate the performances of the models using online BCI, so it is still unclear if it is practically applicable at the bedside.

7.2.1 Robust Strategy of Cross-subject Pain Assessment

The main deficiency of this work concentrated on the limitation of transfer learning performances. In other words, the model is still far from assessing pain in unresponsive patients at the bedside. Hence, the direction of improvement contains attempts following

the two categories of paradigms.

One of the paradigms is selective transfer learning. In this investigation, the strategy to select one subject similar to the novel did not work ideally. Because poor performance was possibly caused by lack of data, for example, data from one subject was only 1/35 of the training set containing all subjects except for the excluded one. Future work could test the effects of multiple similar subjects and utilise some data augmentation algorithms, such as GAN, to make the data size equivalent with the subject-mixed training. Another paradigm is to find the measure of domain similarity between subjects, so that the pain prediction model can be more flexible. The correlation between KL divergence and subject-wise accuracy indicated in this research can be a good source for this strategy.

The deep learning frameworks, such as adversarial learning and partial fine-tuning frameworks evaluated in this work, are also worth further improvement. In the architecture aspect, the layers could be optimised to reduce the effects of individual differences. Moreover, hyperparameter optimisation could also strengthen the performances of the original frameworks.

7.2.2 Generalisation and Standardisation of Datasets for

EEG-based Pain Assessment

All of the work in this thesis was based on the dataset described in Chapter 3. It means that the generalisation of all the models in the other datasets for pain assessment is un-

clear. In different studies that assessed pain with EEG, there were many different factors, including pain inducer methods, recording environments, EEG hardware, levels of pain intensity, etc. [352, 353]. There is a hierarchy to evaluate the model that involves different datasets. The primary objective is to test the accuracy of the prediction and the consistency of the features extracted in the other datasets. Additionally, the performances of different pain prediction models can be compared in the same dataset. An advanced target is to use data from different datasets for data augmentation, i.e., using subjects participating in different experiments can make it possible to detect individual-specific features, where the characteristics associated with environmental and hardware differences can be decomposed more easily [354].

7.2.3 BCI-based Online Pain Assessment System

No matter whether to help the patient's caretakers or just monitor the pain of responsive people, a *naked* model cannot be ready-to-use. The way to introduce pain assessment models to a system accepting EEG signals as input is by building a brain-computer interface (BCI). Since Vidal proposed the concept of BCI in 1973 [355], the technical pipeline for the use of BCI for medicine has matured [356]. In general, we could use the EEG signals as the input to the BCI system, the processing block consists of the preprocessing methods and the machine learning model. Finally, the BCI system will make the prediction of pain will be made by the BCI system as a result. Furthermore, the pain assessment system is also an important component in the bidirectional or closed-loop BCI for pain relief, where an electric stimulus or other treatment will be administered to the nervous

system when pain is detected [118, 357].

Therefore, future work should incorporate the pain prediction model into a BCI system so that it can detect pain from real-time signals. Initially in laboratory environments, the system should be plug-in ready with specific thermode systems, which can work in both virtual testing mode, loading the existent data for testing the online models, and an experimental mode, predicting pain and recording data in the meantime. Furthermore, some optimisation methods, such as reinforcement learning, can be applied in such a BCI system, so that the model's sensitivity to pain can increase with the new signals recorded while running the system [358].

Bibliography

- [1] Marian Osterweis, Arthur Kleinman, and David Mechanic. Pain and disability: Clinical, behavioral, and public policy perspectives. 1987.
- [2] Amelia Williamson and Barbara Hoggart. Pain: a review of three commonly used pain rating scales. *Journal of clinical nursing*, 14(7):798–804, 2005.
- [3] Ronald Melzack and Srinivasa N Raja. The mcgill pain questionnaire: from description to measurement. *The Journal of the American Society of Anesthesiologists*, 103(1):199–202, 2005.
- [4] Guanghao Sun, Zhenfu Wen, Deborah Ok, Lisa Doan, Jing Wang, and Zhe Sage Chen. Detecting acute pain signals from human eeg. *Journal of neuroscience methods*, 347:108964, 2021.
- [5] Zewen Li, Fan Liu, Wenjie Yang, Shouheng Peng, and Jun Zhou. A survey of convolutional neural networks: analysis, applications, and prospects. *IEEE transactions on neural networks and learning systems*, 2021.

- [6] S.J. Panchal and V. Grami. Pain, nociceptive vs. neuropathic. In Michael J. Aminoff and Robert B. Daroff, editors, *Encyclopedia of the Neurological Sciences (Second Edition)*, pages 749–752. Academic Press, Oxford, second edition edition, 2014.
- [7] Danielle Reddi, Natasha Curran, and Robert Stephens. An introduction to pain pathways and mechanisms. *British journal of hospital medicine*, 74(Sup12):C188–C191, 2013.
- [8] Mike X Cohen. *Analyzing neural time series data: theory and practice*. MIT Press, 1st editio edition, 2014.
- [9] Aleksandra Miljevic, Neil W Bailey, Oscar W Murphy, M Prabhavi N Perera, and Paul B Fitzgerald. Alterations in eeg functional connectivity in individuals with depression: A systematic review. *Journal of Affective Disorders*, 2023.
- [10] Adley Tsang, Michael Von Korff, Sing Lee, Jordi Alonso, Elie Karam, Matthias C. Angermeyer, Guilherme Luiz Guimaraes Borges, Evelyn J. Bromet, Giovanni de Girolamo, Ron de Graaf, Oye Gureje, Jean Pierre Lepine, Josep Maria Haro, Daphna Levinson, Mark A. Oakley Browne, Jose Posada-Villa, Soraya Seedat, and Makoto Watanabe. Common Chronic Pain Conditions in Developed and Developing Countries: Gender and Age Differences and Comorbidity With Depression-Anxiety Disorders. *Journal of Pain*, 9(10):883–891, 2008.
- [11] Harald Breivik, Elon Eisenberg, and Tony O’Brien. The individual and societal burden of chronic pain in Europe: The case for strategic prioritisation and action

- to improve knowledge and availability of appropriate care. *BMC Public Health*, 13(1), 2013.
- [12] Alec B OConnor. Neuropathic pain. *Pharmacoeconomics*, 27(2):95–112, 2009.
- [13] C Voscopoulos and M Lema. When does acute pain become chronic? *British journal of anaesthesia*, 105(suppl_1):i69–i85, 2010.
- [14] Christine H Meyer-Frießem, Janne Gierthmühlen, Ralf Baron, Claudia Sommer, Nurcan Üçeyler, and Elena K Enax-Krumova. Pain during and after covid-19 in germany and worldwide: a narrative review of current knowledge. *Pain reports*, 6(1), 2021.
- [15] Amanda C de C Williams. Facial expression of pain: an evolutionary account. *Behavioral and brain sciences*, 25(4):439–455, 2002.
- [16] Ronald Melzack. The mcgill pain questionnaire: major properties and scoring methods. *pain*, 1(3):277–299, 1975.
- [17] Ronald Melzack. The short-form mcgill pain questionnaire. *Pain*, 30(2):191–197, 1987.
- [18] Gillian A Hawker, Samra Mian, Tetyana Kendzerska, and Melissa French. Measures of adult pain: Visual analog scale for pain (vas pain), numeric rating scale for pain (nrs pain), mcgill pain questionnaire (mpq), short-form mcgill pain questionnaire (sf-mpq), chronic pain grade scale (cpgs), short form-36 bodily pain scale

- (sf-36 bps), and measure of intermittent and constant osteoarthritis pain (icoap). *Arthritis care & research*, 63(S11):S240–S252, 2011.
- [19] Marcella Sacco, Michele Meschi, Giuseppe Regolisti, Simona Detrenis, Laura Bianchi, Marcello Bertorelli, Sarah Pioli, Andrea Magnano, Francesca Spagnoli, Pasquale Gianluca Giuri, et al. The relationship between blood pressure and pain. *The journal of clinical hypertension*, 15(8):600–605, 2013.
- [20] Marco L Loggia, Mylène Juneau, and M Catherine Bushnell. Autonomic responses to heat pain: Heart rate, skin conductance, and their relation to verbal ratings and stimulus intensity. *PAIN®*, 152(3):592–598, 2011.
- [21] Chih-Chung Chen, Ghazala Tabasam, and Mark I Johnson. Does the pulse frequency of transcutaneous electrical nerve stimulation (tens) influence hypoalgesia?: A systematic review of studies using experimental pain and healthy human participants. *Physiotherapy*, 94(1):11–20, 2008.
- [22] Lavinia Raeside. Physiological measures of assessing infant pain: a literature review. *British journal of nursing*, 20(21):1370–1376, 2011.
- [23] The Cortical Rhythms of Chronic Back Pain. *Journal of Neuroscience*, 31(39):13981–13990, 2011.
- [24] Jianren Mao. Current challenges in translational pain research. *Trends in pharmacological sciences*, 33(11):568–573, 2012.

- [25] Srinivasa N Raja, Daniel B Carr, Milton Cohen, Nanna B Finnerup, Herta Flor, Stephen Gibson, Francis Keefe, Jeffrey S Mogil, Matthias Ringkamp, Kathleen A Sluka, et al. The revised iasp definition of pain: concepts, challenges, and compromises. *Pain*, 161(9):1976, 2020.
- [26] Markus Ploner, Christian Sorg, and Joachim Gross. Brain rhythms of pain. *Trends in cognitive sciences*, 21(2):100–110, 2017.
- [27] A Vania Apkarian, M Catherine Bushnell, Rolf-Detlef Treede, and Jon-Kar Zubieta. Human brain mechanisms of pain perception and regulation in health and disease. *European journal of pain*, 9(4):463–484, 2005.
- [28] Esther L Meerwijk, Judith M Ford, and Sandra J Weiss. Brain regions associated with psychological pain: implications for a neural network and its relationship to physical pain. *Brain imaging and behavior*, 7:1–14, 2013.
- [29] Junseok A Kim and Karen D Davis. Neural oscillations: understanding a neural code of pain. *The Neuroscientist*, 27(5):544–570, 2021.
- [30] Markus Ploner, Christian Sorg, and Joachim Gross. Brain Rhythms of Pain. *Trends in Cognitive Sciences*, 21(2):100–110, 2017.
- [31] Andrew J Furman, Timothy J Meeker, Jeremy C Rietschel, Sooyoung Yoo, Janusiya Muthulingam, Mariya Prokhorenko, Michael L Keaser, Ronald N Goodman, Ali Mazaheri, and David A Seminowicz. Cerebral peak alpha frequency predicts individual differences in pain sensitivity. *Neuroimage*, 167:203–210, 2018.

- [32] Elia Valentini, Sebastian Halder, Daisy McInnerney, Jason Cooke, Istvan L Gyimes, and Vincenzo Romei. Assessing the specificity of the relationship between brain alpha oscillations and tonic pain. *NeuroImage*, page 119143, 2022.
- [33] Elisabeth S May, Moritz M Nickel, Son Ta Dinh, Laura Tiemann, Henrik Heitmann, Isabel Voth, Thomas R Tölle, Joachim Gross, and Markus Ploner. Prefrontal gamma oscillations reflect ongoing pain intensity in chronic back pain patients. *Human brain mapping*, 40(1):293–305, 2019.
- [34] CC Liu, JH Chien, JH Kim, YF Chuang, DT Cheng, WS Anderson, and FA Lenz. Cross-frequency coupling in deep brain structures upon processing the painful sensory inputs. *Neuroscience*, 303:412–421, 2015.
- [35] Markus Ploner, Michael C Lee, Katja Wiech, Ulrike Bingel, and Irene Tracey. Pre-stimulus functional connectivity determines pain perception in humans. *Proceedings of the National Academy of Sciences*, 107(1):355–360, 2010.
- [36] Maite M Van Der Miesen, Martin A Lindquist, and Tor D Wager. Neuroimaging-based biomarkers for pain: state of the field and current directions. *Pain reports*, 4(4), 2019.
- [37] Tyler Mari, Jessica Henderson, Michelle Maden, Sarah Nevitt, Rui Duarte, and Nicholas Fallon. Systematic review of the effectiveness of machine learning algorithms for classifying pain intensity, phenotype or treatment outcomes using electroencephalogram data. *The Journal of Pain*, 23(3):349–369, 2022.

- [38] Jörn Lötsch and Alfred Ultsch. Machine learning in pain research. *Pain*, 159(4):623, 2018.
- [39] Enrico Schulz, Andrew Zherdin, Laura Tiemann, Claudia Plant, and Markus Ploner. Decoding an individual's sensitivity to pain from the multivariate analysis of eeg data. *Cerebral cortex*, 22(5):1118–1123, 2012.
- [40] Joshua Levitt, Muhammad M Edhi, Ryan V Thorpe, Jason W Leung, Mai Michishita, Suguru Koyama, Satoru Yoshikawa, Keith A Scarfo, Alexios G Carayannopoulos, Wendy Gu, et al. Pain phenotypes classified by machine learning using electroencephalography features. *Neuroimage*, 223:117256, 2020.
- [41] Maryam Vatankhah and Amir Toliyat. Pain level measurement using discrete wavelet transform. *International Journal of Engineering and Technology*, 8(5):380–384, 2016.
- [42] Tahereh Nezam, Reza Boostani, Vahid Abootalebi, and Karim Rastegar. A novel classification strategy to distinguish five levels of pain using the eeg signal features. *IEEE Transactions on Affective Computing*, 12(1):131–140, 2018.
- [43] Stefano Betti, Raffaele Molino Lova, Erika Rovini, Giorgia Acerbi, Luca Santarelli, Manuela Cabiati, Silvia Del Ry, and Filippo Cavallo. Evaluation of an integrated system of wearable physiological sensors for stress monitoring in working environments by using biological markers. *IEEE Transactions on Biomedical Engineering*, 65(8):1748–1758, 2017.

- [44] Mingxin Yu, Yichen Sun, Bofei Zhu, Lianqing Zhu, Yingzi Lin, Xiaoying Tang, Yikang Guo, Guangkai Sun, and Mingli Dong. Diverse frequency band-based convolutional neural networks for tonic cold pain assessment using eeg. *Neurocomputing*, 378:270–282, 2020.
- [45] Gaurav Misra, Wei-en Wang, Derek B Archer, Arnab Roy, and Stephen A Coombes. Automated classification of pain perception using high-density electroencephalography data. *Journal of neurophysiology*, 117(2):786–795, 2017.
- [46] Zitong Wan, Rui Yang, Mengjie Huang, Nianyin Zeng, and Xiaohui Liu. A review on transfer learning in eeg signal analysis. *Neurocomputing*, 421:1–14, 2021.
- [47] Sinno Jialin Pan and Qiang Yang. A survey on transfer learning. *IEEE Transactions on knowledge and data engineering*, 22(10):1345–1359, 2010.
- [48] Yoshua Bengio. Deep learning of representations for unsupervised and transfer learning. In *Proceedings of ICML workshop on unsupervised and transfer learning*, pages 17–36. JMLR Workshop and Conference Proceedings, 2012.
- [49] Tracy P Jackson, Victoria Sutton Stabile, and KA Kelly McQueen. The global burden of chronic pain. *ASA Monitor*, 78(6):24–27, 2014.
- [50] Suyi Zhang, Hiroaki Mano, Michael Lee, Wako Yoshida, Mitsuo Kawato, Trevor W Robbins, and Ben Seymour. The control of tonic pain by active relief learning. *Elife*, 7, 2018.

- [51] R Jason Yong, Peter M Mullins, and Neil Bhattacharyya. Prevalence of chronic pain among adults in the united states. *Pain*, 163(2):e328–e332, 2022.
- [52] Nalini Vadivelu, Sukanya Mitra, Roberta Hines, Maxwell Elia, and Richard W Rosenquist. Acute pain in undergraduate medical education: an unfinished chapter! *Pain Practice*, 12(8):663–671, 2012.
- [53] Emma V Briggs, Eloise CJ Carr, and Maggie S Whittaker. Survey of undergraduate pain curricula for healthcare professionals in the united kingdom. *European Journal of Pain*, 15(8):789–795, 2011.
- [54] Nalini Sehgal, Laxmaiah Manchikanti, and Howard S Smith. Prescription opioid abuse in chronic pain: a review of opioid abuse predictors and strategies to curb opioid abuse. *Pain physician*, 15(3 Suppl):ES67–ES92, 2012.
- [55] Puja Seth, Rose A Rudd, Rita K Noonan, and Tamara M Haegerich. Quantifying the epidemic of prescription opioid overdose deaths, 2018.
- [56] Beth Han, Wilson M Compton, Carlos Blanco, Elizabeth Crane, Jinhee Lee, and Christopher M Jones. Prescription opioid use, misuse, and use disorders in us adults: 2015 national survey on drug use and health. *Annals of internal medicine*, 167(5):293–301, 2017.
- [57] Douglas J Hsu, Ellen P McCarthy, Jennifer P Stevens, and Kenneth J Mukamal. Hospitalizations, costs and outcomes associated with heroin and prescription

- opioid overdoses in the united states 2001–12. *Addiction*, 112(9):1558–1564, 2017.
- [58] Karen D Davis. Legal and ethical issues of using brain imaging to diagnose pain. *Pain Reports*, 1(4), 2016.
- [59] Dirk De Ridder, Jarek Maciaczyk, and Sven Vanneste. The future of neuromodulation: Smart neuromodulation. *Expert Review of Medical Devices*, 18(4):307–317, 2021.
- [60] Paulina Świeboda, Rafał Filip, Andrzej Prystupa, and Mariola Drozd. Assessment of pain: types, mechanism and treatment. *Pain*, 2(7), 2013.
- [61] Luana Colloca, Taylor Ludman, Didier Bouhassira, Ralf Baron, Anthony H Dickenson, David Yarnitsky, Roy Freeman, Andrea Truini, Nadine Attal, Nanna B Finnerup, et al. Neuropathic pain. *Nature reviews Disease primers*, 3(1):1–19, 2017.
- [62] Mark J Millan. The induction of pain: an integrative review. *Progress in neurobiology*, 57(1):1–164, 1999.
- [63] Steven J Middleton, Allison M Barry, Maddalena Comini, Yan Li, Pradipta R Ray, Stephanie Shiers, Andreas C Themistocleous, Megan L Uhelski, Xun Yang, Patrick M Dougherty, et al. Studying human nociceptors: from fundamentals to clinic. *Brain*, 144(5):1312–1335, 2021.
- [64] BL Kidd and LA Urban. Mechanisms of inflammatory pain. *British journal of anaesthesia*, 87(1):3–11, 2001.

- [65] Daniel Vardeh, Richard J Mannion, and Clifford J Woolf. Toward a mechanism-based approach to pain diagnosis. *The Journal of Pain*, 17(9):T50–T69, 2016.
- [66] R-D Treede, TS Jensen, JN Campbell, G Cruccu, JO Dostrovsky, JW Griffin, PM-DDDDS Hansson, R Hughes, TMDP Nurmikko, and J Serra. Neuropathic pain: redefinition and a grading system for clinical and research purposes. *Neurology*, 70(18):1630–1635, 2008.
- [67] Molly C Basch, Erika T Chow, Deirdre E Logan, Neil L Schechter, and Laura E Simons. Perspectives on the clinical significance of functional pain syndromes in children. *Journal of Pain Research*, 8:675, 2015.
- [68] Naomi I Eisenberger. Social pain and the brain: controversies, questions, and where to go from here. *Annual review of psychology*, 66(1):601–629, 2015.
- [69] John C Liebeskind and Linda A Paul. Psychological and physiological mechanisms of pain. *Annual review of psychology*, 28(1):41–60, 1977.
- [70] Andrea Chadwick, Andrew Frazier, Talal W Khan, and Erin Young. Understanding the psychological, physiological, and genetic factors affecting precision pain medicine: A narrative review. *Journal of Pain Research*, 14:3145, 2021.
- [71] KP Grichnik and FM Ferrante. The difference between acute and chronic pain. *The Mount Sinai journal of medicine, New York*, 58(3):217–220, 1991.
- [72] Daniel B Carr and Leonidas C Goudas. Acute pain. *The Lancet*, 353(9169):2051–2058, 1999.

- [73] Rolf-Detlef Treede, Winfried Rief, Antonia Barke, Qasim Aziz, Michael I Bennett, Rafael Benoliel, Milton Cohen, Stefan Evers, Nanna B Finnerup, Michael B First, et al. A classification of chronic pain for icd-11. *Pain*, 156(6):1003, 2015.
- [74] F Sicuteri, Pierangelo Geppetti, S Marabini, and F Lembeck. Pain relief by somatostatin in attacks of cluster headache. *Pain*, 18(4):359–365, 1984.
- [75] Harold Ed Merskey. Classification of chronic pain: Descriptions of chronic pain syndromes and definitions of pain terms. *Pain*, 1986.
- [76] DB Carr and MJ Cousins. Spinal route of analgesia: opioids and future options. *Neural blockade in clinical anesthesia and management of pain*. Philadelphia: Lippincott-Raven, pages 915–83, 1998.
- [77] HE Torebjörk, LE Lundberg, and RH LaMotte. Central changes in processing of mechanoreceptive input in capsaicin-induced secondary hyperalgesia in humans. *The Journal of physiology*, 448(1):765–780, 1992.
- [78] Bill McCarberg and John Peppin. Pain pathways and nervous system plasticity: learning and memory in pain. *Pain Medicine*, 20(12):2421–2437, 2019.
- [79] Prasad Shirvalkar, Jordan Prosky, Gregory Chin, Parima Ahmadipour, Omid G Sani, Maansi Desai, Ashlyn Schmitgen, Heather Dawes, Maryam M Shanechi, Philip A Starr, et al. First-in-human prediction of chronic pain state using intracranial neural biomarkers. *Nature neuroscience*, pages 1–10, 2023.

- [80] Lorne M. Mendell. Nociceptors. In V.S. Ramachandran, editor, *Encyclopedia of the Human Brain*, pages 613–624. Academic Press, New York, 2002.
- [81] Kieran Rea, Siobhain M O’Mahony, and John F Cryan. High and mighty? cannabinoids and the microbiome in pain. *Neurobiology of Pain*, 9:100061, 2021.
- [82] Adrienne E Dubin, Ardem Patapoutian, et al. Nociceptors: the sensors of the pain pathway. *The Journal of clinical investigation*, 120(11):3760–3772, 2010.
- [83] Laiche Djouhri and Sally N Lawson. $A\beta$ -fiber nociceptive primary afferent neurons: a review of incidence and properties in relation to other afferent a-fiber neurons in mammals. *Brain research reviews*, 46(2):131–145, 2004.
- [84] Breanne L Harty and Kelly R Monk. Unwrapping the unappreciated: recent progress in remak schwann cell biology. *Current Opinion in Neurobiology*, 47:131–137, 2017.
- [85] Florian Beissner, Amadeus Brandau, Christian Henke, Lisa Felden, Ulf Baumgärtner, Rolf-Detlef Treede, Bruno G Oertel, and Jörn Lötsch. Quick discrimination of adelta and c fiber mediated pain based on three verbal descriptors. *PloS one*, 5(9):e12944, 2010.
- [86] Allan I Basbaum. Spinal mechanisms of acute and persistent pain. *Regional anesthesia and pain medicine*, 24(1):59–67, 1999.
- [87] Ronald Melzack. From the gate to the neuromatrix. *Pain*, 82:S121–S126, 1999.

- [88] Sarah Bourne, Andre G Machado, and Sean J Nagel. Basic anatomy and physiology of pain pathways. *Neurosurgery Clinics*, 25(4):629–638, 2014.
- [89] William J Roberts and Mark E Foglesong. I. spinal recordings suggest that wide-dynamic-range neurons mediate sympathetically maintained pain. *Pain*, 34(3):289–304, 1988.
- [90] Donald D Price. Psychological and neural mechanisms of the affective dimension of pain. *Science*, 288(5472):1769–1772, 2000.
- [91] Mark J Millan. Descending control of pain. *Progress in neurobiology*, 66(6):355–474, 2002.
- [92] Michael H Ossipov, Kozo Morimura, and Frank Porreca. Descending pain modulation and chronification of pain. *Current opinion in supportive and palliative care*, 8(2):143, 2014.
- [93] Pierre Rainville. Brain mechanisms of pain affect and pain modulation. *Current opinion in neurobiology*, 12(2):195–204, 2002.
- [94] Roland Peyron, Bernard Laurent, and Luis Garcia-Larrea. Functional imaging of brain responses to pain. a review and meta-analysis (2000). *Neurophysiologie Clinique/Clinical Neurophysiology*, 30(5):263–288, 2000.
- [95] Tetsuo Koyama, Keichiro Kato, and Akichika Mikami. During pain-avoidance neurons activated in the macaque anterior cingulate and caudate. *Neuroscience letters*, 283(1):17–20, 2000.

- [96] Eric A Moulton, Jeremy D Schmahmann, Lino Becerra, and David Borsook. The cerebellum and pain: passive integrator or active participator? *Brain research reviews*, 65(1):14–27, 2010.
- [97] Volker Neugebauer. Amygdala pain mechanisms. *Pain control*, pages 261–284, 2015.
- [98] Haley N Harris and Yuan B Peng. Evidence and explanation for the involvement of the nucleus accumbens in pain processing. *Neural regeneration research*, 15(4):597, 2020.
- [99] David Borsook, Jaymin Upadhyay, Eric H Chudler, and Lino Becerra. A key role of the basal ganglia in pain and analgesia-insights gained through human functional imaging. *Molecular pain*, 6:1744–8069, 2010.
- [100] Ronald Melzack. Phantom limbs and the concept of a neuromatrix. *Trends in neurosciences*, 13(3):88–92, 1990.
- [101] Gian Domenico Iannetti and André Mouraux. From the neuromatrix to the pain matrix (and back). *Experimental brain research*, 205:1–12, 2010.
- [102] Chantal Villemure and M Catherine Bushnell. Cognitive modulation of pain: how do attention and emotion influence pain processing? *Pain*, 95(3):195–199, 2002.
- [103] Tanvi Khera and Valluvan Rangasamy. Cognition and pain: a review. *Frontiers in psychology*, 12:1819, 2021.

- [104] DM Torta, Valéry Legrain, André Mouraux, and Elia Valentini. Attention to pain! a neurocognitive perspective on attentional modulation of pain in neuroimaging studies. *Cortex*, 89:120–134, 2017.
- [105] David J Moore, Edmund Keogh, and Christopher Eccleston. The interruptive effect of pain on attention. *Quarterly journal of experimental psychology*, 65(3):565–586, 2012.
- [106] Monika Hasenbring. Attentional control of pain and the process of chronification. 2000.
- [107] Aleda Erskine, Stephen Morley, and Shirley Pearce. Memory for pain: a review. *Pain*, 41(3):255–265, 1990.
- [108] Stéphanie Mazza, Maud Frot, and Amandine E Rey. A comprehensive literature review of chronic pain and memory. *Progress in Neuro-Psychopharmacology and Biological Psychiatry*, 87:183–192, 2018.
- [109] John J Bonica. History of pain concepts and pain therapy. *The Mount Sinai journal of medicine, New York*, 58(3):191–202, 1991.
- [110] Kenneth M Hargreaves, Emanuel S Troullos, and Raymond A Dionne. Pharmacologic rationale for the treatment of acute pain. *Dental Clinics of North America*, 31(4):675–694, 1987.
- [111] Mai-Phuong Huynh and John A Yagiela. Current concepts in acute pain management. *Journal of the California Dental Association*, 31(5):419–427, 2003.

- [112] Ronald Melzack and Patrick D Wall. Pain mechanisms: A new theory: A gate control system modulates sensory input from the skin before it evokes pain perception and response. *Science*, 150(3699):971–979, 1965.
- [113] Alejandro R Jadad and George P Browman. The who analgesic ladder for cancer pain management: stepping up the quality of its evaluation. *Jama*, 274(23):1870–1873, 1995.
- [114] Jane C Ballantyne and Jianren Mao. Opioid therapy for chronic pain. *New England Journal of Medicine*, 349(20):1943–1953, 2003.
- [115] V Mehta and RM Langford. Acute pain management for opioid dependent patients. *Anaesthesia*, 61(3):269–276, 2006.
- [116] Christopher T Plastaras, Seth Schran, Natasha Kim, Susan Sorosky, Deborah Darr, Mary Susan Chen, and Rebecca Lansky. Complementary and alternative treatment for neck pain: chiropractic, acupuncture, tens, massage, yoga, tai chi, and feldenkrais. *Physical Medicine and Rehabilitation Clinics*, 22(3):521–537, 2011.
- [117] FA Hazime, AF Baptista, DG De Freitas, RL Monteiro, RL Maretto, RH Hasue, and SMA Joao. Treating low back pain with combined cerebral and peripheral electrical stimulation: A randomized, double-blind, factorial clinical trial. *European Journal of Pain*, 21(7):1132–1143, 2017.

- [118] Julian C Motzkin, Ishan Kanungo, Mark DEsposito, and Prasad Shirvalkar. Network targets for therapeutic brain stimulation: towards personalized therapy for pain. *Frontiers in Pain Research*, 4:1156108, 2023.
- [119] Moritz M Nickel, Elisabeth S May, Laura Tiemann, Paul Schmidt, Martina Postorino, Son Ta Dinh, Joachim Gross, and Markus Ploner. Brain oscillations differentially encode noxious stimulus intensity and pain intensity. *Neuroimage*, 148:141–147, 2017.
- [120] Tetsuo Koyama, John G McHaffie, Paul J Laurienti, and Robert C Coghill. The subjective experience of pain: where expectations become reality. *Proceedings of the National Academy of Sciences*, 102(36):12950–12955, 2005.
- [121] Lisa Victor and Steven H Richeimer. Trustworthiness as a clinical variable: The problem of trust in the management of chronic, nonmalignant pain. *Pain Medicine*, 6(5):385–391, 2005.
- [122] CS Cleeland and KM8080219 Ryan. Pain assessment: global use of the brief pain inventory. *Annals of the Academy of Medicine, Singapore*, 23(2):129–138, 1994.
- [123] Mathias Haefeli and Achim Elfering. Pain assessment. *European spine journal*, 15:S17–S24, 2006.
- [124] Owen Doody and Maria E. Bailey. Pain and pain assessment in people with intellectual disability: issues and challenges in practice. *British Journal of Learning Disabilities*, 45(3):157–165, 2017.

- [125] Larry Lindenbaum and David J Milia. Pain management in the icu. *Surgical Clinics*, 92(6):1621–1636, 2012.
- [126] Joseph T Giacino, Kathleen Kalmar, and John Whyte. The jfk coma recovery scale-revised: measurement characteristics and diagnostic utility. *Archives of physical medicine and rehabilitation*, 85(12):2020–2029, 2004.
- [127] Davinia Fernández-Espejo and Adrian M Owen. Detecting awareness after severe brain injury. *Nature Reviews Neuroscience*, 14(11):801–809, 2013.
- [128] Steven Laureys and Nicholas D Schiff. Coma and consciousness: paradigms (re) framed by neuroimaging. *Neuroimage*, 61(2):478–491, 2012.
- [129] Hubert Van Griensven and Jenny Strong. *Pain-E-Book: A textbook for health professionals*. Elsevier Health Sciences, 2022.
- [130] A Hassaan, Anthony Jones, and Manoj Sivan. The brain alpha rhythm in the perception and modulation of pain. *Advances in Clinical Neuroscience and Rehabilitation*, 2020.
- [131] Denise Li, Kathleen Puntillo, and Christine Miaskowski. A review of objective pain measures for use with critical care adult patients unable to self-report. *The journal of pain*, 9(1):2–10, 2008.
- [132] Michael E Robinson, Cynthia D Myers, Ian J Sadler, Joseph L Riley III, Steven A Kvaal, and Michael E Geisser. Bias effects in three common self-report pain assessment measures. *The Clinical journal of pain*, 13(1):74–81, 1997.

- [133] Timothy H Wideman, Robert R Edwards, David M Walton, Marc O Martel, Anne Hudon, and David A Seminowicz. The multimodal assessment model of pain: a novel framework for further integrating the subjective pain experience within research and practice. *The Clinical journal of pain*, 35(3):212, 2019.
- [134] Robert C Aitken. Measurement of feelings using visual analogue scales. *Proceedings of the royal society of medicine*, 62(10):989, 1969.
- [135] GB Langley and H Sheppard. The visual analogue scale: its use in pain measurement. *Rheumatology international*, 5(4):145–148, 1985.
- [136] JANE Scott and EC Huskisson. Accuracy of subjective measurements made with or without previous scores: an important source of error in serial measurement of subjective states. *Annals of the Rheumatic Diseases*, 38(6):558–559, 1979.
- [137] C Aun, YM Lam, and B Collett. Evaluation of the use of visual analogue scale in chinese patients. *Pain*, 25(2):215–221, 1986.
- [138] Craig T Hartrick, Juliann P Kovan, and Sharon Shapiro. The numeric rating scale for clinical pain measurement: a ratio measure? *Pain Practice*, 3(4):310–316, 2003.
- [139] Mark P Jensen and Paul Karoly. Comparative self-evaluation and depressive affect among chronic pain patients: An examination of selective evaluation theory. *Cognitive Therapy and Research*, 16:297–308, 1992.

- [140] Sangeetha Nayak, Samuel C Shiflett, Sussie Eshun, and Fredric M Levine. Culture and gender effects in pain beliefs and the prediction of pain tolerance. *Cross-cultural research*, 34(2):135–151, 2000.
- [141] Chris J Main. Pain assessment in context: a state of the science review of the mcgill pain questionnaire 40 years on. *Pain*, 157(7):1387–1399, 2016.
- [142] Michael K Nicholas. The pain self-efficacy questionnaire: taking pain into account. *European journal of pain*, 11(2):153–163, 2007.
- [143] Sandra Merkel, Terri Voepel-Lewis, and Shobha Malviya. Pain control: pain assessment in infants and young children: the flacc scale. *The American journal of nursing*, 102(10):55–58, 2002.
- [144] Terri Voepel-Lewis, Jay R Shayevitz, and Shobha Malviya. The flacc: a behavioral scale for scoring postoperative pain in young children. *Pediatr Nurs*, 23(3):293–297, 1997.
- [145] Victoria Warden, Ann C Hurley, and Ladislav Volicer. Development and psychometric evaluation of the pain assessment in advanced dementia (painad) scale. *Journal of the American Medical Directors Association*, 4(1):9–15, 2003.
- [146] M Mosele, EM Inelmen, ED Toffanello, A Girardi, A Coin, G Sergi, and E Manzato. Psychometric properties of the pain assessment in advanced dementia scale compared to self assessment of pain in elderly patients. *Dementia and geriatric cognitive disorders*, 34(1):38–43, 2012.

- [147] Sandra MG Zwakhalen, Jan PH Hamers, and Martijn PF Berger. The psychometric quality and clinical usefulness of three pain assessment tools for elderly people with dementia. *Pain*, 126(1-3):210–220, 2006.
- [148] Matthias Siegfried Schuler, Stefanie Becker, Roman Kaspar, Thorsten Nikolaus, Andreas Kruse, and Heinz Dieter Basler. Psychometric properties of the german pain assessment in advanced dementia scale (painad-g) in nursing home residents. *Journal of the American Medical Directors Association*, 8(6):388–395, 2007.
- [149] Margaret Fry and Rosalind Elliott. Pragmatic evaluation of an observational pain assessment scale in the emergency department: The pain assessment in advanced dementia (painad) scale. *Australasian emergency care*, 21(4):131–136, 2018.
- [150] Jeanne Young, Jo Siffleet, Sue Nikoletti, and Th  rese Shaw. Use of a behavioural pain scale to assess pain in ventilated, unconscious and/or sedated patients. *Intensive and Critical Care Nursing*, 22(1):32–39, 2006.
- [151] Jean-Francois Payen, Olivier Bru, Jean-Luc Bosson, Anna Lagrasta, Eric Novel, Isabelle Deschaux, Pierre Lavagne, and Claude Jacquot. Assessing pain in critically ill sedated patients by using a behavioral pain scale. *Critical care medicine*, 29(12):2258–2263, 2001.
- [152] Youn  s A  ssaoui, Amine Ali Zeggwagh, A  cha Zekraoui, Khalid Abidi, and Redouane Abouqal. Validation of a behavioral pain scale in critically ill, sedated,

- and mechanically ventilated patients. *Anesthesia & Analgesia*, 101(5):1470–1476, 2005.
- [153] Hanne Cathrine Birkedal, Marie Hamilton Larsen, Simen A Steindal, and Marianne Trygg Solberg. Comparison of two behavioural pain scales for the assessment of procedural pain: A systematic review. *Nursing Open*, 8(5):2050–2060, 2021.
- [154] Dennis C Turk and Akiko Okifuji. Assessment of patients' reporting of pain: an integrated perspective. *The Lancet*, 353(9166):1784–1788, 1999.
- [155] Brent D Winslow, Rebecca Kwasinski, Kyle Whirlow, Emily Mills, Jeffrey Hullfish, and Meredith Carroll. Automatic detection of pain using machine learning. *Frontiers in Pain Research*, 3:1044518, 2022.
- [156] Roy Bjørkholt Olsen, Stephen Bruehl, Christopher Sivert Nielsen, Leiv Arne Roseland, Anne Elise Eggen, and Audun Stubhaug. Hypertension prevalence and diminished blood pressure-related hypoalgesia in individuals reporting chronic pain in a general population: The tromsø study. *Pain*, 154(2):257–262, 2013.
- [157] Stefan Duschek, W Schwarzkopf, and Rainer Schandry. Increased pain sensitivity in low blood pressure. *Journal of Psychophysiology*, 22(1):20–27, 2008.
- [158] William Maixner, Roger Fillingim, Shelley Kincaid, Asgeir Sigurdsson, and M Brennan Harris. Relationship between pain sensitivity and resting arterial blood pres-

- sure in patients with painful temporomandibular disorders. *Psychosomatic medicine*, 59(5):503–511, 1997.
- [159] Rui Cao, Seyed Amir Hossein Aqajari, Emad Kasaeyan Naeini, and Amir M Rahmani. Objective pain assessment using wrist-based ppg signals: A respiratory rate based method. In *2021 43rd Annual International Conference of the IEEE Engineering in Medicine & Biology Society (EMBC)*, pages 1164–1167. IEEE, 2021.
- [160] D Wildemeersch, N Peeters, V Saldien, M Vercauteren, and G Hans. Pain assessment by pupil dilation reflex in response to noxious stimulation in anaesthetized adults. *Acta Anaesthesiologica Scandinavica*, 62(8):1050–1056, 2018.
- [161] Wolfgang Ellermeier and Wolfgang Westphal. Gender differences in pain ratings and pupil reactions to painful pressure stimuli. *Pain*, 61(3):435–439, 1995.
- [162] C Richard Chapman, Shunichi Oka, David H Bradshaw, Robert C Jacobson, and Gary W Donaldson. Phasic pupil dilation response to noxious stimulation in normal volunteers: relationship to brain evoked potentials and pain report. *Psychophysiology*, 36(1):44–52, 1999.
- [163] Thomas Ledowski, J Bromilow, J Wu, MJ Paech, H Storm, and SA Schug. The assessment of postoperative pain by monitoring skin conductance: results of a prospective study. *Anaesthesia*, 62(10):989–993, 2007.
- [164] Hanne Storm. Changes in skin conductance as a tool to monitor nociceptive stimulation and pain. *Current Opinion in Anesthesiology*, 21(6):796–804, 2008.

- [165] Sibylle I Ziegler. Positron emission tomography: principles, technology, and recent developments. *Nuclear Physics A*, 752:679–687, 2005.
- [166] Mélanie Boly, Marie-Elisabeth Faymonville, Caroline Schnakers, Philippe Peigneux, Bernard Lambermont, Christophe Phillips, Patrizio Lancellotti, Andre Luxen, Maurice Lamy, Gustave Moonen, et al. Perception of pain in the minimally conscious state with pet activation: an observational study. *The Lancet Neurology*, 7(11):1013–1020, 2008.
- [167] Andrew CN Chen. New perspectives in eeg/meg brain mapping and pet/fmri neuroimaging of human pain. *International Journal of Psychophysiology*, 42(2):147–159, 2001.
- [168] Seiji Ogawa, Tso-Ming Lee, Asha S Nayak, and Paul Glynn. Oxygenation-sensitive contrast in magnetic resonance image of rodent brain at high magnetic fields. *Magnetic resonance in medicine*, 14(1):68–78, 1990.
- [169] Edson Amaro Jr and Gareth J Barker. Study design in fmri: basic principles. *Brain and cognition*, 60(3):220–232, 2006.
- [170] Marianne C Reddan and Tor D Wager. Modeling pain using fmri: from regions to biomarkers. *Neuroscience bulletin*, 34:208–215, 2018.
- [171] Tor D Wager, Lauren Y Atlas, Martin A Lindquist, Mathieu Roy, Choong-Wan Woo, and Ethan Kross. An fmri-based neurologic signature of physical pain. *New England Journal of Medicine*, 368(15):1388–1397, 2013.

- [172] Malcolm Proudfoot, Mark W Woolrich, Anna C Nobre, and Martin R Turner. Magnetoencephalography. *Practical neurology*, 14(5):336–343, 2014.
- [173] Markus Ploner and Elisabeth S May. Electroencephalography and magnetoencephalography in pain researchcurrent state and future perspectives. *Pain*, 159(2):206–211, 2018.
- [174] Po-Chih Kuo, Yi-Ti Chen, Yong-Sheng Chen, and Li-Fen Chen. Decoding the perception of endogenous pain from resting-state meg. *Neuroimage*, 144:1–11, 2017.
- [175] Hamid R Mohseni, Penny P Smith, Christine E Parsons, Katherine S Young, Jonathan A Hyam, Alan Stein, John F Stein, Alexander L Green, Tipu Z Aziz, and Morten L Kringelbach. Meg can map short and long-term changes in brain activity following deep brain stimulation for chronic pain. *PLoS One*, 7(6):e37993, 2012.
- [176] Teena Hassan, Dominik Seuß, Johannes Wollenberg, Katharina Weitz, Miriam Kunz, Stefan Lautenbacher, Jens-Uwe Garbas, and Ute Schmid. Automatic detection of pain from facial expressions: a survey. *IEEE transactions on pattern analysis and machine intelligence*, 43(6):1815–1831, 2019.
- [177] Philipp Werner, Daniel Lopez-Martinez, Steffen Walter, Ayoub Al-Hamadi, Sascha Gruss, and Rosalind W Picard. Automatic recognition methods supporting pain assessment: A survey. *IEEE Transactions on Affective Computing*, 13(1):530–552, 2019.

- [178] Samah Jamal Fodeh, Dezon Finch, Lina Bouayad, Stephen L Luther, Han Ling, Robert D Kerns, and Cynthia Brandt. Classifying clinical notes with pain assessment using machine learning. *Medical & biological engineering & computing*, 56:1285–1292, 2018.
- [179] David A Kaiser. Basic principles of quantitative eeg. *Journal of Adult Development*, 12:99–104, 2005.
- [180] Jayant N Acharya and Vinita J Acharya. Overview of eeg montages and principles of localization. *Journal of Clinical Neurophysiology*, 36(5):325–329, 2019.
- [181] Guiomar Niso, Elena Romero, Jeremy T Moreau, Alvaro Araujo, and Laurens R Krol. Wireless eeg: A survey of systems and studies. *NeuroImage*, 269:119774, 2023.
- [182] Munsif Ali Jatoi, Nidal Kamel, Aamir Saeed Malik, Ibrahima Faye, and Tahamina Begum. A survey of methods used for source localization using eeg signals. *Biomedical Signal Processing and Control*, 11:42–52, 2014.
- [183] György Buzsáki, Costas A Anastassiou, and Christof Koch. The origin of extracellular fields and currentseeg, ecog, lfp and spikes. *Nature reviews neuroscience*, 13(6):407–420, 2012.
- [184] William J Ray and Harry W Cole. Eeg alpha activity reflects attentional demands, and beta activity reflects emotional and cognitive processes. *Science*, 228(4700):750–752, 1985.

- [185] Wolfgang Klimesch, Michael Doppelmayr, Harald Russegger, Thomas Pachinger, and Jens Schwaiger. Induced alpha band power changes in the human eeg and attention. *Neuroscience letters*, 244(2):73–76, 1998.
- [186] LA Finelli, H Baumann, AA Borbély, and P Achermann. Dual electroencephalogram markers of human sleep homeostasis: correlation between theta activity in waking and slow-wave activity in sleep. *Neuroscience*, 101(3):523–529, 2000.
- [187] Rony-Reuven Nir, Alon Sinai, Ruth Moont, Eyal Harari, and David Yarnitsky. Tonic pain and continuous eeg: prediction of subjective pain perception by alpha-1 power during stimulation and at rest. *Clinical Neurophysiology*, 123(3):605–612, 2012.
- [188] Robert Dowman, Daniel Rissacher, and Stephanie Schuckers. Eeg indices of tonic pain-related activity in the somatosensory cortices. *Clinical Neurophysiology*, 119(5):1201–1212, 2008.
- [189] Florian Chouchou, Caroline Perchet, and Luis Garcia-Larrea. Eeg changes reflecting pain: is alpha suppression better than gamma enhancement? *Neurophysiologie Clinique*, 51(3):209–218, 2021.
- [190] Elisabeth S May, Markus Butz, Nina Kahlbrock, Meike Brenner, Nienke Hoogenboom, Gerald Kircheis, Dieter Häussinger, and Alfons Schnitzler. Hepatic encephalopathy is associated with slowed and delayed stimulus-associated somatosensory alpha activity. *Clinical neurophysiology*, 125(12):2427–2435, 2014.

- [191] Andrew J Furman, Mariya Prokhorenko, Michael L Keaser, Jing Zhang, Shuo Chen, Ali Mazaheri, and David A Seminowicz. Sensorimotor peak alpha frequency is a reliable biomarker of prolonged pain sensitivity. *Cerebral Cortex*, 30(12):6069–6082, 2020.
- [192] Ali Mazaheri, David A Seminowicz, and Andrew J Furman. Peak alpha frequency as a candidate biomarker of pain sensitivity: the importance of distinguishing slow from slowing. *NeuroImage*, 262:119560, 2022.
- [193] Rony Reuven Nir, Alon Sinai, Einat Raz, Elliot Sprecher, and David Yarnitsky. Pain assessment by continuous eeg: Association between subjective perception of tonic pain and peak frequency of alpha oscillations during stimulation and at rest. *Brain Research*, 1344:77–86, 2010.
- [194] Elia Valentini, Alina Shindy, Viktor Witkovsky, Anne Stankewitz, and Enrico Schulz. Interindividual variability and individual stability of pain-and touch-related neuronal gamma oscillations. *Journal of Neurophysiology*, 2023.
- [195] Phanomporn Veerasarn and Christian S Stohler. The effect of experimental muscle pain on the background electrical brain activity. *Pain*, 49(3):349–360, 1992.
- [196] Suresh D Muthukumaraswamy. High-frequency brain activity and muscle artifacts in meg/eeg: a review and recommendations. *Frontiers in human neuroscience*, 7:138, 2013.

- [197] Stefano Ferracuti, Stefano Seri, Donatella Mattia, and Giorgio Cruccu. Quantitative eeg modifications during the cold water pressor test: hemispheric and hand differences. *International journal of psychophysiology*, 17(3):261–268, 1994.
- [198] MT Huber, J Bartling, D v Pachur, SV Woikowsky-Biedau, and S Lautenbacher. Eeg responses to tonic heat pain. *Experimental brain research*, 173:14–24, 2006.
- [199] Panagiotis Zis, Andreas Liampas, Artemios Artemiadis, Gabriela Tsalamandris, Panagiota Neophytou, Zoe Unwin, Vasilios K Kimiskidis, Georgios M Hadjigeorgiou, Giustino Varrassi, Yifan Zhao, et al. Eeg recordings as biomarkers of pain perception: Where do we stand and where to go? *Pain and Therapy*, 11(2):369–380, 2022.
- [200] Brian W LeBlanc, Theresa R Lii, Andrew E Silverman, Robert T Alleyne, and Carl Y Saab. Cortical theta is increased while thalamocortical coherence is decreased in rat models of acute and chronic pain. *PAIN®*, 155(4):773–782, 2014.
- [201] Barbara S Hulka, Timothy C Wilcosky, and Jack D Griffith. Biological markers in epidemiology. (*No Title*), 1990.
- [202] Tzyy-Ping Jung, Scott Makeig, Magnus Stensmo, and Terrence J Sejnowski. Estimating alertness from the eeg power spectrum. *IEEE transactions on biomedical engineering*, 44(1):60–69, 1997.

- [203] Pradjkij Panavaranan and Yodchanan Wongsawat. Eeg-based pain estimation via fuzzy logic and polynomial kernel support vector machine. In *The 6th 2013 Biomedical Engineering International Conference*, pages 1–4. IEEE, 2013.
- [204] Tianao Cao, Qisong Wang, Dan Liu, Jinwei Sun, and Ou Bai. Resting state eeg-based sudden pain recognition method and experimental study. *Biomedical Signal Processing and Control*, 59:101925, 2020.
- [205] Johannes Sarnthein, Jair Stern, Christoph Aufenberg, Valentin Rousson, and Daniel Jeanmonod. Increased eeg power and slowed dominant frequency in patients with neurogenic pain. *Brain*, 129(1):55–64, 2006.
- [206] Ricardo Ramos-Aguilar, J Arturo Olvera-López, Ivan Olmos-Pineda, and Susana Sánchez-Urrieta. Feature extraction from eeg spectrograms for epileptic seizure detection. *Pattern Recognition Letters*, 133:202–209, 2020.
- [207] Yiheng Tu, Ao Tan, Yanru Bai, Yeung Sam Hung, and Zhiguo Zhang. Decoding subjective intensity of nociceptive pain from pre-stimulus and post-stimulus brain activities. *Frontiers in computational neuroscience*, 10:32, 2016.
- [208] Longhao Yuan and Jianting Cao. Patients eeg data analysis via spectrogram image with a convolution neural network. In *Intelligent Decision Technologies 2017: Proceedings of the 9th KES International Conference on Intelligent Decision Technologies (KES-IDT 2017)–Part I 9*, pages 13–21. Springer, 2018.

- [209] Hui Wen Loh, Chui Ping Ooi, Emrah Aydemir, Turker Tuncer, Sengul Dogan, and U Rajendra Acharya. Decision support system for major depression detection using spectrogram and convolution neural network with eeg signals. *Expert Systems*, 39(3):e12773, 2022.
- [210] Leontios J Hadjileontiadis. Eeg-based tonic cold pain characterization using wavelet higher order spectral features. *IEEE Transactions on Biomedical Engineering*, 62(8):1981–1991, 2015.
- [211] Rami Alazrai, Mohammad Momani, Hussein Abu Khudair, and Mohammad I Daoud. Eeg-based tonic cold pain recognition system using wavelet transform. *Neural Computing and Applications*, 31:3187–3200, 2019.
- [212] Leontios J Hadjileontiadis. Continuous wavelet transform and higher-order spectrum: combinatory potentialities in breath sound analysis and electroencephalogram-based pain characterization. *Philosophical Transactions of the Royal Society A: Mathematical, Physical and Engineering Sciences*, 376(2126):20170249, 2018.
- [213] Ingrid Daubechies. The wavelet transform, time-frequency localization and signal analysis. *IEEE transactions on information theory*, 36(5):961–1005, 1990.
- [214] Vishal Vijayakumar, Michelle Case, Sina Shirinpour, and Bin He. Quantifying and characterizing tonic thermal pain across subjects from eeg data using random

- forest models. *IEEE Transactions on Biomedical Engineering*, 64(12):2988–2996, 2017.
- [215] Jian Kong, Karin Jensen, Rita Loiotile, Alexandra Cheetham, Hsiao-Ying Wey, Ying Tan, Bruce Rosen, Jordan W Smoller, Ted J Kaptchuk, and Randy L Gollub. Functional connectivity of the frontoparietal network predicts cognitive modulation of pain. *PAIN®*, 154(3):459–467, 2013.
- [216] Marwan N Baliki, Bogdan Petre, Souraya Torbey, Kristina M Herrmann, Lejian Huang, Thomas J Schnitzer, Howard L Fields, and A Vania Apkarian. Corticostriatal functional connectivity predicts transition to chronic back pain. *Nature neuroscience*, 15(8):1117–1119, 2012.
- [217] Yohan Attal, Manik Bhattacharjee, Jerome Yelnik, Benoit Cottureau, Julien Lefèvre, Yoshio Okada, Eric Bardinet, Marie Chupin, and Sylvain Baillet. Modeling and detecting deep brain activity with meg & eeg. In *2007 29th Annual International Conference of the IEEE Engineering in Medicine and Biology Society*, pages 4937–4940. IEEE, 2007.
- [218] Marina De Tommaso, Gabriele Trotta, Eleonora Vecchio, Katia Ricci, Frederik Van de Steen, Anna Montemurno, Marta Lorenzo, Daniele Marinazzo, Roberto Bellotti, and Sebastiano Stramaglia. Functional connectivity of eeg signals under laser stimulation in migraine. *Frontiers in human neuroscience*, 9:640, 2015.

- [219] Leah Shafran Topaz, Alex Frid, Yelena Granovsky, Rabab Zubidat, Shoshana Crystal, Chen Buxbaum, Noam Bosak, Rafi Hadad, Erel Domany, Tayir Alon, et al. Electroencephalography functional connectivitya biomarker for painful polyneuropathy. *European Journal of Neurology*, 30(1):204–214, 2023.
- [220] Foroogh Shamsi, Ali Haddad, et al. Recognizing pain in motor imagery eeg recordings using dynamic functional connectivity graphs. In *2020 42nd Annual International Conference of the IEEE Engineering in Medicine & Biology Society (EMBC)*, pages 2869–2872. IEEE, 2020.
- [221] Ryan T Canolty and Robert T Knight. The functional role of cross-frequency coupling. *Trends in cognitive sciences*, 14(11):506–515, 2010.
- [222] Sven Vanneste and Dirk De Ridder. Chronic pain as a brain imbalance between pain input and pain suppression. *Brain Communications*, 3(1):fcab014, 2021.
- [223] Daniel Jacobs, Trevor Hilton, Martin Del Campo, Peter L Carlen, and Berj L Bardakjian. Classification of pre-clinical seizure states using scalp eeg cross-frequency coupling features. *IEEE Transactions on Biomedical Engineering*, 65(11):2440–2449, 2018.
- [224] Wenjing Wang. Brain network features based on theta-gamma cross-frequency coupling connections in eeg for emotion recognition. *Neuroscience Letters*, 761:136106, 2021.

- [225] Teresa H Sanders, Mark McCurry, and Mark A Clements. Sleep stage classification with cross frequency coupling. In *2014 36th Annual International Conference of the IEEE Engineering in Medicine and Biology Society*, pages 4579–4582. IEEE, 2014.
- [226] Stavros I Dimitriadis, Christos Salis, and David Linden. A novel, fast and efficient single-sensor automatic sleep-stage classification based on complementary cross-frequency coupling estimates. *Clinical Neurophysiology*, 129(4):815–828, 2018.
- [227] Robert W Thatcher, Duane North, and C Biver. Eeg and intelligence: relations between eeg coherence, eeg phase delay and power. *Clinical neurophysiology*, 116(9):2129–2141, 2005.
- [228] Sheida Malekpour, John A Gubner, and William A Sethares. Measures of generalized magnitude-squared coherence: Differences and similarities. *Journal of the Franklin Institute*, 355(5):2932–2950, 2018.
- [229] David Joffe. Connectivity assessment and training: a partial directed coherence approach. *Journal of Neurotherapy*, 12(2-3):111–122, 2008.
- [230] Luiz A Baccalá and Koichi Sameshima. Partial directed coherence: a new concept in neural structure determination. *Biological cybernetics*, 84(6):463–474, 2001.
- [231] Richard Taylor. Interpretation of the correlation coefficient: a basic review. *Journal of diagnostic medical sonography*, 6(1):35–39, 1990.

- [232] Jean-Philippe Lachaux, Eugenio Rodriguez, Jacques Martinerie, and Francisco J Varela. Measuring phase synchrony in brain signals. *Human brain mapping*, 8(4):194–208, 1999.
- [233] Cornelis J Stam, Guido Nolte, and Andreas Daffertshofer. Phase lag index: assessment of functional connectivity from multi channel eeg and meg with diminished bias from common sources. *Human brain mapping*, 28(11):1178–1193, 2007.
- [234] Mohammad-Parsa Hosseini, Amin Hosseini, and Kiarash Ahi. A review on machine learning for eeg signal processing in bioengineering. *IEEE reviews in biomedical engineering*, 14:204–218, 2020.
- [235] Danilo Bzdok and Andreas Meyer-Lindenberg. Machine learning for precision psychiatry: opportunities and challenges. *Biological Psychiatry: Cognitive Neuroscience and Neuroimaging*, 3(3):223–230, 2018.
- [236] Corinna Cortes and Vladimir Vapnik. Support-vector networks. *Machine learning*, 20:273–297, 1995.
- [237] Vladimir Vapnik. The support vector method of function estimation. In *Nonlinear modeling: Advanced black-box techniques*, pages 55–85. Springer, 1998.
- [238] William S Noble. What is a support vector machine? *Nature biotechnology*, 24(12):1565–1567, 2006.

- [239] Maryam Vatankhah, Vahid Asadpour, and Reza Fazel-Rezai. Perceptual pain classification using anfis adapted rbf kernel support vector machine for therapeutic usage. *Applied Soft Computing*, 13(5):2537–2546, 2013.
- [240] Atsushi Kimura, Yasue Mitsukura, Akihito Oya, Morio Matsumoto, Masaya Nakamura, Arihiko Kanaji, and Takeshi Miyamoto. Objective characterization of hip pain levels during walking by combining quantitative electroencephalography with machine learning. *Scientific reports*, 11(1):3192, 2021.
- [241] Laith Alzubaidi, Jinglan Zhang, Amjad J Humaidi, Ayad Al-Dujaili, Ye Duan, Omran Al-Shamma, José Santamaría, Mohammed A Fadhel, Muthana Al-Amidie, and Laith Farhan. Review of deep learning: Concepts, cnn architectures, challenges, applications, future directions. *Journal of big Data*, 8:1–74, 2021.
- [242] Fengjie Wu, Weijian Mai, Yisheng Tang, Qingkun Liu, Jiangtao Chen, and Ziqian Guo. Learning spatial-spectral-temporal eeg representations with deep attentive-recurrent-convolutional neural networks for pain intensity assessment. *Neuroscience*, 481:144–155, 2022.
- [243] Sinno Jialin Pan, Ivor W Tsang, James T Kwok, and Qiang Yang. Domain adaptation via transfer component analysis. *IEEE transactions on neural networks*, 22(2):199–210, 2010.
- [244] Vinay Jayaram, Morteza Alamgir, Yasemin Altun, Bernhard Scholkopf, and Moritz Grosse-Wentrup. Transfer learning in brain-computer interfaces. *IEEE Computa-*

- tional Intelligence Magazine*, 11(1):20–31, 2016.
- [245] Zirui Lan, Olga Sourina, Lipo Wang, Reinhold Scherer, and Gernot R Müller-Putz. Domain adaptation techniques for eeg-based emotion recognition: A comparative study on two public datasets. *IEEE Transactions on Cognitive and Developmental Systems*, 11(1):85–94, 2018.
- [246] Jesús S García-Salinas, Luis Villaseñor-Pineda, Carlos A Reyes-García, and Alejandro A Torres-García. Transfer learning in imagined speech eeg-based bcis. *Biomedical Signal Processing and Control*, 50:151–157, 2019.
- [247] Jinpeng Li, Shuang Qiu, Yuan-Yuan Shen, Cheng-Lin Liu, and Huiguang He. Multi-source transfer learning for cross-subject eeg emotion recognition. *IEEE transactions on cybernetics*, 50(7):3281–3293, 2019.
- [248] Yonghao Song, Lie Yang, Xueyu Jia, and Longhan Xie. Common spatial generative adversarial networks based eeg data augmentation for cross-subject brain-computer interface. *arXiv preprint arXiv:2102.04456*, 2021.
- [249] Hong Zeng and Wael Zakaria. A new common spatial pattern-based unified channels algorithm for drivers fatigue eeg signals classification. *Neural Computing and Applications*, 35(2):1423–1445, 2023.
- [250] Wenlong Hang, Wei Feng, Ruoyu Du, Shuang Liang, Yan Chen, Qiong Wang, and Xuejun Liu. Cross-subject eeg signal recognition using deep domain adaptation network. *IEEE Access*, 7:128273–128282, 2019.

- [251] Michal Granot, Irit Weissman-Fogel, Yonathan Crispel, Dorit Pud, Yelena Granovsky, Elliot Sprecher, and David Yarnitsky. Determinants of endogenous analgesia magnitude in a diffuse noxious inhibitory control (dnic) paradigm: do conditioning stimulus painfulness, gender and personality variables matter? *Pain*, 136(1-2):142–149, 2008.
- [252] Scott Makeig, Anthony J Bell, Tzyy-Ping Jung, and Terrence J Sejnowski. Independent component analysis of electroencephalographic data. In *Advances in neural information processing systems*, pages 145–151, 1996.
- [253] Sebastianus Petrus van den Broek, F Reinders, M Donderwinkel, and MJ Peters. Volume conduction effects in eeg and meg. *Electroencephalography and clinical neurophysiology*, 106(6):522–534, 1998.
- [254] Henry K Beecher. Generalization from pain of various types and diverse origins. *Science*, 130(3370):267–268, 1959.
- [255] Bill Noble, David Clark, Marcia Meldrum, Henk Ten Have, Jane Seymour, Michelle Winslow, and Silvia Paz. The measurement of pain, 1945–2000. *Journal of pain and symptom management*, 29(1):14–21, 2005.
- [256] Camille Chatelle, Aurore Thibaut, John Whyte, Marie Danièle De Val, Steven Laureys, and Caroline Schnakers. Pain issues in disorders of consciousness. *Brain Injury*, 28(9):1202–1208, 2014.

- [257] Stephen Bruehl, Charles R Carlson, and James A McCubbin. The relationship between pain sensitivity and blood pressure in normotensives. *Pain*, 48(3):463–467, 1992.
- [258] Bradley M Appelhans and Linda J Luecken. Heart rate variability and pain: associations of two interrelated homeostatic processes. *Biological psychology*, 77(2):174–182, 2008.
- [259] Hassan Jafari, Ali Gholamrezaei, Mathijs Franssen, Lukas Van Oudenhove, Qasim Aziz, Omer Van den Bergh, Johan WS Vlaeyen, and Ilse Van Diest. Can slow deep breathing reduce pain? an experimental study exploring mechanisms. *The Journal of Pain*, 21(9-10):1018–1030, 2020.
- [260] Fan Yang, Tanvi Banerjee, Kalindi Narine, and Nirmish Shah. Improving pain management in patients with sickle cell disease from physiological measures using machine learning techniques. *Smart Health*, 7:48–59, 2018.
- [261] Olivia K Harrison, Anja Hayen, Tor D Wager, and Kyle TS Pattinson. Investigating the specificity of the neurologic pain signature against breathlessness and finger opposition. *Pain*, 162(12):2933–2944, 2021.
- [262] Predrag Petrovic, Karl Magnus Petersson, PH Ghatan, S Stone-Elander, and Martin Ingvar. Pain-related cerebral activation is altered by a distracting cognitive task. *Pain*, 85(1-2):19–30, 2000.

- [263] Joshua Levitt and Carl Y. Saab. What does a pain biomarker' mean and can a machine be taught to measure pain? *Neuroscience Letters*, 702(November 2018):40–43, 2019.
- [264] Maite van der Miesen, Martin Lindquist, and Tor Wager. Neuroimaging-based biomarkers for pain: state of the field and current directions. *PAIN Reports*, 4(4):e751, 2019.
- [265] H Merskey and N Bogduk. Iasp pain terminology. *Classification of Chronic Pain*, pages 209–214, 1994.
- [266] A Vania Apkarian, Javeria A Hashmi, and Marwan N Baliki. Pain and the brain: specificity and plasticity of the brain in clinical chronic pain. *Pain*, 152(3 Suppl):S49, 2011.
- [267] Marina de Tommaso, Gabriele Trotta, Eleonora Vecchio, Katia Ricci, Frederik Van de Steen, Anna Montemurno, Marta Lorenzo, Daniele Marinazzo, Roberto Bellotti, and Sebastiano Stramaglia. Functional connectivity of EEG signals under laser stimulation in migraine. *Frontiers in Human Neuroscience*, 9(NOV):1–10, 2015.
- [268] Andrew J. Furman, Timothy J. Meeker, Jeremy C. Rietschel, Sooyoung Yoo, Janusiya Muthulingam, Mariya Prokhorenko, Michael L. Keaser, Ronald N. Goodman, Ali Mazaheri, and David A. Seminowicz. Cerebral peak alpha frequency

- predicts individual differences in pain sensitivity. *NeuroImage*, 167(November 2017):203–210, 2018.
- [269] Moritz M. Nickel, Elisabeth S. May, Laura Tiemann, Paul Schmidt, Martina Postorino, Son Ta Dinh, Joachim Gross, and Markus Ploner. Brain oscillations differentially encode noxious stimulus intensity and pain intensity. *NeuroImage*, 148(January):141–147, 2017.
- [270] Joachim Gross, Alfons Schnitzler, Lars Timmermann, and Markus Ploner. Gamma oscillations in human primary somatosensory cortex reflect pain perception. *PLoS biology*, 5(5):e133, 2007.
- [271] Sarah Katie Zeller Ihnen, Jessica A Church, Steven E Petersen, and Bradley L Schlaggar. Lack of generalizability of sex differences in the fmri bold activity associated with language processing in adults. *Neuroimage*, 45(3):1020–1032, 2009.
- [272] Z. G. Zhang, L. Hu, Y. S. Hung, A. Mouraux, and G. D. Iannetti. Gamma-band oscillations in the primary somatosensory cortex-A direct and obligatory correlate of subjective pain intensity. *Journal of Neuroscience*, 32(22):7429–7438, 2012.
- [273] Enrico Schulz, Elisabeth S May, Martina Postorino, Laura Tiemann, Moritz M Nickel, Viktor Witkovsky, Paul Schmidt, Joachim Gross, and Markus Ploner. Prefrontal gamma oscillations encode tonic pain in humans. *Cerebral cortex*, 25(11):4407–4414, 2015.

- [274] Cornelis J Stam, BF Jones, Ilonka Manshanden, AM van Cappellen Van Walsum, T Montez, Jeroen PA Verbunt, Jan C de Munck, Bob W van Dijk, Henk W Berendse, and Philip Scheltens. Magnetoencephalographic evaluation of resting-state functional connectivity in alzheimer's disease. *Neuroimage*, 32(3):1335–1344, 2006.
- [275] C. C. Liu, J. H. Chien, J. H. Kim, Y. F. Chuang, D. T. Cheng, W. S. Anderson, and F. A. Lenz. Cross-frequency coupling in deep brain structures upon processing the painful sensory inputs. *Neuroscience*, 303:412–421, 2015.
- [276] Mingxin Yu, Hao Yan, Jing Han, Yingzi Lin, Lianqing Zhu, and Xiaoying Tang. EEG-based tonic cold pain assessment using extreme learning machine. *Intelligent Data Analysis*, 24:163–182, 2020.
- [277] Li Wang, Yan Xiao, Richard D Urman, and Yingzi Lin. Cold pressor pain assessment based on eeg power spectrum. *SN Applied Sciences*, 2(12):1–8, 2020.
- [278] Fu-Jung Hsiao, Wei-Ta Chen, Li-Ling Hope Pan, Hung-Yu Liu, Yen-Feng Wang, Shih-Pin Chen, Kuan-Lin Lai, and Shuu-Jiun Wang. Machine learning–based prediction of heat pain sensitivity by using resting-state eeg. *Frontiers in Bioscience-Landmark*, 26(12):1537–1547, 2021.
- [279] Cornelis J. Stam, Guido Nolte, and Andreas Daffertshofer. Phase lag index: Assessment of functional connectivity from multi channel EEG and MEG with diminished bias from common sources. *Human Brain Mapping*, 28(11):1178–1193, 2007.

- [280] Moritz M. Nickel, Son Ta Dinh, Elisabeth S. May, Laura Tiemann, Vanessa D. Hohn, Joachim Gross, and Markus Ploner. Neural oscillations and connectivity characterizing the state of tonic experimental pain in humans. *Human Brain Mapping*, (August):1–13, 2019.
- [281] Dietrich Lehmann, Pascal L Faber, Lorena RR Gianotti, Kieko Kochi, and Roberto D Pascual-Marqui. Coherence and phase locking in the scalp eeg and between loreta model sources, and microstates as putative mechanisms of brain temporo-spatial functional organization. *Journal of Physiology-Paris*, 99(1):29–36, 2006.
- [282] Jean-Philippe Lachaux, Eugenio Rodriguez, Michel Le Van Quyen, Antoine Lutz, Jacques Martinerie, and Francisco J Varela. Studying single-trials of phase synchronous activity in the brain. *International Journal of Bifurcation and Chaos*, 10(10):2429–2439, 2000.
- [283] Andrew CN Chen, Samuel F Dworkin, Joanna Haug, and John Gehrig. Human pain responsivity in a tonic pain model: psychological determinants. *Pain*, 37(2):143–160, 1989.
- [284] Gary L Kreps and Linda Neuhauser. Artificial intelligence and immediacy: designing health communication to personally engage consumers and providers. *Patient education and counseling*, 92(2):205–210, 2013.
- [285] Ulla Mitzdorf. Current source-density method and application in cat cerebral cortex: investigation of evoked potentials and eeg phenomena. *Physiological reviews*,

- 65(1):37–100, 1985.
- [286] Jürgen Kayser and Craig E Tenke. On the benefits of using surface laplacian (current source density) methodology in electrophysiology. *International journal of psychophysiology: official journal of the International Organization of Psychophysiology*, 97(3):171, 2015.
- [287] Andjela Markovic, Peter Achermann, Thomas Rusterholz, and Leila Tarokh. Heritability of sleep eeg topography in adolescence: results from a longitudinal twin study. *Scientific reports*, 8(1):1–13, 2018.
- [288] Wei Yang, Kuanquan Wang, and Wangmeng Zuo. Neighborhood component feature selection for high-dimensional data. *Journal of Computers*, 7(1):162–168, 2012.
- [289] J. A.K. Suykens and J. Vandewalle. Least squares support vector machine classifiers. *Neural Processing Letters*, 9(3):293–300, 1999.
- [290] Rony Reuven Nir, Alon Sinai, Ruth Moont, Eyal Harari, and David Yarnitsky. Tonic pain and continuous EEG: Prediction of subjective pain perception by alpha-1 power during stimulation and at rest. *Clinical Neurophysiology*, 123(3):605–612, 2012.
- [291] Wolfgang Klimesch. Eeg alpha and theta oscillations reflect cognitive and memory performance: a review and analysis. *Brain Research Reviews*, 29(2):169–195, 1999.

- [292] Michael Breakspear. Nonlinear phase desynchronization in human electroencephalographic data. *Human brain mapping*, 15(3):175–198, 2002.
- [293] Matteo Frascini, Matteo Demuru, Alessandra Crobe, Francesco Marrosu, Cornelis J Stam, and Arjan Hillebrand. The effect of epoch length on estimated eeg functional connectivity and brain network organisation. *Journal of neural engineering*, 13(3):036015, 2016.
- [294] Somayeh Afrasiabi, Reza Boostani, Mohammad Ali Masnadi-Shirazi, and Tahereh Nezam. An eeg based hierarchical classification strategy to differentiate five intensities of pain. *Expert Systems with Applications*, 180:115010, 2021.
- [295] P Modares-Haghighi, Reza Boostani, Mohammad Nami, and Saeid Sanei. Quantification of pain severity using eeg-based functional connectivity. *Biomedical Signal Processing and Control*, 69:102840, 2021.
- [296] Son Ta Dinh, Moritz M Nickel, Laura Tiemann, Elisabeth S May, Henrik Heitmann, Vanessa D Hohn, Günther Edenharter, Daniel Utpadel-Fischler, Thomas R Tölle, Paul Sauseng, et al. Brain dysfunction in chronic pain patients assessed by resting-state electroencephalography. *Pain*, 160(12):2751, 2019.
- [297] Louis Mayaud, H el ene Wu, Quentin Barth el emy, Patrick Favennec, Yannick Delpierre, Marco Congedo, Arnaud Dupeyron, and Michel Ritz. Alpha-phase synchrony eeg training for multi-resistant chronic low back pain patients: an open-label pilot study. *European Spine Journal*, 28(11):2487–2501, 2019.

- [298] Danny Camfferman, G Lorimer Moseley, Kevin Gertz, Mark W Pettet, and Mark P Jensen. Waking eeg cortical markers of chronic pain and sleepiness. *Pain Medicine*, 18(10):1921–1931, 2017.
- [299] Christoph Baumgartner, Andreas Doppelbauer, William W Sutherling, Gerald Lindinger, Michel F Levesque, Susanne Aull, Josef Zeitlhofer, and Lüder Deecke. Somatotopy of human hand somatosensory cortex as studied in scalp eeg. *Electroencephalography and Clinical Neurophysiology/Evoked Potentials Section*, 88(4):271–279, 1993.
- [300] Valentin Riedl, Michael Valet, Andreas Wöller, Christian Sorg, Dominik Vogel, Till Sprenger, Henning Boecker, Afra M Wohlschläger, and Thomas R Tölle. Repeated pain induces adaptations of intrinsic brain activity to reflect past and predict future pain. *Neuroimage*, 57(1):206–213, 2011.
- [301] Yiheng Tu, Binlong Zhang, Jin Cao, Georgia Wilson, Zhiguo Zhang, and Jian Kong. Identifying inter-individual differences in pain threshold using brain connectome: a test-retest reproducible study. *Neuroimage*, 202:116049, 2019.
- [302] Tamas Spisak, Balint Kincses, Frederik Schlitt, Matthias Zunhammer, Tobias Schmidt-Wilcke, Zsigmond T Kincses, and Ulrike Bingel. Pain-free resting-state functional brain connectivity predicts individual pain sensitivity. *Nature communications*, 11(1):1–12, 2020.

- [303] Yiyuan Han, Elia Valentini, and Sebastian Halder. Classification of tonic pain experience based on phase connectivity in the alpha frequency band of the electroencephalogram using convolutional neural networks. In *2022 44th Annual International Conference of the IEEE Engineering in Medicine & Biology Society (EMBC)*, pages 3542–3545. IEEE, 2022.
- [304] Enrico Schulz, Andrew Zherdin, Laura Tiemann, Claudia Plant, and Markus Ploner. Decoding an individual’s sensitivity to pain from the multivariate analysis of EEG data. *Cerebral Cortex*, 22(5):1118–1123, 2012.
- [305] Yiyuan Han, Elia Valentini, and Sebastian Halder. Validation of cross-individual pain assessment with individual recognition model from electroencephalogram. In *2023 45th Annual International Conference of the IEEE Engineering in Medicine & Biology Society (EMBC)*. IEEE, 2023.
- [306] T. Nezam, R. Boostani, V. Abootalebi, and K. Rastegar. A novel classification strategy to distinguish five levels of pain using the eeg signal features. *IEEE Transactions on Affective Computing*, 12(1):131–140, 2021.
- [307] Karl Weiss, Taghi M Khoshgoftaar, and DingDing Wang. A survey of transfer learning. *Journal of Big data*, 3(1):1–40, 2016.
- [308] Wei-Long Zheng and Bao-Liang Lu. Personalizing eeg-based affective models with transfer learning. In *Proceedings of the twenty-fifth international joint conference on artificial intelligence*, pages 2732–2738, 2016.

- [309] Niklas Smedemark-Margulies, Ye Wang, Toshiaki Koike-Akino, and Deniz Erdogmus. Autotransfer: Subject transfer learning with censored representations on biosignals data. In *2022 44th Annual International Conference of the IEEE Engineering in Medicine & Biology Society (EMBC)*, pages 3159–3165. IEEE, 2022.
- [310] David Bethge, Philipp Hallgarten, Ozan Özdenizci, Ralf Mikut, Albrecht Schmidt, and Tobias Grosse-Puppenthal. Exploiting multiple eeg data domains with adversarial learning. *arXiv preprint arXiv:2204.07777*, 2022.
- [311] Saad Albawi, Tareq Abed Mohammed, and Saad Al-Zawi. Understanding of a convolutional neural network. In *2017 international conference on engineering and technology (ICET)*, pages 1–6. Ieee, 2017.
- [312] Theekshana Dissanayake, Tharindu Fernando, Simon Denman, Sridha Sridharan, Houman Ghaemmaghami, and Clinton Fookes. A robust interpretable deep learning classifier for heart anomaly detection without segmentation. *IEEE Journal of Biomedical and Health Informatics*, 25(6):2162–2171, 2020.
- [313] Jeroen Van Der Donckt, Jonas Van Der Donckt, Emiel Deprost, Nicolas Vandembussche, Michael Rademaker, Gilles Vandewiele, and Sofie Van Hoecke. Do not sleep on traditional machine learning: Simple and interpretable techniques are competitive to deep learning for sleep scoring. *Biomedical Signal Processing and Control*, 81:104429, 2023.

- [314] Guang Yang, Arvind Rao, Christine Fernandez-Maloigne, Vince Calhoun, and Gloria Menegaz. Explainable ai (xai) in biomedical signal and image processing: Promises and challenges. In *2022 IEEE International Conference on Image Processing (ICIP)*, pages 1531–1535. IEEE, 2022.
- [315] Ramprasaath R Selvaraju, Michael Cogswell, Abhishek Das, Ramakrishna Vedantam, Devi Parikh, and Dhruv Batra. Grad-cam: Visual explanations from deep networks via gradient-based localization. In *Proceedings of the IEEE international conference on computer vision*, pages 618–626, 2017.
- [316] Thuan TT Dao and Linda LeResche. Gender differences in pain. *Journal of orofacial pain*, 14(3), 2000.
- [317] Stephen J Gibson and Michael Farrell. A review of age differences in the neurophysiology of nociception and the perceptual experience of pain. *The Clinical journal of pain*, 20(4):227–239, 2004.
- [318] Aristidis Likas, Nikos Vlassis, and Jakob J Verbeek. The global k-means clustering algorithm. *Pattern recognition*, 36(2):451–461, 2003.
- [319] Jasmine Irani, Nitin Pise, and Madhura Phatak. Clustering techniques and the similarity measures used in clustering: A survey. *International journal of computer applications*, 134(7):9–14, 2016.

- [320] Zhongqi Lu, Erheng Zhong, Lili Zhao, Evan Wei Xiang, Weike Pan, and Qiang Yang. Selective transfer learning for cross domain recommendation. In *Proceedings of the 2013 SIAM International Conference on Data Mining*, pages 641–649. SIAM, 2013.
- [321] Chun-Shu Wei, Yuan-Pin Lin, Yu-Te Wang, Tzyy-Ping Jung, Nima Bigdely-Shamlo, and Chin-Teng Lin. Selective transfer learning for eeg-based drowsiness detection. In *2015 IEEE International Conference on Systems, Man, and Cybernetics*, pages 3229–3232. IEEE, 2015.
- [322] AR Ajiboye, Ruzaini Abdullah-Arshah, and Q Hongwu. Evaluating the effect of dataset size on predictive model using supervised learning technique. 2015.
- [323] Kay Gregor Hartmann, Robin Tibor Schirrmeyer, and Tonio Ball. Eeg-gan: Generative adversarial networks for electroencephalographic (eeg) brain signals. *arXiv preprint arXiv:1806.01875*, 2018.
- [324] Yaroslav Ganin, Evgeniya Ustinova, Hana Ajakan, Pascal Germain, Hugo Larochelle, François Laviolette, Mario Marchand, and Victor Lempitsky. Domain-adversarial training of neural networks. *The journal of machine learning research*, 17(1):2096–2030, 2016.
- [325] Barbara Plank and Gertjan Van Noord. Effective measures of domain similarity for parsing. In *Proceedings of the 49th Annual Meeting of the Association for Computational Linguistics: Human Language Technologies*, pages 1566–1576, 2011.

- [326] Yanru Bai, Gan Huang, Yiheng Tu, Ao Tan, Yeung Sam Hung, and Zhiguo Zhang. Normalization of pain-evoked neural responses using spontaneous eeg improves the performance of eeg-based cross-individual pain prediction. *Frontiers in computational neuroscience*, 10:31, 2016.
- [327] Francesca Fardo, Ryszard Auksztulewicz, Micah Allen, Martin J Dietz, Andreas Roepstorff, and Karl J Friston. Expectation violation and attention to pain jointly modulate neural gain in somatosensory cortex. *Neuroimage*, 153:109–121, 2017.
- [328] Jieun Kim, Ishtiaq Mawla, Jian Kong, Jeungchan Lee, Jessica Gerber, Ana Ortiz, Hyungjun Kim, Suk-Tak Chan, Marco L Loggia, Ajay D Wasan, et al. Somatotopically-specific primary somatosensory connectivity to salience and default mode networks encodes clinical pain. *Pain*, 160(7):1594, 2019.
- [329] Björn Horing, Christian Sprenger, and Christian Büchel. The parietal operculum preferentially encodes heat pain and not salience. *PLoS biology*, 17(8):e3000205, 2019.
- [330] MC Bushnell, GH Duncan, RK Hofbauer, B Ha, J-I Chen, and B Carrier. Pain perception: is there a role for primary somatosensory cortex? *Proceedings of the National Academy of Sciences*, 96(14):7705–7709, 1999.
- [331] Li-Ling Hope Pan, Wei-Ta Chen, Yen-Feng Wang, Shih-Pin Chen, Kuan-Lin Lai, Hung-Yu Liu, Fu-Jung Hsiao, and Shuu-Jiun Wang. Resting-state occipital alpha

- power is associated with treatment outcome in patients with chronic migraine. *Pain*, 163(7):1324–1334, 2022.
- [332] He He and Dongrui Wu. Transfer learning for brain–computer interfaces: A euclidean space data alignment approach. *IEEE Transactions on Biomedical Engineering*, 67(2):399–410, 2019.
- [333] Gintare Karolina Dziugaite, Daniel M Roy, and Zoubin Ghahramani. Training generative neural networks via maximum mean discrepancy optimization. *arXiv preprint arXiv:1505.03906*, 2015.
- [334] David Hübner, Thibault Verhoeven, Klaus-Robert Müller, Pieter-Jan Kindermans, and Michael Tangermann. Unsupervised learning for brain-computer interfaces based on event-related potentials: Review and online comparison [research frontier]. *IEEE Computational Intelligence Magazine*, 13(2):66–77, 2018.
- [335] Sumanto Dutta and Anup Nandy. Data augmentation for ambulatory eeg based cognitive state taxonomy system with rnn-lstm. In *International Conference on Innovative Techniques and Applications of Artificial Intelligence*, pages 468–473. Springer, 2019.
- [336] Zhiqiang Shen, Zechun Liu, Jie Qin, Marios Savvides, and Kwang-Ting Cheng. Partial is better than all: revisiting fine-tuning strategy for few-shot learning. In *Proceedings of the AAAI Conference on Artificial Intelligence*, volume 35, pages 9594–9602, 2021.

- [337] Wei Bian, Dacheng Tao, and Yong Rui. Cross-domain human action recognition. *IEEE Transactions on Systems, Man, and Cybernetics, Part B (Cybernetics)*, 42(2):298–307, 2011.
- [338] Andrea Soddu, Audrey Vanhauzenhuyse, Athena Demertzi, Marie-Aurélié Bruno, Luaba Tshibanda, Haibo Di, Mélanie Boly, Michele Papa, Steven Laureys, and Quentin Noirhomme. Resting state activity in patients with disorders of consciousness. *Functional neurology*, 26(1):37, 2011.
- [339] Elia Valentini, Meng Liang, Salvatore Maria Aglioti, and Gian Domenico Iannetti. Seeing touch and pain in a stranger modulates the cortical responses elicited by somatosensory but not auditory stimulation. *Human brain mapping*, 33(12):2873–2884, 2012.
- [340] Antonia Creswell, Tom White, Vincent Dumoulin, Kai Arulkumaran, Biswa Sengupta, and Anil A Bharath. Generative adversarial networks: An overview. *IEEE signal processing magazine*, 35(1):53–65, 2018.
- [341] Solomon Kullback and Richard A Leibler. On information and sufficiency. *The annals of mathematical statistics*, 22(1):79–86, 1951.
- [342] Thorsten Pohlert. Pmcnr: Calculate pairwise multiple comparisons of mean rank sums (version 4.0), 12 2015.

- [343] Dominik Scherer, Andreas Müller, and Sven Behnke. Evaluation of pooling operations in convolutional architectures for object recognition. In *International conference on artificial neural networks*, pages 92–101. Springer, 2010.
- [344] ME Hoeppli, H Nahman-Averbuch, WA Hinkle, E Leon, J Peugh, M Lopez-Sola, CD King, KR Goldschneider, and RC Coghill. Dissociation between individual differences in self-reported pain intensity and underlying fmri brain activation. *Nature communications*, 13(1):3569, 2022.
- [345] Qianqian Lin, Linling Li, Jia Liu, Weixiang Liu, Gan Huang, and Zhiguo Zhang. Influence of individual differences in fmri-based pain prediction models on between-individual prediction performance. *Frontiers in neuroscience*, 12:569, 2018.
- [346] Kevin N Ochsner, David H Ludlow, Kyle Knierim, Josh Hanelin, Tara Ramachandran, Gary C Glover, and Sean C Mackey. Neural correlates of individual differences in pain-related fear and anxiety. *Pain*, 120(1-2):69–77, 2006.
- [347] Tim V Salomons, Tom Johnstone, Misha-Miroslav Backonja, Alexander J Shackman, and Richard J Davidson. Individual differences in the effects of perceived controllability on pain perception: critical role of the prefrontal cortex. *Journal of cognitive neuroscience*, 19(6):993–1003, 2007.
- [348] Marina López-Solà, Jesus Pujol, Rosa Hernández-Ribas, Ben J Harrison, Héctor Ortiz, Carles Soriano-Mas, Joan Deus, José M Menchón, Julio Vallejo, and Nar-

- cís Cardoner. Dynamic assessment of the right lateral frontal cortex response to painful stimulation. *Neuroimage*, 50(3):1177–1187, 2010.
- [349] Philip A Kragel, Michiko Kano, Lukas Van Oudenhove, Huynh Giao Ly, Patrick Dupont, Amandine Rubio, Chantal Delon-Martin, Bruno L Bonaz, Stephen B Marnock, Peter J Gianaros, et al. Generalizable representations of pain, cognitive control, and negative emotion in medial frontal cortex. *Nature neuroscience*, 21(2):283–289, 2018.
- [350] Fadel Zeidan, Oleg V Lobanov, Robert A Kraft, and Robert C Coghill. Brain mechanisms supporting violated expectations of pain. *Pain*, 156(9):1772, 2015.
- [351] Matthias Feurer and Frank Hutter. Hyperparameter optimization. *Automated machine learning: Methods, systems, challenges*, pages 3–33, 2019.
- [352] Paul Theo Zebhauser, Cristina Gil Ávila, and Markus Ploner. Chronic pain eeg dataset, Jan 2023.
- [353] Daniela M. Zolezzi. Chronic neuropathic pain eeg raw data in ec (5 min) and eo (5 min), Jul 2021.
- [354] Lichao Xu, Minpeng Xu, Yufeng Ke, Xingwei An, Shuang Liu, and Dong Ming. Cross-dataset variability problem in eeg decoding with deep learning. *Frontiers in human neuroscience*, 14:103, 2020.
- [355] Jacques J Vidal. Toward direct brain-computer communication. *Annual review of Biophysics and Bioengineering*, 2(1):157–180, 1973.

- [356] Jerry J Shih, Dean J Krusienski, and Jonathan R Wolpaw. Brain-computer interfaces in medicine. In *Mayo clinic proceedings*, volume 87, pages 268–279. Elsevier, 2012.
- [357] Naoki Yoshida, Yasunari Hashimoto, Mio Shikota, and Tetsuo Ota. Relief of neuropathic pain after spinal cord injury by brain–computer interface training. *Spinal Cord Series and Cases*, 2(1):1–4, 2016.
- [358] Anna Buttfeld, Pierre W Ferrez, and Jd R Millan. Towards a robust bci: error potentials and online learning. *IEEE Transactions on Neural Systems and Rehabilitation Engineering*, 14(2):164–168, 2006.